KANSAS GEOLOGICAL SURVEY
OPEN-FILE REPORT 82-27

Distribution, Petrology and Depositional Environment
of "Bush City Shoestring Sandstone" and
"Centerville Lagonda Sandstone" in
Cherokee Group (Middle Pennsylvanian),
Southeastern Kansas

by

Philip N. Reinholtz

KANSAS GEOLOGICAL SURVEY
1930 Constant Avenue
University of Kansas
Lawrence, KS 66047

DISTRIBUTION, PETROLOGY AND DEPOSITIONAL ENVIRONMENT OF "BUSH CITY SHOESTRING SANDSTONE" AND "CENTERVILLE LAGONDA SANDSTONE" IN CHEROKEE GROUP (MIDDLE PENNSYLVANIAN), SOUTHEASTERN KANSAS

by

Philip N. Reinholtz

A thesis submitted in partial fulfillment
of the requirements for the degree of
Master of Science in Geology
in the Graduate College of
the University of Iowa

July, 1982

Thesis supervisor:Assistant Professor Robert L. Brenner

Graduate College
The University of Iowa
Iowa City, Iowa

CERTIFICATE OF APPROVAL

MASTER'S THESIS

This is to certify that the Master's thesis of

Philip N. Reinholtz

has been approved by the Examining Committee for the thesis requirement for the Master of Science degree in Geology at the July, 1982 graduation.

Thesis committee: Robert R Brenner
Thesis Supervisor

Member

Member

ACKNOWLEDGMENTS

I would like to extend my gratitude to the Kansas Geological Survey for the financial assistance which made this project possible, and especially to Lynn Watney and the many fine people of that organization.

Special thanks are extended to my committee chairman, Dr. Robert L. Brenner, for his guidance and advice from the conception to completion of this project. I would also like to thank Dr. Keene Swett and Dr. P. H. Heckel for their assistance and critique of the manuscript.

Many thanks to the following individuals who contributed their time and information which made this study possible; Eugene Cornish, Ray Marmon, Dennis Feuerborn, S. A. Mitchell, John Marvin, Orville Sobba, and especially Glenn Caldwell.

Thanks are also due Ken Kern for his assistance in thin section preparation. I would like to thank Steve Pearson, Leon Aden, and Ahmet Dogan for their assistance in microprobe, x-ray, and S.E.M. investigations and to the rest of the graduate students of the geology department who have made the last two years very enjoyable.

ABSTRACT

During the Middle Pennsylvanian (Desmoinesian), sedimentation patterns in eastern Kansas and the entire mid-continent were influenced by the periodic influx of siliciclastic materials and eustatic changes in sea level. Abundant siliciclastic detritus resulted in the progradation of delta systems in the shallow seas of the Cherokee platform, with carbonate deposition occurring during periods of low sediment input.

In Anderson County, Kansas, the shales and thin sandstones of the "Lagonda" interval of the upper Cherokee Group represent the advancement of a prograding delta system. Subsequent alluvial channels incised and modified the previously deposited sediments, resulting in fining-upward sequences such as those within the Centerville "Lagonda" sandstone, which are interpreted as representing point-bar deposits.

A lowering of sea level resulted in the incisement of the Bush City Channel. During later transgression of the Cherokee Sea, this channel was filled by the aggradational deposits of a moderately sinuous alluvial stream, resulting

in numerous, irregular, lenslike bodies composed of well sorted, quartz-rich sands containing highly variable amounts of matrix. Small-scale sedimentary structures consisting of rippled laminae and thin beds are prevalent. Minor high-angle cross stratification also occurs.

Following initial compaction, diagenetic alterations further modified the sediments. Major authigenic cements include Fe-calcite and quartz overgrowths. Minor amounts of pyrite, sericite, kaolinite, siderite, gypsum, and iron oxide were also formed.

TABLE OF CONTENTS

LIST OF FIGURES

LIST OF TABLES

INTRODUCTION

The Middle Pennsylvanian (Desmoinesian) Cherokee Group of Kansas (Figure 1) consists mostly of mudrocks with numerous sandstone lenses, persistant thin limestones, black shales, and coal beds. The elongate lenticular sandstone bodies are known as "shoestring sands" and have long been the target of drillers in search of hydrocarbons. The first "shoestring" discovered, which produced oil, was the Paola trend discovered in 1917 (Powell and Eakin, 1953).

Location

The upper Cherokee "Lagonda" sandstones of the Bush City Shoestring and Centerville trend are the main focus of this study. The Bush City trend is located in east-central Anderson County, Kansas (Figure 2). The Bush City, discovered in 1923 (Rich, 1923), is believed to be an extension of the Goodrich-Parker Shoestring in Linn County (Jewett, 1954) (Figure 2). The Graves oil and gas field is also believed to be related to the Bush City trend (Jewett, 1954) (Figure 2). The Centerville trend, discovered in 1919 (Jewett, 1954), is located southeast of the Bush City trend in Anderson County and extends southeastward into Linn County (Figure 2).

Figure 1. Stratigraphic column of Cherokee Group in Kansas. (From Zeller, 1968).

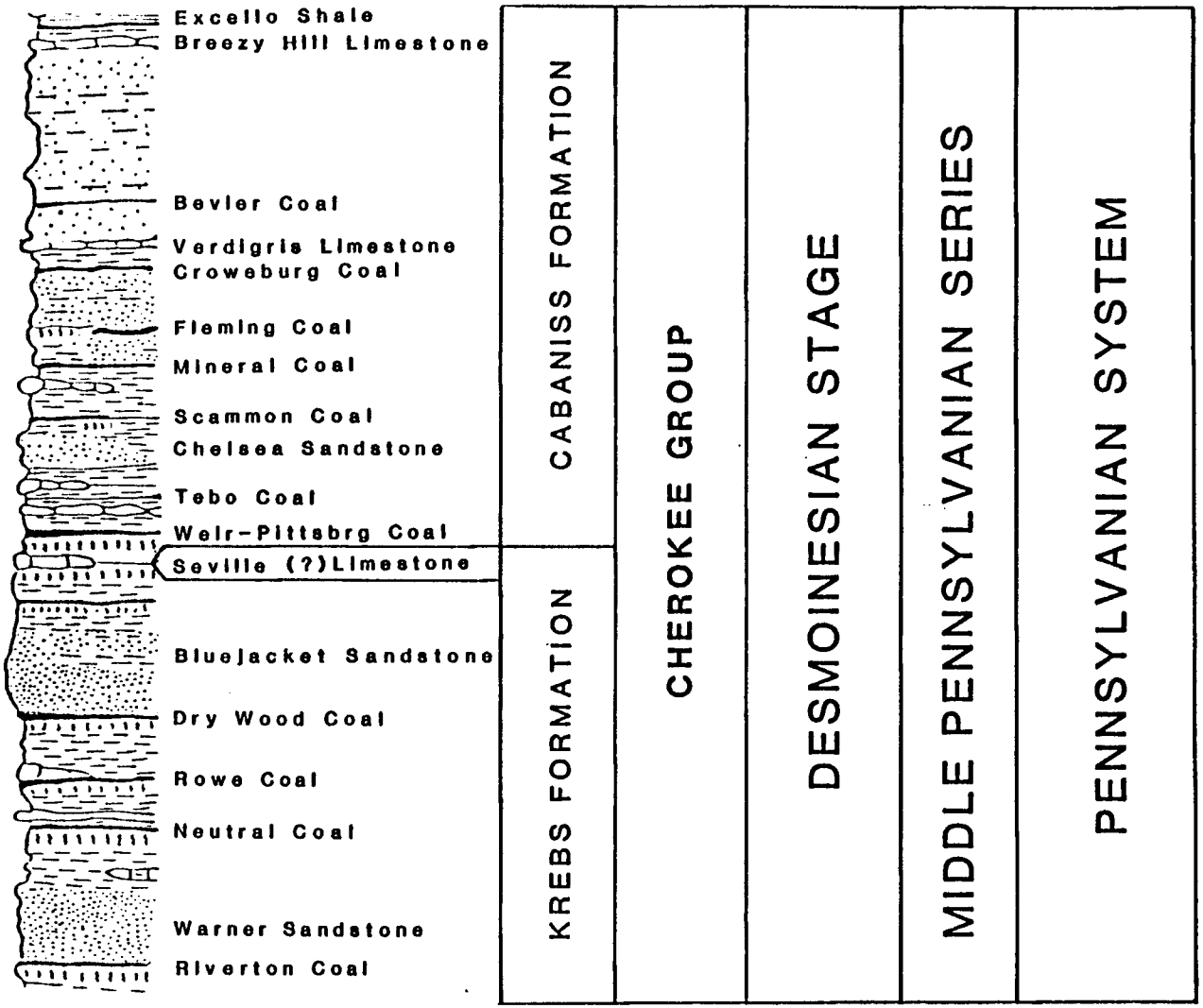
Excello Shale
Breezy Hill Limestone
Bevier Coal
Verdigris Limestone
Croweburg Coal
Fleming Coal
Mineral Coal
Scammon Coal
Chelsea Sandstone
Tebo Coal
Weir-Pittsbrg Coal
Seville (?)Limestone
Bluejacket Sandstone
Dry Wood Coal
Rowe Coal
Neutral Coal
Warner Sandstone
Riverton Coal
CABANISS FORMATION
KREBS FORMATION
CHEROKEE GROUP
DESMOINESIAN STAGE
MIDDLE PENNSYLVANIAN SERIES
PENNSYLVANIAN SYSTEM

Figure 1

Figure 2. Location map of study area, Anderson County, Kansas. Names indicate Bush City Shoestring and other Lagonda sandstone trends: Goodrich-Parker, Colony-Welda, Centerville, Garnett, and Graves. Well log locations are indicated by dots and core locations by squares. A-A' and L-L' illustrate regional cross-section positions.

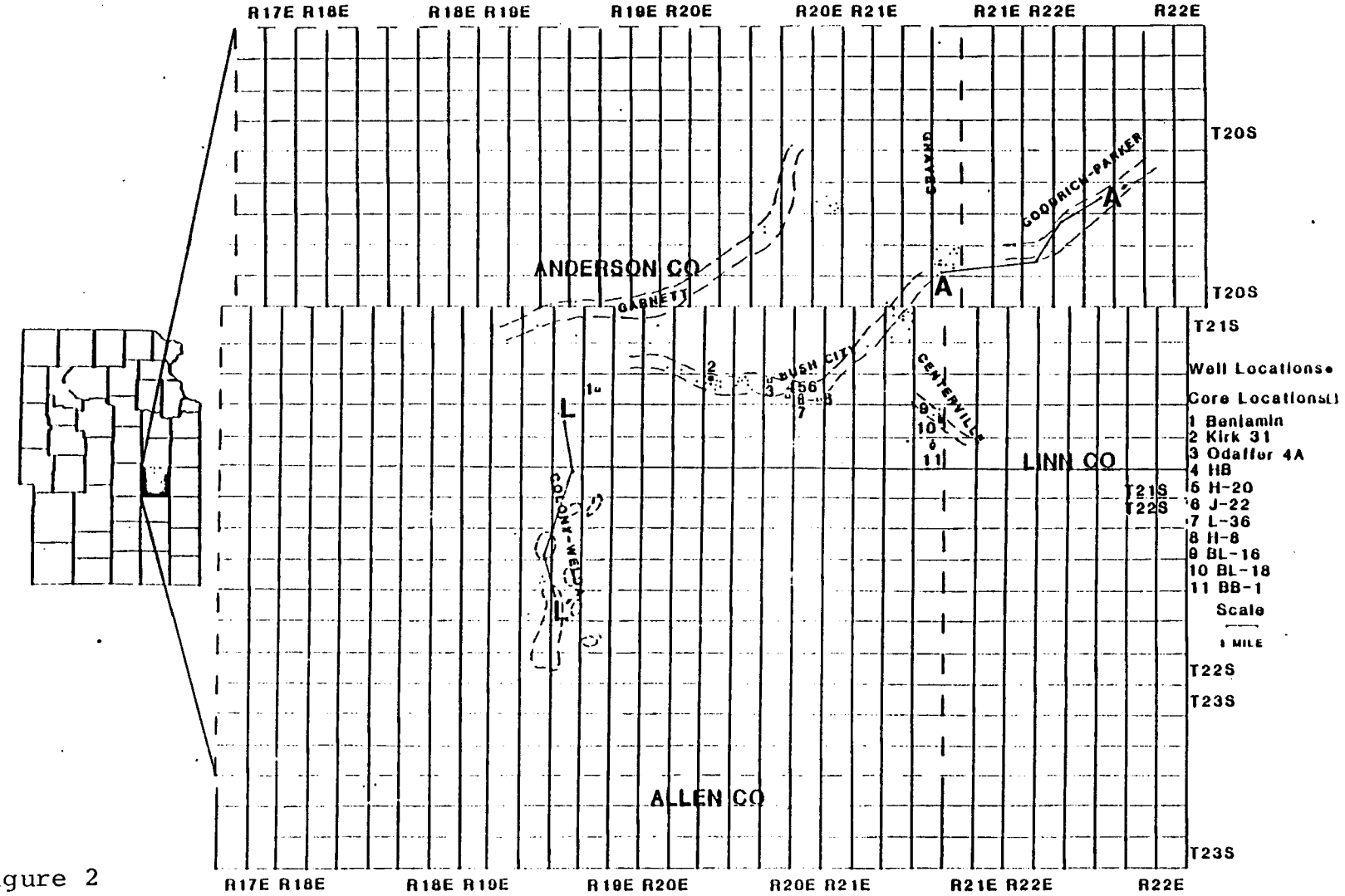
R17E R18E
R18E R19E
R19E R20E
R20E R21E
R21E R22E
R22E
T20S
T20S
T21S
T22S
T23S
ANDERSON CO
ALLEN CO
LINN CO
GARNETT
GOODRICH-PARKER
CENTERVILLE
BUSH CITY
COLONY-WELDA
A
A'
L
L'
Well Locations•
Core Locations(1)
1 Benlamin
2 Kirk 31
3 Odaffer 4A
4 HB
5 H-20
6 J-22
7 L-36
8 H-8
9 BL-16
10 BL-18
11 BB-1
Scale
1 MILE

Figure 2

Objectives

The objectives of this study are: 1) to determine facies variation and delineate the geometry of the Bush City Shoestring; 2) to determine the mineralogical composition of and the stratigraphic relations between the Bush City and Centerville sandstones; 3) to determine source area(s) for siliciclastic materials; 4) to determine the diagenetic history of the sandstones and the effects of diagenetic alterations upon sandstone reservoir characteristics; 5) to determine the depositional environments of the Bush City and Centerville sandstones.

PREVIOUS INVESTIGATIONS

The stratigraphy of Cherokee strata (Desmoinesian) occurring in the Forest City and Cherokee Basins of eastern Kansas has been the subject of studies by Moore (1936), Lee (1943), Searight and others (1953), Howe (1956), Zeller (1968) and Wells and Anderson (1968).

The cyclic nature of Pennsylvanian deposition in the mid-continent has long been recognized. This aspect of sedimentation in Kansas has been the focus of studies by Moore (1931, 1964), Wanless and others (1963), Merriam (1963), Heckel (1977, 1980).

Exploration for petroleum in the irregular "shoestring" sandstones of the Cherokee Group led to several early studies on shallow-shelf depositional environments. In Anderson County, Charles (1927, 1941) and Rich (1923,1926) studied the nature of the Bush City Shoestring. Bass (1934) investigated shoestring sandstones occurring in Greenwood and Butler Counties, Kansas. Weirich (1953) studied the principles of the generation and migration of oil on shallow shelves.

Recent work on Pennsylvanian deltaic sedimentation has been focused in Oklahoma by Visher (1968), Visher and others (1971), and Busch (1971). Fluvial and deltaic sedimentary environments in the mid-continent have been examined by Moore (1979) and Brown (1979). The latest work in Anderson County, Kansas focused on a sandstone unit in the Kincaid oil field (Van Dyke, 1975).

METHODS OF INVESTIGATION

Well Log Analyses

Geophysical well-logs and core material from the upper Cherokee "Lagonda" interval in the Bush City and Centerville fields and adjacent areas were obtained from the Kansas Geological Survey and private driller operators (Figure 2). Neutron logs were used in conjunction with gamma-ray logs to identify lithology. Coals produce high neutron porosities and low gamma-ray counts. Limestones are usually recognized by their low gamma-ray counts and neutron porosity readings. Shales will normally cause moderate gamma-ray counts and neutron porosities. Phosphatic black shales cause extremely high gamma-ray readings that are due to the high concentration of uranium. These responses of the logging tools to lithology are illustrated in Figure 3.

The gamma-ray and neutron logs were used in conjunction with the cores to investigate the stratigraphic relations of the sandstone bodies within and between the Bush City and Centerville trends. Cross-sections were constructed on a regional (Figure 2) and local scale (Figure 4) to illustrate stratigraphic relations and varying well-log signatures.

Figure 3. Gamma-ray and neutron log recordings of Lagonda interval. Phosphatic black shales (Little Osage, Excello, and Verdigris) produce extremely high gamma-ray "kicks" because of a high concentration of uranium. Bevier coal located at approximately 634 ft. (193.0m) causes a low gamma-ray count and high neutron porosity. Fort Scott Limestone is characterized by low gamm-ray and low neutron readings. Shaley intervals characterized by irregular "serrate" gamma-ray patterns.

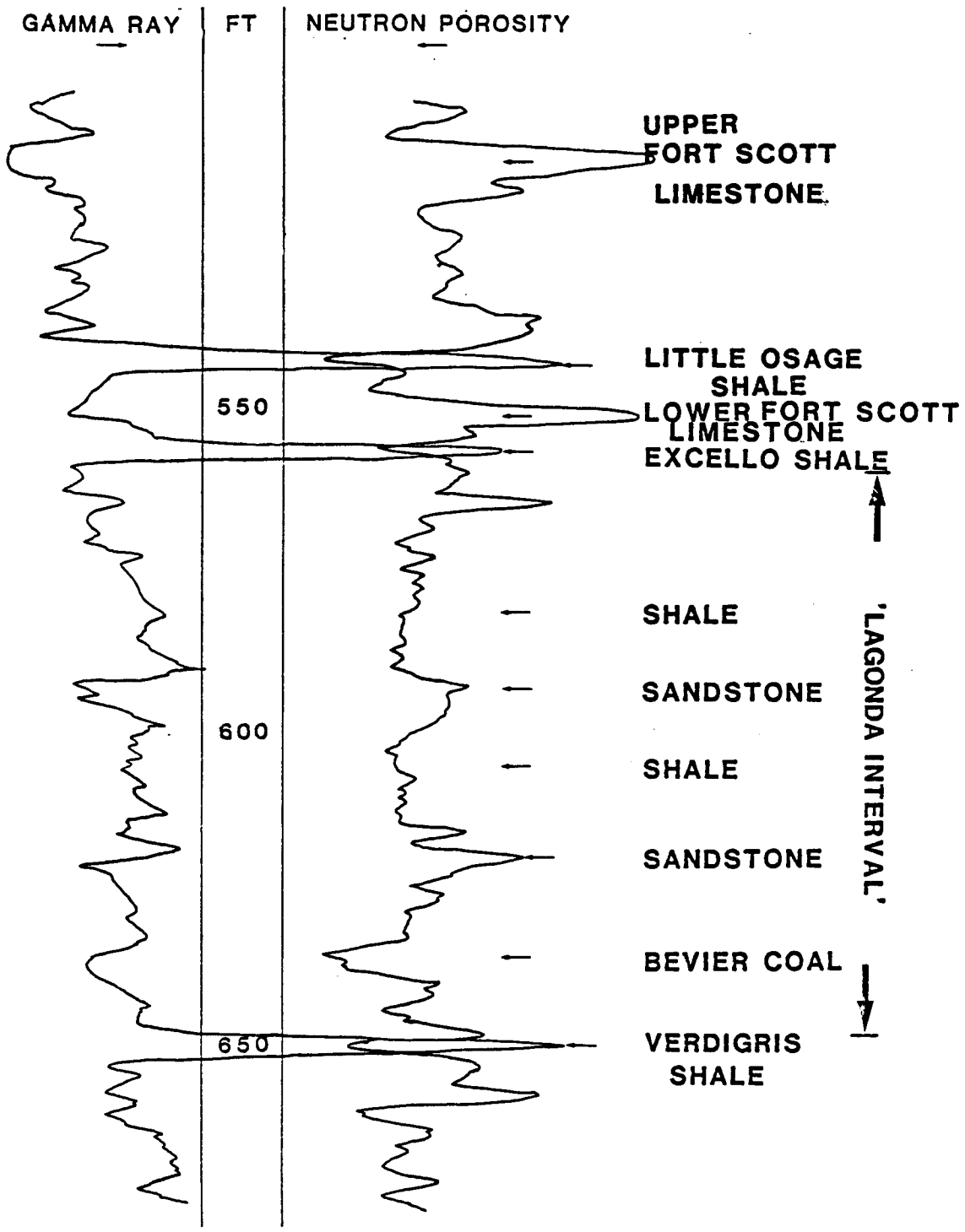
GAMMA RAY
FT
NEUTRON POROSITY
UPPER
FORT SCOTT
LIMESTONE
LITTLE OSAGE
SHALE
550
LOWER FORT SCOTT
LIMESTONE
EXCELLO SHALE
SHALE
SANDSTONE
600
SHALE
SANDSTONE
BEVIER COAL
650
VERDIGRIS
SHALE
'LAGONDA INTERVAL'

Figure 3

Figure 4. Map showing position of cross-sections in Bush City Shoestring area.

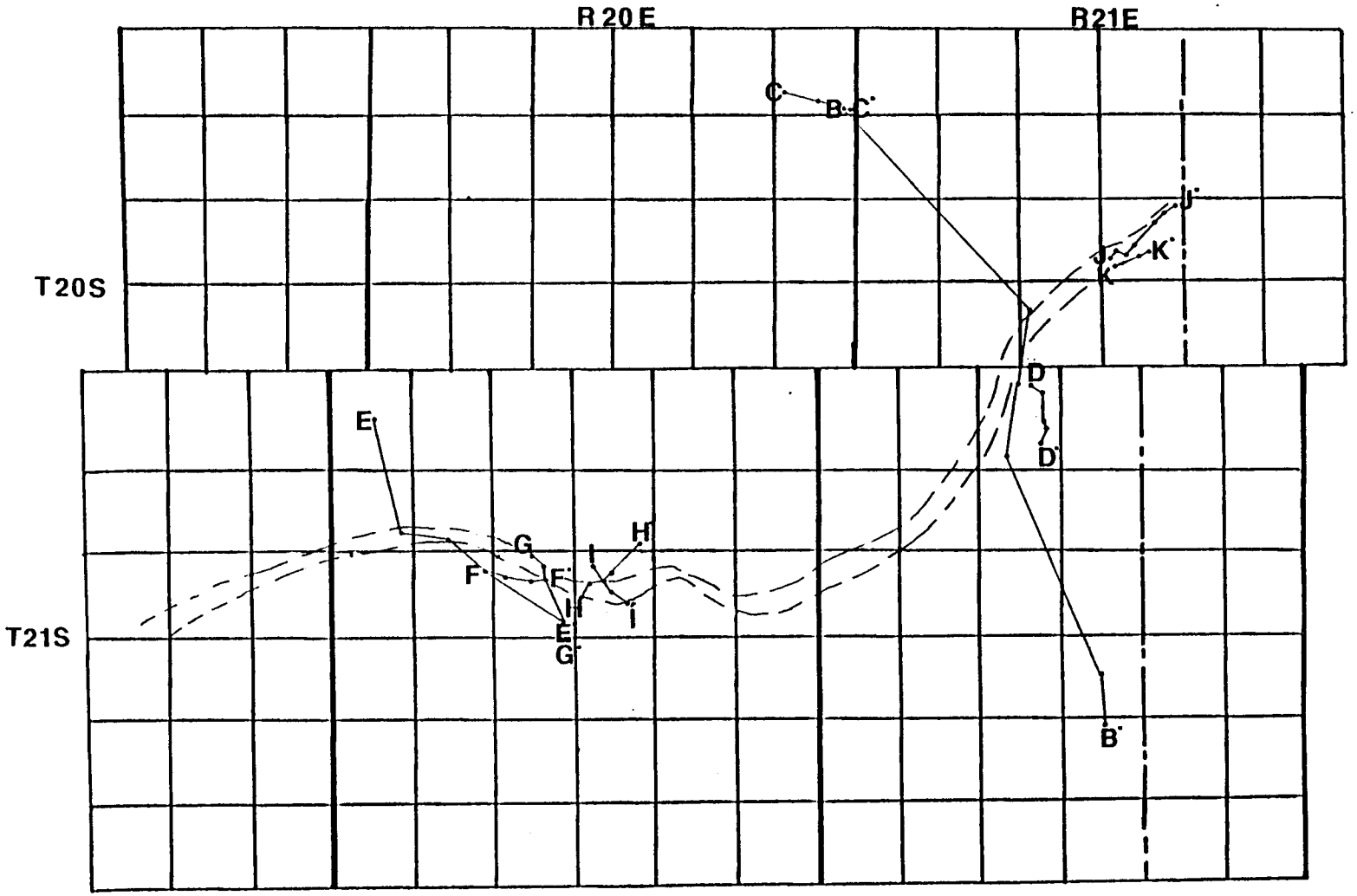

Figure 4

Core Analyses

Eight cores from the Bush City and three from the Centerville were available for sedimentologic and petrographic analyses (APPENDIX A). Stratigraphic position of these cores within the Lagonda interval was determined through the use of both gamma-ray logs and drillers logs (Table 1). The cores were vertically slabbed to examine the lithologic sequences, textures, and sedimentary structures of the sandstones. Descriptions of bedding characteristics were based on criteria suggested by Moore and Scruton (1957). "Regular" strata are uniform beds or laminations which extend completely across the width of the core, while in contrast, "irregular" strata differ in thickness or pinch out across the core.

Petrographic Analyses

Cores were sampled at regular intervals for petrographic analysis. The sandstone chips of wells Bailey-Bailey No. 1 and Bailey-Lohrengel 16 and 18 were cleaned of petroleum using the soxhlet extraction method at the University of Kansas Tertiary Oil Recovery Project. In this process tetrahydronaphthalene (THN) is flushed through the rock, removing hydrocarbon residue. All rock chips were impregnated with blue epoxy in order that pore space would be recognized. Selected thin sections from each core were

Table 1. Position of cores within the Lagonda Interval.

WELL	DEPTH BELOW EXCELLO SHALE (feet)	LOCATION TOWNSHIP-RANGE
Bailey-Lohrengel 16 *	55.0-68.0 (16.8-20.7m)	660FNL 660FEL $SE\frac{1}{4}$ of $NE\frac{1}{4}$ Sec. 22 T21S-R21E
Bailey-Lohrengel 18 *	51.0-57.0 (15.6-17.4m)	1100FEL 660FNL $SE\frac{1}{4}$ of $NE\frac{1}{4}$ Sec. 22 T21S-R21E
Bailey-Bailey 1	53.0-70.0 (16.2-21.3m) (?)	$NW\frac{1}{4}$ of $NW\frac{1}{4}$ of $NE\frac{1}{4}$ Sec. 27 T21S-R21E
Kirk 31 *	37.0-63.5 (11.3-19.4m)	$NW\frac{1}{4}$ of $NW\frac{1}{4}$ Sec. 16 T21S-R20E
H-8-2	21.0-55.0 (6.4-16.8m)	$W\frac{1}{2}$ of $E\frac{1}{2}$ of $SE\frac{1}{4}$ Sec. 13 T21S-R20E
H-20	33.0-53.0 (10.0-16.2m)	1100FNL 1155FEL $SW\frac{1}{4}$ Sec. 13 T21S-R20E
J-22	27.0-47.0 (8.2-14.5m)	C $SW\frac{1}{4}$ Sec. 13 T21S-R20E
L-36	?	$NE\frac{1}{4}$ of $SE\frac{1}{4}$ Sec. 13 T21S-R20E
H-B	?	$SW\frac{1}{4}$ of $NE\frac{1}{4}$ of $SE\frac{1}{4}$ Sec. 14 T21S-R20E
Odaffer 4A	?	165FWL 880FNL $W\frac{1}{2}$ of $NW\frac{1}{4}$ Sec. 14 T21S-R20E
Benjamin	?	Sec. 14 T21S-R19E

Table 1

stained using alizarin red "S" and potassium ferricyanide. These solutions stain carbonates in the following manner: calcite-pale pink to red; ferroan calcite-mauve purple to dark blue; ferroan dolomite-pale to deep turquoise; non-ferroan dolomite-no effect (Dickson, 1965). Compositions of the Bush City and Centerville sandstones were determined through petrographic microscope examination of 120 thin sections. Modal analyses were determined for 39 thin sections from nine cores (APPENDIX B). The sandstones were classified using Folk's (1974) classification scheme (Figure 5). Sandstones having a clay matrix content equal to or greater than 10% were classified as wackes. Point counts were carried out perpendicular to stratification. In addition, the S.E.M. was used to observe diagenetic alterations and their effects on pore-throat geometries, and microprobe and x-ray analyses were used to determine compositional differences between similar-appearing carbonate cements that occur in the sandstones.

Figure 5. Sandstone classification scheme used in study. (After Folk, 1974).

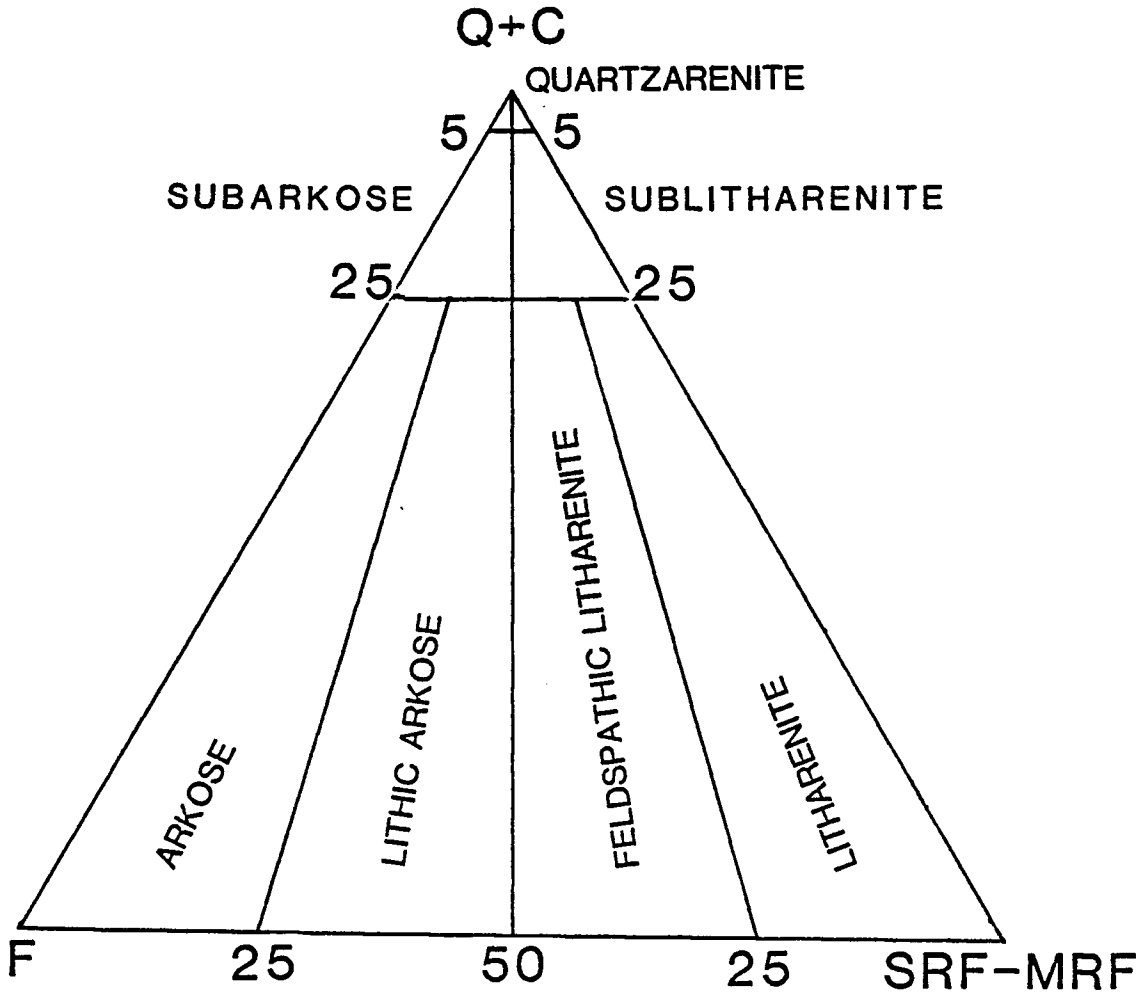
Q+C
QUARTZARENITE
5
5
SUBARKOSE
SUBLITHARENITE
25
25
ARKOSE
LITHIC ARKOSE
FELDSPATHIC LITHARENITE
LITHARENITE
F
25
50
25
SRF-MRF

Figure 5

TECTONIC SETTING OF THE MIDCONTINENT

Tectonic activity increased in the mid-continent following Mississippian time. South of Kansas the Arkoma and Anadarko Basins were developing, possibly in response to the continental suturing to the south resulting from the collision between the North American and South American-African plates (Kluth and Coney,1981). In the eastern Kansas area the main structural features produced by the activity were the Nemaha Uplift and Bourbon Arch (Merriam, 1963) (Figure 6).

The Nemaha Uplift divided the Kansas Basin into two regions, the Salina Basin to the west and Forest City and Cherokee Basins to the east (Merriam,1963). The Nemaha Uplift extended south into Kansas from present-day Nemaha County to Sumner County, and is generally steeper on its eastern flank than on the west, interpreted as an eastward-facing fault escarpment (Lee, 1943). The steep western boundary of the Forest City Basin created by the Nemaha Uplift produced an asymmetrical profile with the deeper part of the basin adjacent to the uplift.

Figure 6. Structural features of mid-continent area during Middle Pennsylvanian. (Modified from Van Dyke, 1975).

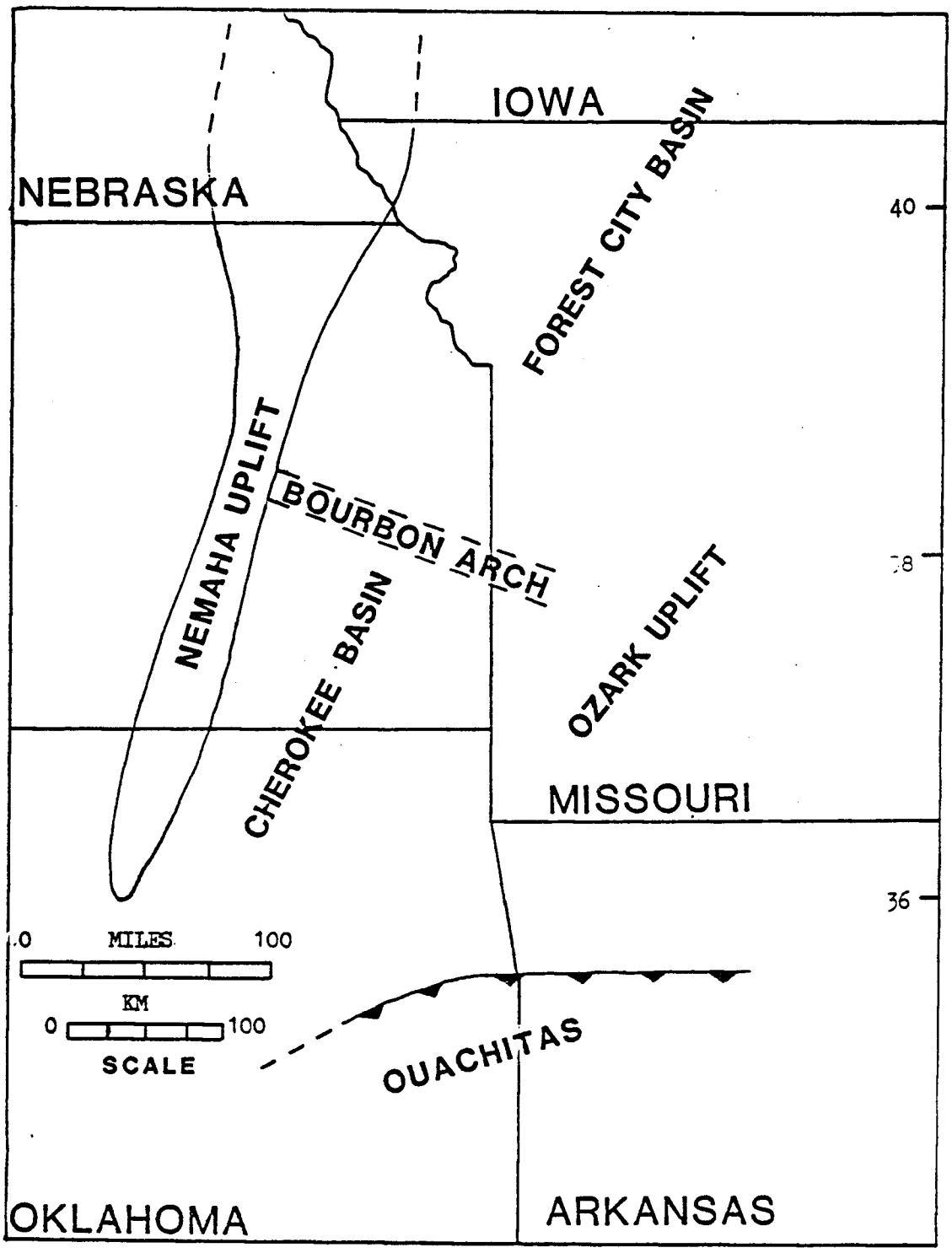
IOWA
NEBRASKA
FOREST CITY BASIN
40
NEMAHA UPLIFT
BOURBON ARCH
CHEROKEE BASIN
OZARK UPLIFT
38
MISSOURI
36
0 MILES 100
KM
0 100
SCALE
OUACHITAS
OKLAHOMA
ARKANSAS

Figure 6

The Cherokee Basin, a shelf-like extension of the Arkoma Basin of Oklahoma, was separated from the Forest City Basin by the Bourbon Arch, a positive feature at various times during the Pennsylvanian, trending NW to SE through east-central Kansas and into Missouri (Merriam, 1963) (Figure 6). The Ozark uplift forms the eastern boundary of the Cherokee Basin and the southeastern boundary of the Forest City Basin (Figure 6).

During the Pennsylvanian, the sea advanced northward from Oklahoma reworking the sediments derived from the newly uplifted source areas. The Nemaha Uplift and Bourbon Arch were major influences on sedimentation in Kansas, in that older Pennsylvanian deposits were confined to the basinal areas with younger rocks overstepping one another on the positive areas (Merriam, 1963; Visher and others, 1971). However, recent work has shown that the Bourbon Arch did not conspicuously influence depositional characteristics of the Lagonda interval (R. L. Brenner, personal communication, 1982).

The Cherokee Group in Kansas records the first occurrence of the well known cyclic deposits of the mid-continent. Eustatic sea level changes resulting from Gondwana glaciation have been suggested to account for the broad patterns of cyclicity (Heckel, 1980), with deltaic progradation having modifying effects near the shoreline.

STRATIGRAPHIC OVERVIEW

Cherokee Group

The Cherokee Group in eastern Kansas is the lowest division of the Desmoinesian Stage, Middle Pennsylvanian Series, Pennsylvanian System. Cherokee strata were divided into the Krebs and Cabaniss subgroups in 1953 (Oakes, 1953) and were later divided into 17 formations (Howe, 1956) in which the lower 6 formations were placed in the Krebs and the upper 11 in the Cabaniss subgroup. The Krebs is approximately 60 to 75 meters thick in southeastern Kansas, and the Cabiniss 60 meters thick (Howe, 1956). Cherokee Group nomenclature currently used in Missouri, Kansas, and Oklahoma is shown in Figure 7.

The base of the Cherokee Group lies unconformably on Mississippian strata in eastern Kansas, but in anticlinal areas and faulted highs such as the Nemaha Uplift the age of the underlying strata varies from Devonian to Precambrian (Ham and Wilson, 1967). The upper limit of the Cherokee is the base of the Fort Scott Limestone of the Marmaton Group.

The Cherokee Group crops out in a southwest-northeast band across southeastern Kansas (Figure 8). The type area

Figure 7. Current nomenclature of Cherokee Group used in Kansas, Missouri, and Oklahoma. (After Ebanks, 1979).

MISSOURI		KANSAS		OKLAHOMA	
CHEROKEE GROUP	CABANISS SUBGROUP: 12 CYCLOTHEM FORMATIONS	CHEROKEE GROUP	CABANISS FORMATION	CABANISS GP.	SENORA FORMATION
	KREBS SUBGROUP: 6 CYCLOTHEM FORMATIONS		KREBS FORMATION	KREBS GROUP	BOGGY FORMATION SAVANNA FORMATION MCALESTER FORMATION HARTSHORNE FORMATION

Figure 7

Figure 8. Outcrop belt of Cherokee Group in southeast Kansas. (After Moore, 1949).

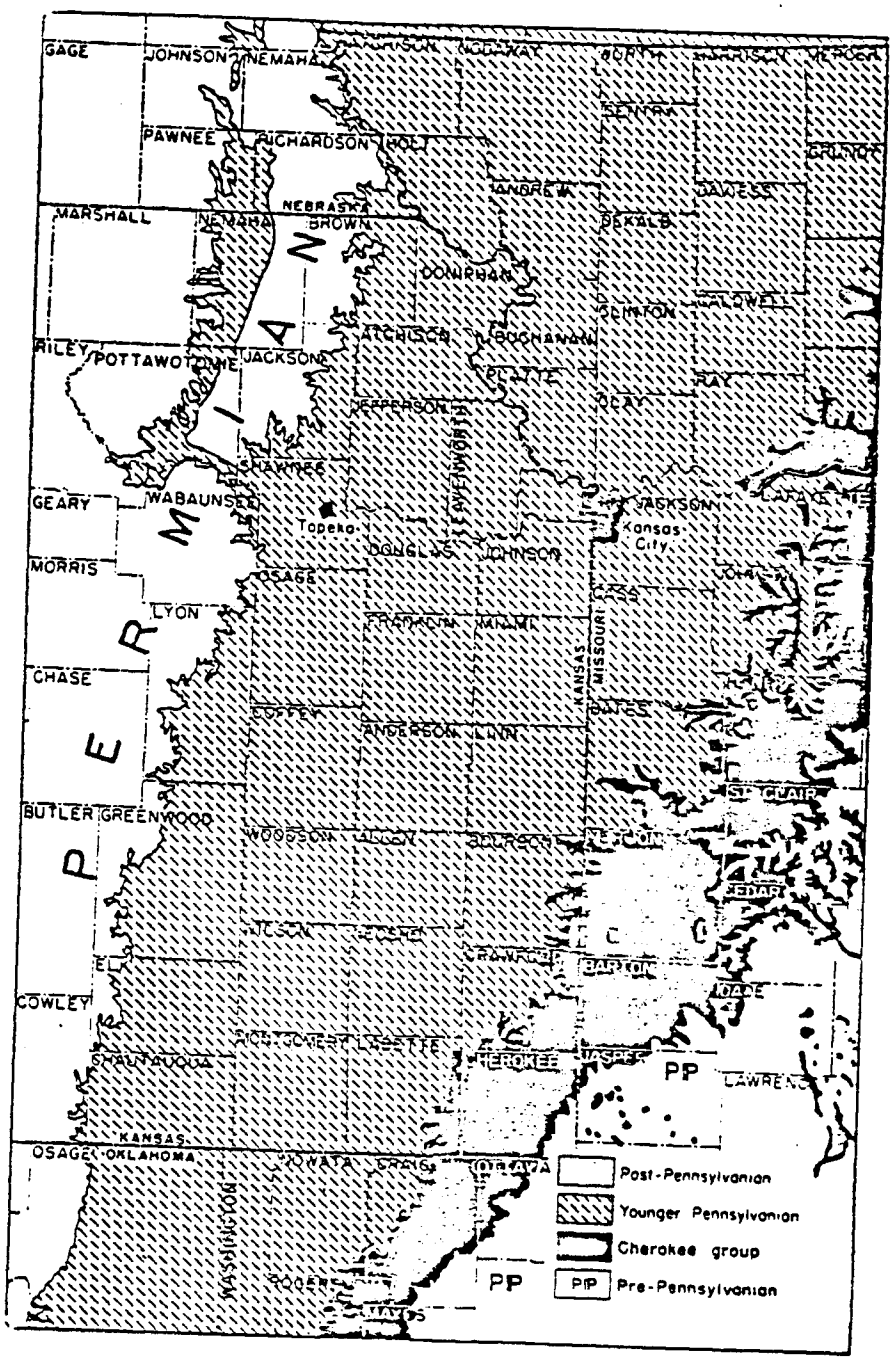
GAGE
JOHNSON
NEMAHA
PAWNEE
RICHARDSON
NEBRASKA
MARSHALL
NEMAHA
BROWN
DONIPHAN
ATCHISON
BUCHANAN
RILEY
POTTAWATOMIE
JACKSON
PLATTE
CLAY
JEFFERSON
LEAVENWORTH
SHAWNEE
WABAUNSEE
GEARY
Topeka
JACKSON
Kansas City
DOUGLAS
JOHNSON
MORRIS
OSAGE
LYON
FRANKLIN
MIAMI
CHASE
COFFEY
ANDERSON
LINN
BATES
BUTLER
GREENWOOD
WOODSON
ALLEN
BOURBON
NEOSHO
LABETTE
CHEROKEE
CRAWFORD
CHAUTAUQUA
MONTGOMERY
COWLEY
KANSAS
OKLAHOMA
OSAGE
KAY
PAWNEE
GRANT
HARPER
SUMNER
HARVEY
MARION
BUTLER
CHASE
COWLEY
SEDGWICK
HARPER
KINGMAN
HARPER
SUMNER
HARVEY
MARION
MCPHERSON
REPUBLIC
CLOUD
OTTAWA
WASHINGTON
CRAIG
OTTAWA
ROGERS
MAYES
PP
PP
Post-Pennsylvanian
Younger Pennsylvanian
Cherokee group
Pre-Pennsylvanian

Figure 8

for the group is Cherokee County, Kansas. Cherokee strata dip 3 to 5 meters per km to the northwest as a result of post-Permian deformation (Jewett, 1954). The dominant lithology of the Cherokee Group is shale, which accounts for approximately 80% of the strata (Howe, 1956).

Lagonda Interval

The term Lagonda was first used by Gordon (1893) to designate strata between the Bevier Coal and the underclay of the Mulky Coal in Missouri (Howe, 1956). Searight and others (1953) placed the Lagonda interval from above the Bevier Coal to the top of the Iron Post Coal. In this study the "Lagonda" is defined as the strata lying above the Verdigris Limestone to the base of the Excello Shale. However, since the Verdigris Limestone is often impossible to detect on geophysical well-logs, a black shale beneath it is often used as the Lagonda lower boundary. The upper limit of the interval is delineated by the "hot shale" response of the Excello Shale (Figure 3). The top of the Lagonda interval in the Bush City trend and surrounding area increases in depth from east to west, ranging from 167.0 meters to 259.0 meters below the surface (Rich, 1923).

Verdigris Limestone

The Verdigris Limestone is the most widespread limestone in the Cabaniss Formation (Howe, 1956). The unit

was first described at its outcrop along the Verdigris River in Rogers County, Oklahoma. In southeast Kansas the Verdigris averages 1.5 meters in thickness and consists of three limestone beds interbedded with shale (Howe, 1956). The Verdigris is a finely crystalline, fossiliferous, and dense limestone. A black phosphatic shale, which is widespread through eastern Kansas, Oklahoma, and Iowa, occurs immediately below the limestone and serves as a valuable subsurface stratigraphic marker, since it has a characteristically high gamma-ray count (Figure 3).

Bevier Coal

The Bevier Coal in the type area in Macon County, Missouri, consists of two distinct coal beds separated by a shale parting (Howe, 1956). In southeast Kansas a single coal bed is overlain by thin beds of limestone and calcareous shale. The underclay of the coal often rests directly on the Verdigris Limestone but also overlies a sandstone or shale above the limestone (Howe, 1956). The Bevier Coal is usually present in the Bush City and Centerville trends at approximately 23.8 to 25.6 meters below the Excello Shale.

Squirrel Sandstone

The "squirrel" sandstone received its nickname when oil was discovered in an upper Cherokee sandstone on the farm of

Lenny Squirrel (Visher, 1968). Drillers called irregularly occurring sand bodies the "squirrel" because they "jumped" wildly around in the subsurface. This name is widely used among oil field operators to label sandstone bodies that occur above the Verdigris Limestone in the upper 30.0 meters of the Cherokee Group (Jewett, 1954). The thickness of the "squirrel" sandstone varies from 3.0 to 24.4 meters (Lee, 1943). The sandstone is fine to very fine-grained, micaceous, and exhibits fine laminations and ripple structures. The "squirrel" of Kansas is equivalent to the Prue of Oklahoma (Visher and others, 1971). The depositional environment of the "squirrel" sandstone is variable, and interpretations range from marine bar to valley fill (Charles, 1927).

Breezy Hill Limestone

The Breezy Hill Limestone in Kansas occurs above the Lagonda sandstone and below the underclay of the Mulky Coal. The lithology of the Breezy Hill ranges from an irregular bedded, sandy, conglomeratic limestone present in southeast Kansas to a thin bedded, massive, dense to medium-grained limestone in northern Oklahoma (Howe, 1956). The Breezy Hill of southeast Kansas has been suggested to have been deposited as a fresh-water limestone or as an "underlimestone" associated with the deposition of the Mulky

Coal (Heckel, personal communication, 1981). Thickness of the Breezy Hill is about 0.6 meters in the Breezy Hill, Kansas area.

Mulky Coal

The Mulky is the uppermost coal of the Cherokee Group. It reaches a maximum thickness of 0.5 meters in northeast Crawford and eastern Bourbon Counties, where it was mined (Howe, 1956).

Excello Shale

The Excello Shale is the uppermost unit of the Cabaniss Formation. It is a black, phosphatic shale, which varies from 0.6 to 1.5 meters in thickness and is widespread over Kansas, Missouri, and Oklahoma (Howe, 1956). The Excello Shale overlies the Mulky Coal and is overlain by the Blackjack Creek Limestone Member of the Fort Scott Formation. It has been interpreted as being deposited at a maximum transgression of the Cherokee Sea when the development of a thermocline led to anoxic bottom conditions (James, 1970). The high gamma-ray count of the shale and its lateral continuity throughout eastern Kansas makes it an excellent subsurface stratigraphic marker for the top of the Cherokee Group and the "Lagonda" interval (Figure 3).

SEDIMENTOLOGIC ANALYSIS

Sedimentologic analyses of the Lagonda interval were based primarily on subsurface core material. Four cores that lacked sufficient information to be accurately placed within the Lagonda interval include H-B, Odaffer, L-36, and Benjamin. These cores were included in the study because of their value in the overall depositional analysis. Core samples were available from as deep as 21.3 meters to as shallow as 6.4 meters below the Excello Shale (Table 1).

Slabbed core material was described in detail (APPENDIX A). Units were subdivided on the basis of grain size, bedding characteristics, sedimentary structures, and depositional sequence. These descriptions were then used to establish five main lithofacies in the Bush City and Centerville trends to serve as a basis for stratigraphic and sedimentologic interpretations.

Lithofacies A

Lithofacies A is a uniform, massive, fine-grained, micaceous sandstone. The cores of Bailey-Lohrengel 16 and 18 are composed entirely of this facies. Thickness of this facies ranges from 0.1 to 4.6 meters. The only significant

compositional variations observed in lithofacies A are thin horizons of shale-chip conglomerate that occur in the basal section of Bailey-Lohrengel 16 (181.0 m) and in the upper portion (184.4 m) of Bailey-Lohrengel 18 (Figure 9). The clasts are finely laminated, dark silty shales, and range up to 5 cm in length and 2 cm in width. These clasts suggest a short transport of local sediments ripped up during high flow periods. Burrowing is absent in lithofacies A. Sedimentary characteristics of lithofacies A suggest deposition in a high-energy environment.

Lithofacies B

Fine-grained sandstone beds interstratified with lesser amounts of silt and clay shales are the major lithologic components of lithofacies B. Bedding character and sedimentary structures vary significantly within this unit. Thickness of this facies ranges from 0.3 to 1.6 meters.

Regular and irregular wavy bedding are the most abundant stratification types. The bedding surfaces are only slightly to moderately undulating, with individual beds rarely exceeding 4.0 cm. Rippled sandstones with well defined basal erosional surfaces show small-scale trough cross-bedding in several horizons of lithofacies B (Figure 10). This type of trough cross-stratification has been attributed to the migration of linguoid ripples (Blatt and

Figure 9. Photograph showing massive bedding of Lithofacies A. Silt-shale chip conglomerate present in otherwise structureless unit in slabbed core of Bailey-Lohrengel 18.

Figure 10. Photograph showing small-scale trough cross-bedding in Lithofacies B. Slabbed core Kirk 31.

Figure 9

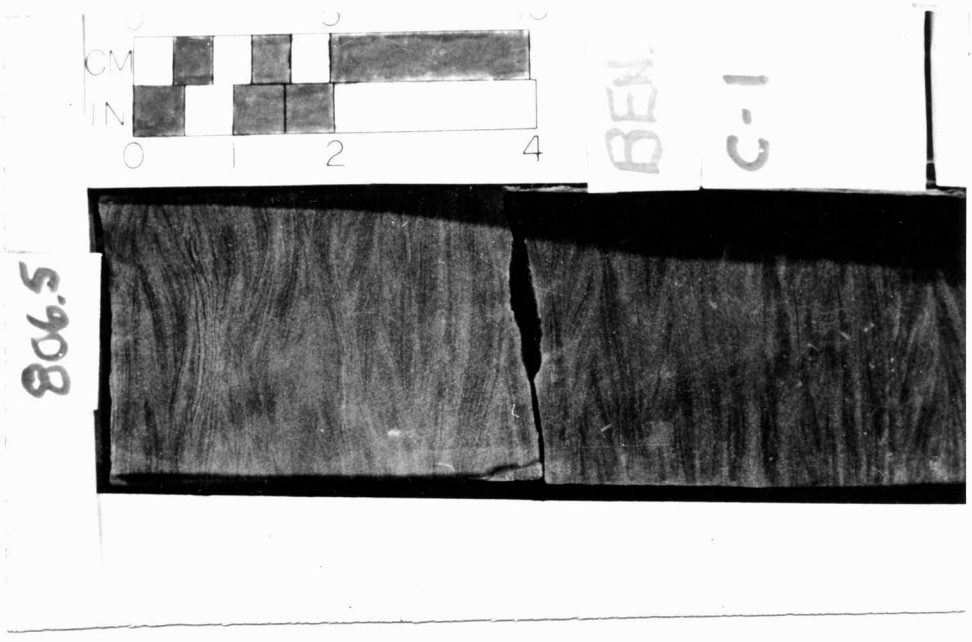

Figure 10

others, 1980). High angle cross-bedding not exceeding 0.3 meters in thickness is infrequently observed. Massive sandstone beds 2.0 to 10.0 cm in thickness are often interstratified with silt and clay shales. Commonly finer grained sediments succeed lithofacies B, resulting in thin fining-upward sequences, as illustrated in well Kirk 31 in the interval 244.4 to 243.4 meters (Figure 11). The following vertical sequence of bedforms occurs: 1) medium scale rippling (amplitudes from 1.0 to 3.0 cm); 2) irregular wavy laminae and thin beds; 3) thin, lenticular sandstone and shale beds. Minor burrowing is present in this lithofacies (Figure 12). The diversity of bedform and grain size suggests that lithofacies B was deposited under fluctuating energy conditions, dominantly in the lower flow regime.

Lithofacies C

Subequal amounts of fine sandstone and silty or clay rich shales constitute lithofacies C. Thickness of this facies ranges from 0.2 to 1.4 meters. The dominant bedding features are regular and irregular planar to wavy thin beds, laminations, and lenticular beds (Figure 13). Ripples with small amplitudes (1.0 to 2.5 cm) are infrequently observed. Distorted bedding, the result of soft sediment deformation, occurs in the silt and clay shales. Due to a lack of

Figure 11. Photograph showing fining upward sequences of Lithofacies B in slabbed core Kirk 31. Rippled intervals are followed upsection by increased amount of silt and clay detritus. Base of each sequence is indicated by an arrow.

Figure 12. Photograph showing vertical burrow structure within Lithofacies B. Slabbed core L-36-2.

Figure 11

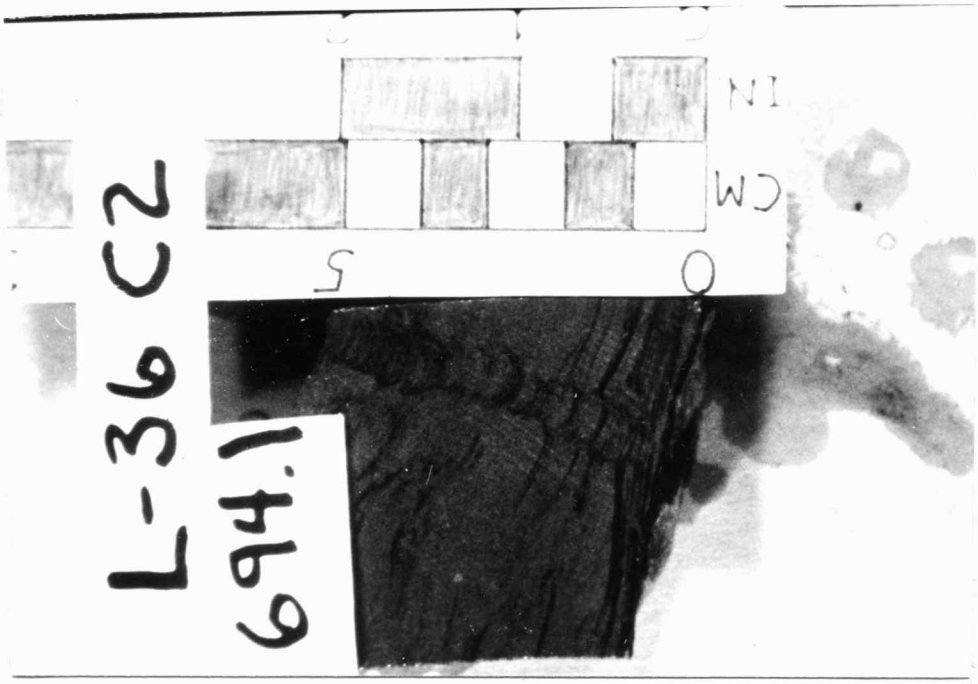

Figure 12

gradation, contacts between sandstone and shale units are sharp. Micaceous partings are abundant with macerated plant fragments observed on the bedding planes. Clay-shale horizons are often slightly mottled but horizontal burrows are rare. Pyrite is common, often replacing plant fragments. Lithofacies C was deposited predominantly in lower flow regime.

Lithofacies D

Siltstone and silty shale are the dominant lithologies of lithofacies D. The thickness of this lithofacies ranges from 0.06 to 3.7 meters. Irregular and regular planar to wavy laminations are the most abundant stratification types (Figure 14). These thin, alternating laminae of silt and clay shale, commonly ripple laminated, are common in the cores in the Bush City Shoestring trend. One instance of high angle cross-strata (25 degrees) of a set thickness of 0.2 meters was observed in core L-36-2 from 209.6 to 209.4 meters (687.6 to 687.0 ft) , and represents deposition under higher energy conditions than the laminated lithologies. Wood fragments and organic material are abundant on prevalent micaceous partings. Mottling and burrows are rare. Although sharp contacts are predominant within this lithofacies, it is overlain, underlain, and grades into lithofacies B, C, and E. Lithofacies D is finer grained and

Figure 13. Photograph showing wavy regular and irregular thin beds and laminations in Lithofacies C. Abundant cross-stratification suggests ripple migration. Slabbed core H-20.

Figure 14. Photograph showing planar, fining-upward sequence of regular and irregular laminations in Lithofacies D. Slabbed core Kirk 31.

Figure 13

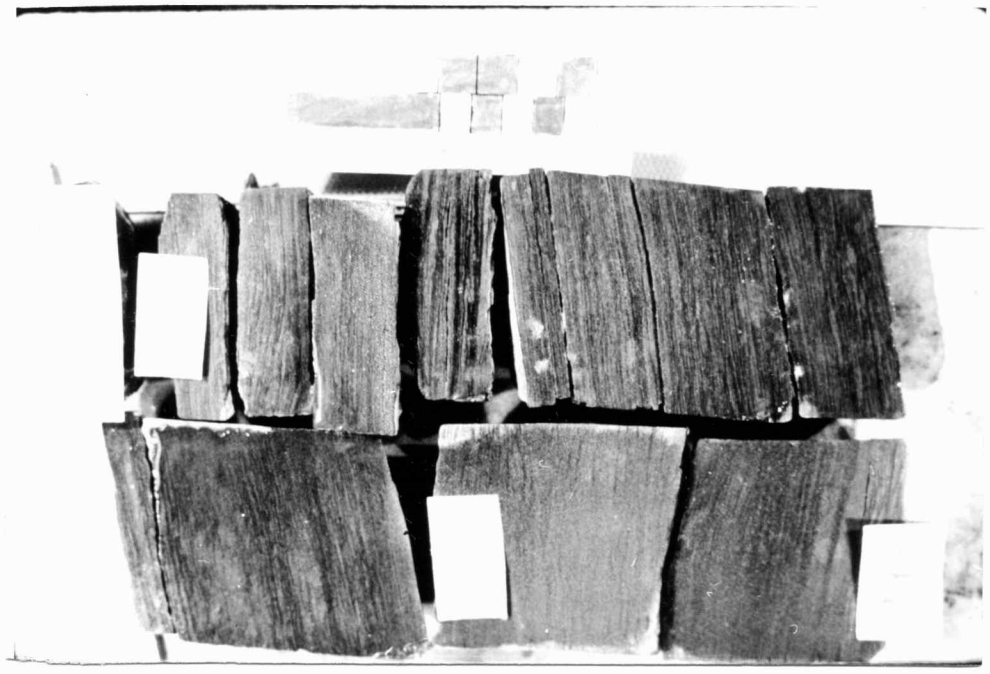

Figure 14

more commonly laminated than lithofacies C. The majority of lithofacies D is interpreted as having been deposited in the lower flow regime.

Lithofacies E

Lithofacies E consists mostly of mudrocks with small amounts of siltstone. Thickness of this lithofacies ranges from 0.1 to 1.6 meters. Clayey-shales with minor amounts of silt exhibit faint irregular and regular planar laminations (Figure 15). Soft-sediment deformation structures are common (Figure 16). The shales are commonly color mottled. Distinct burrows are rare. Basal contacts are normally sharp but minor gradation into silt-shales does occur. Plant matter, which includes possible carbonized leaf imprints, is present as are small amounts of pyrite. Intervals composed of dominantly clay and clayey shales represent suspension deposition under low-energy conditions.

Figure 15. Photograph showing clay-shale with minor silt laminations in Lithofacies E. Slabbed core Benjamin.

Figure 16. Photograph showing soft-sediment deformation in Lithofacies E. Slabbed core HB-C2.

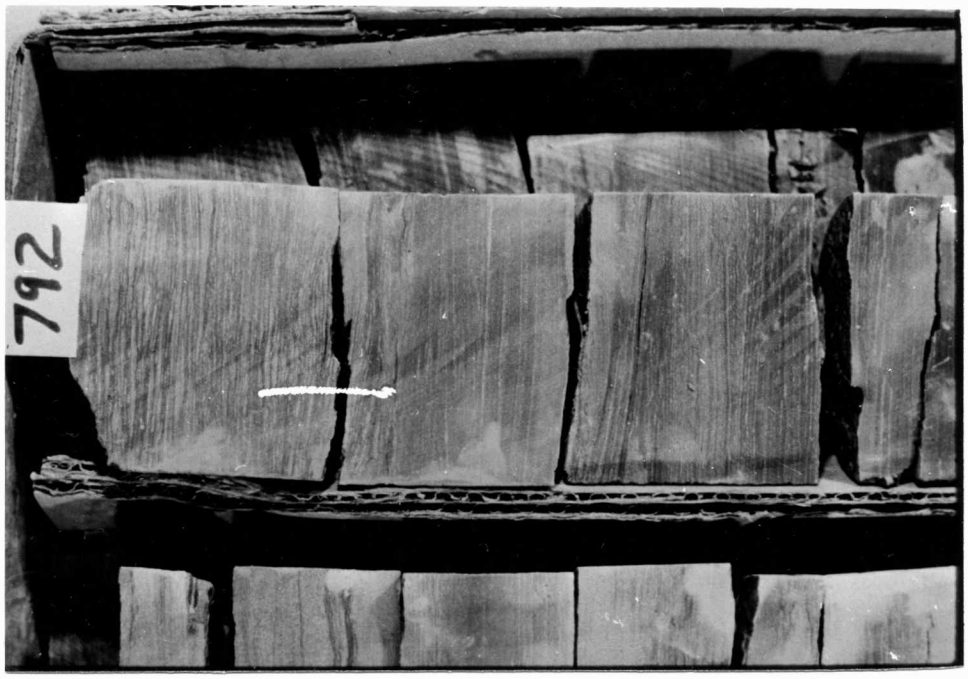

Figure 15

Figure 16

STRATIGRAPHY

Geophysical well-log curves are direct responses to variation in lithologic characteristics and interstitial fluid chemistry. Well-log signatures and core descriptions of lithology and structure were compared to obtain a clearer understanding of depositional and stratigraphic relationships of lithofacies A-E within the Bush City Shoestring and between it and the surrounding Centerville, Garnett, and Goodrich-Parker horizons of the Lagonda interval.

Well Log - Lithology Relationships

Wells Bailey-Lohrengel 16 and 18 are located in the Centerville oil and gas field (Figure 2). Production from these wells is from a sandstone of lithofacies A which is present from 21.3 to 9.1 meters below the Excello Shale. Gamma-ray log response for the interval is well defined and forms a half-bell shape (Figure 17). The sharp deflection of the gamma-ray log to the left at the base of the sandstone indicates a rapid change in lithology from the underlying strata, possibly caused by an erosional contact. A coal is present in this section at approximately 24.4

Figure 17. Bailey-Lohrengel 16 gamma-ray recording. Cored interval from 182.0 to 177.4 meters is expanded on right side of diagram. A single fining-upward sandstone-shale sequence follows the sharp basal contact at 182.0 meters. Gamma-ray response is uniform due to a lack of abundant interbeds of sandstone and shale. Abbreviations: Fg = Fine-grained; Ss = Sandstone; Ints = Interstratified; Sil Sh = Silty shale.

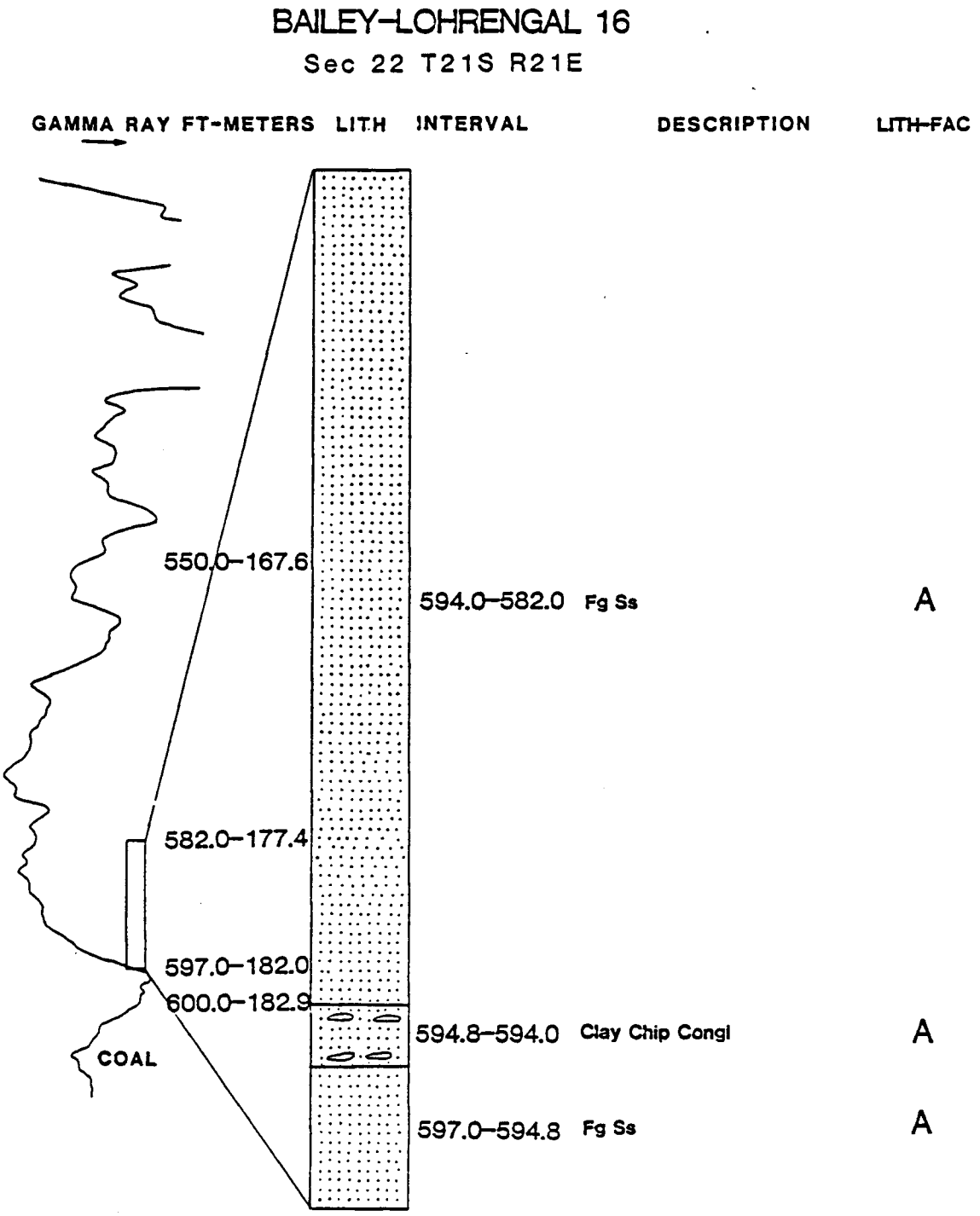
BAILEY-LOHRENGAL 16
Sec 22 T21S R21E
GAMMA RAY FT-METERS
LITH
INTERVAL
DESCRIPTION
LITH-FAC
550.0-167.6
582.0-177.4
597.0-182.0
600.0-182.9
COAL
594.0-582.0 Fg Ss
A
594.8-594.0 Clay Chip Congl
A
597.0-594.8 Fg Ss
A

Figure 17

meters below the Excello Shale. The basal 4.6 meters of the sandstone in BaileyLohrengel 16 was examined in slabbed core and thin section. Major sedimentologic features were previously described under lithofacies A. Grain size of the sandstone is very uniform with no shale or siltstone interbeds.

Well Kirk 31 is located in the Bush City trend (Figure 2). The gamma-ray log response of this well is variable because of the presence of interbeds and laminae of silt and clay shales (Figure 18). Core was obtained from this well in the interval 251.3 to 241.0 meters. Lithofacies A is limited to the basal 1.7 meters of the core, where the maximum sand deflection is recorded on the gamma-ray log (Figure 18). The remainder the core is dominated by lithofacies B, C, and D, which represent lower but variable hydraulic conditions. The upper 6.0 meters is a coarsening-upward interval as shown by the decreasing gamma-ray curve (Figure 18).

Using the available log-core relationships as a guide, the stratigraphic relationships within and surrounding the Bush City Shoestring were investigated. A majority of the wells in the Bush City trend were drilled before the introduction of modern logging tools, resulting in an unavoidable bias to the data base used in this study, which is from wells drilled primarily in the 1970's in known

Figure 18. Kirk 31 gamma-ray recording. Cored interval from 251.8 to 241.0 meters is expanded on right side of diagram. Irregular gamma-ray response reflects interstratified nature of the core. Shaley horizons (arrows) correlate well with an increase in gamma-ray radiation.

KIRK 31

Sec 16 T21S R20E

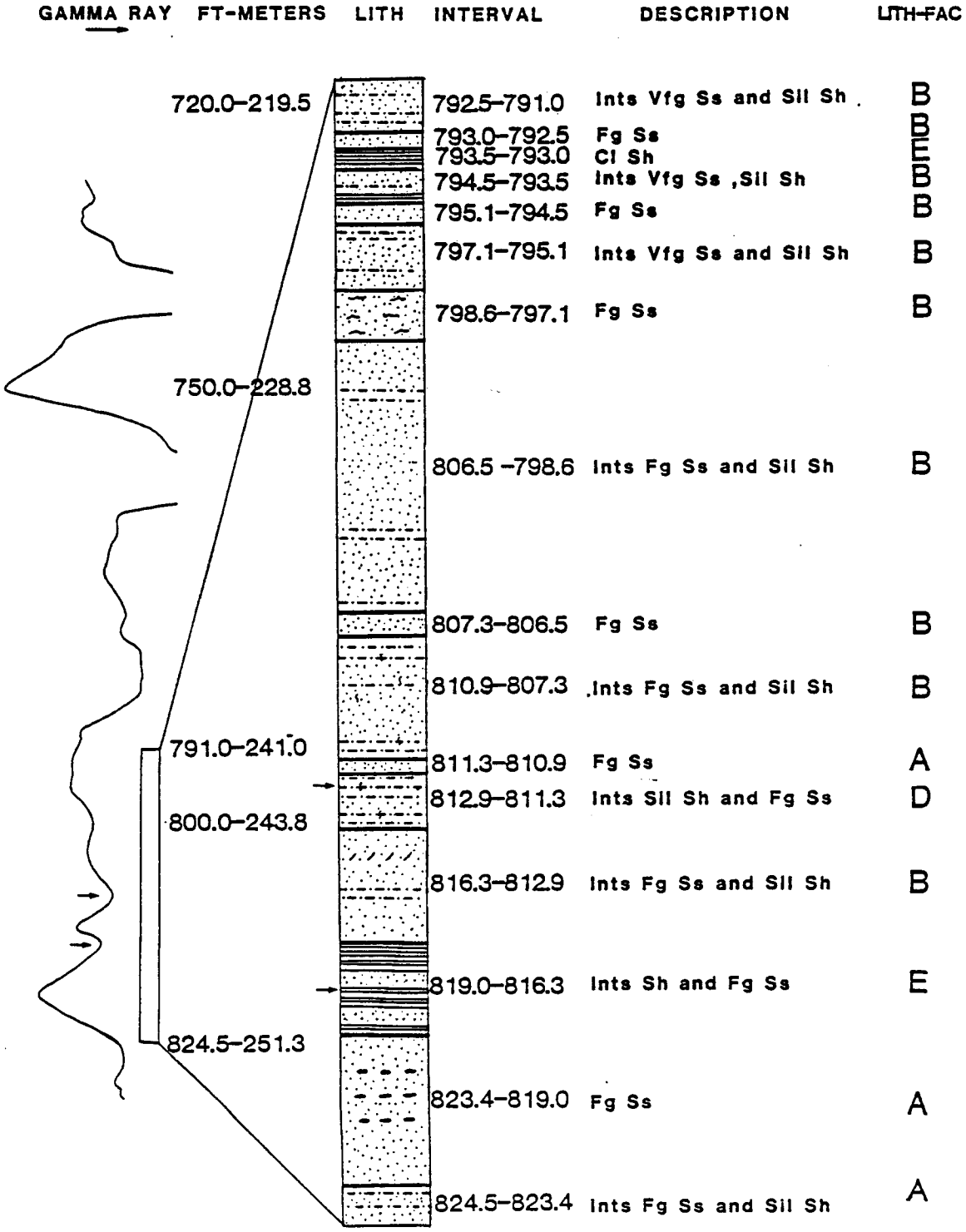

Figure 18

producing trends. Stratigraphic information for the subsurface outside of known sandstone trends is limited.

Charles (1927, 1941) delineated the Bush City "channel" using drillers logs and was able to map the main boundaries of the sandstone (Figure 19). A major goal of this study was to determine stratigraphic relations between this and other sandstone units using modern gamma-ray logs.

Three important parameters were considered when delineating sand-dominated intervals by the use of gamma-ray log signatures: 1) irregularity of the trace; 2) similarities of coarsening- or fining-upward sequences; 3) distance between wells. The irregularity or "serrated" nature of the gamma-ray log response is due to the presense of silt and clay shale interbeds. A large degree of irregular deflection in a sand-dominated interval was considered to limit the lateral continuity of that interval. Similarities, in both well-log character and stratigraphic position of the sandstone horizons, were also noted. Where nearly identical well log signatures are observed, lateral continuity of lithologies between the wells is suggested. Distance between well-log locations is taken into consideration because of the lateral variation in lithology that is possible, and without tight well log control, miscorrelation can easily occur.

Figure 19. Map showing delineation of Bush City Shoestring. Cross-sections A-A' to D-D' show the variation in thickness and overall geometry of the sandstone body. (After Charles, 1941).

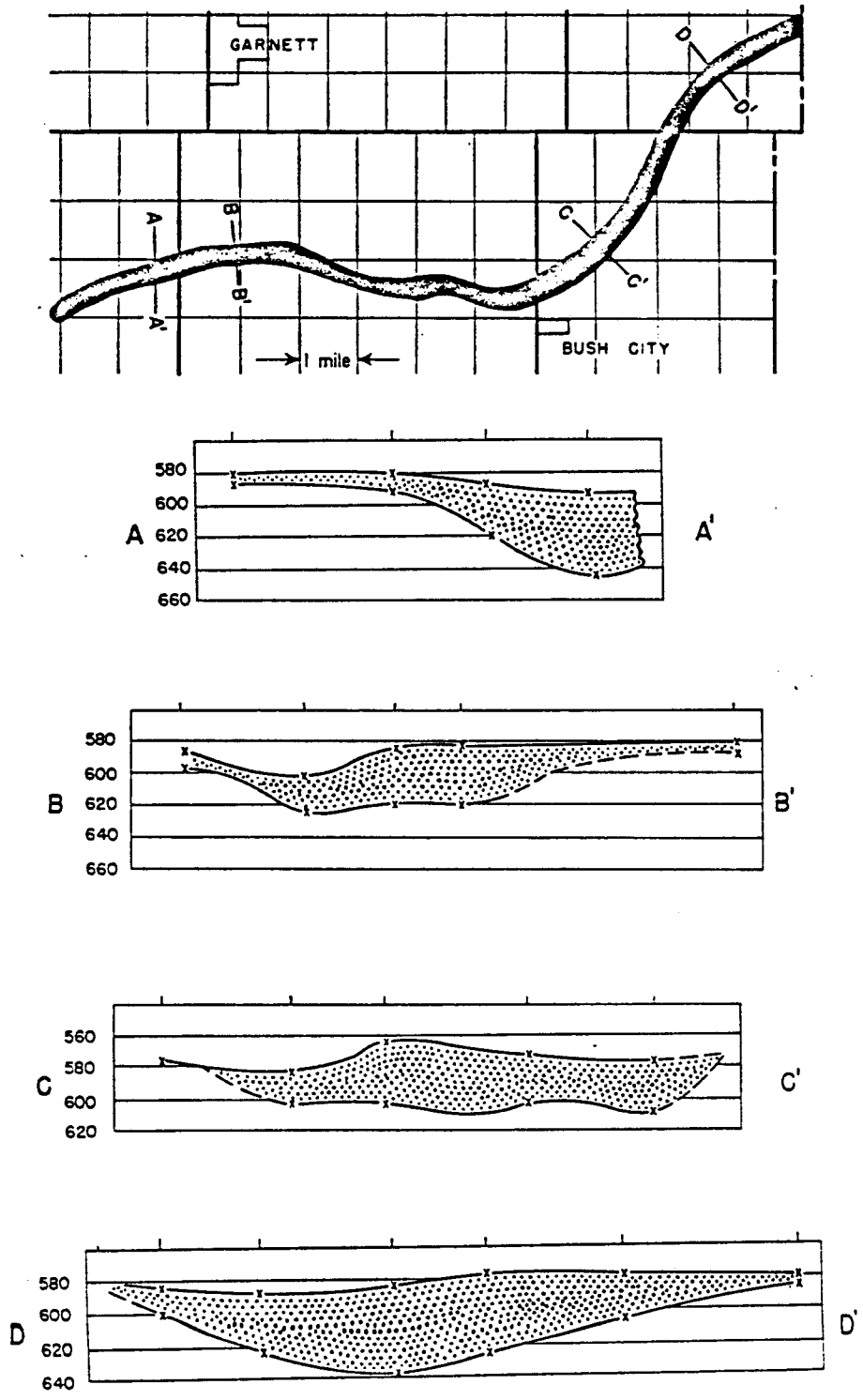
GARNETT
BUSH CITY
1 mile
A
A'
B
B'
C
C'
D
D'
580
600
620
640
660
560
580
600
620
640

Figure 19

Figure 20. Depth horizons established for the Lagonda interval. Position of sandstone-dominated intervals within the Lagonda is related to these horizons.

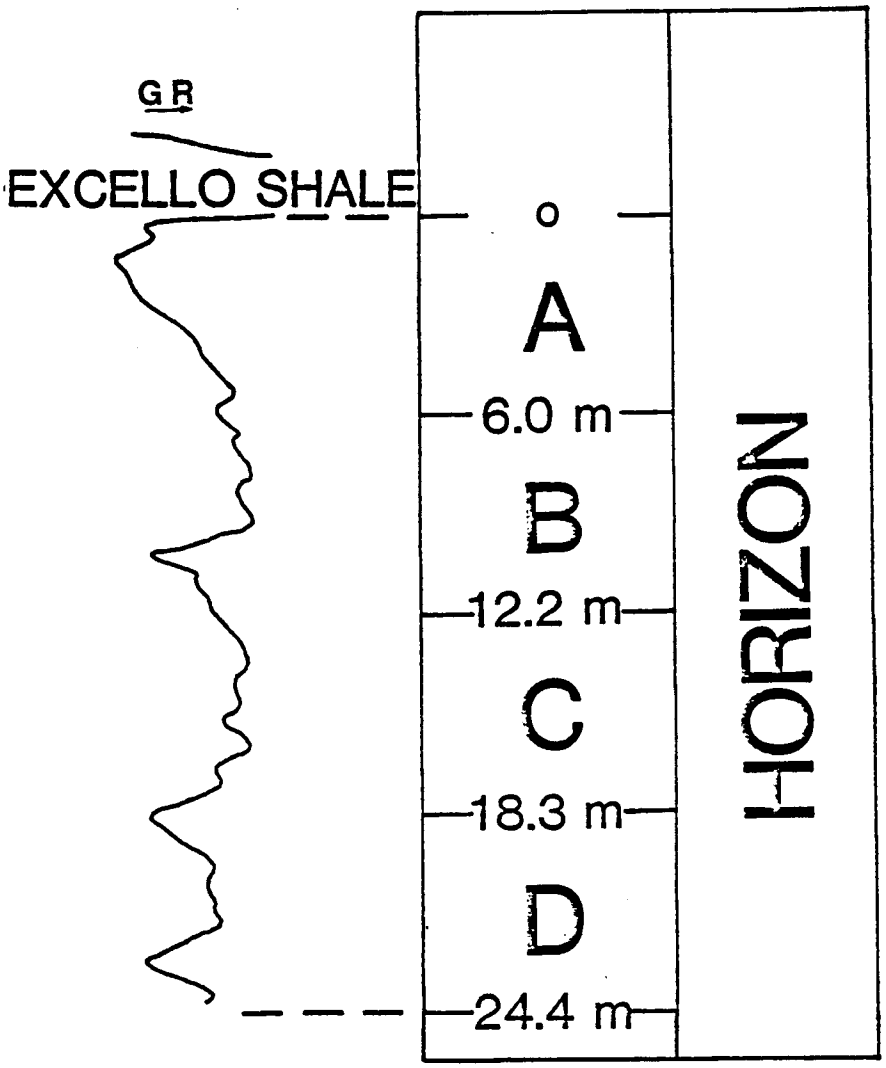

Figure 20

The Lagonda interval was divided into four horizons, A through D, on the basis of depth in meters of that interval below the Excello Shale (Figure 20). In the stratigraphic section that follows, the depths of sandstone-dominated horizons will be identified by reference to these horizons.

Stratigraphy of Bush City Trend

The Bush City trend is thought to be an extension of the Goodrich-Parker shoestring of western Linn County, Kansas (Figure 2). A SW to NE cross section (A-A') was constructed (Figure 21). The lack of well control in Sec. 28, T. 21 S., R. 21 E. hindered correlation. In wells 3 and 4, correlation of a basal fining-upward sandstone in horizon C and D is possible. The sandstone is absent in wells 1 and 2. Two thinner sandstones separated by a shale bed are present in horizons A and B in all the wells with the exception of well 3. The sandstone in horizon A coarsens upward in these wells. The sandstone in horizon B coarsens upward and then fines irregularly in its upper portion (Figure 21). These correlations do not confirm the connection between the Bush City and Goodrich-Parker sandstones. However, the inconsistent nature of the "squirrel" sand, similar depositional strike of the two sandstones, similar upper sandstones, and a lack of tight well control do not rule out the possibility that the two sandstones are connected.

Figure 21. Cross-section A-A' showing stratigraphic relationship between Bush City and Goodrich-Parker trends. Lack of tight well log control prevents positive correlation between these two shoestrings that are strongly believed by local drillers to be essentially one sandstone trend.

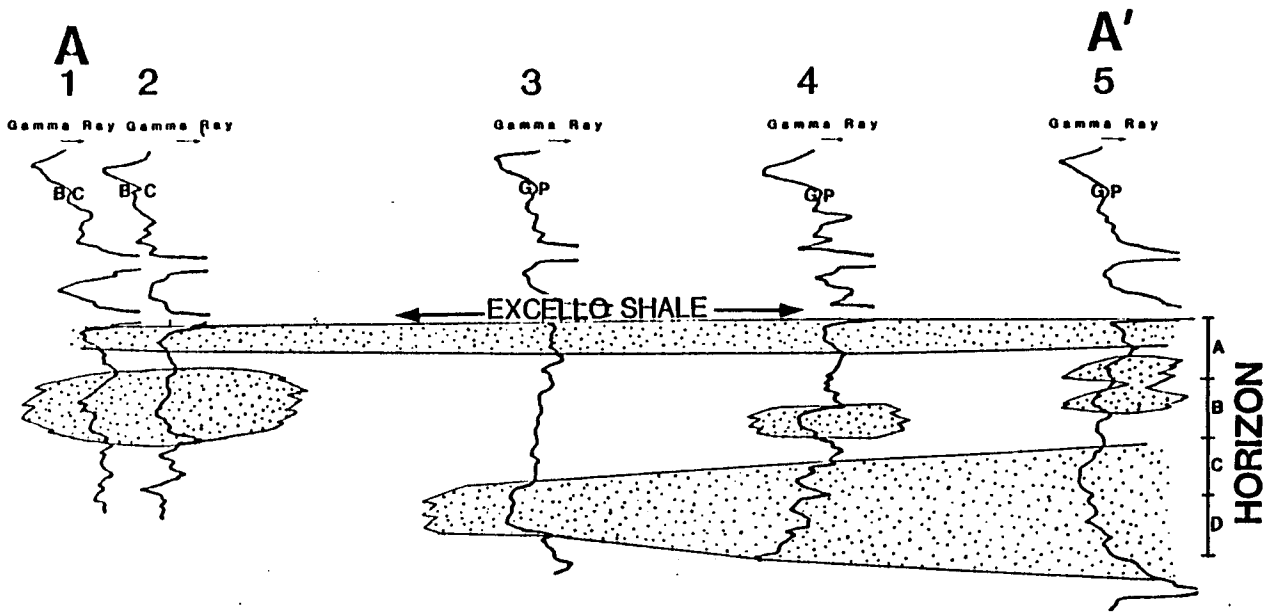

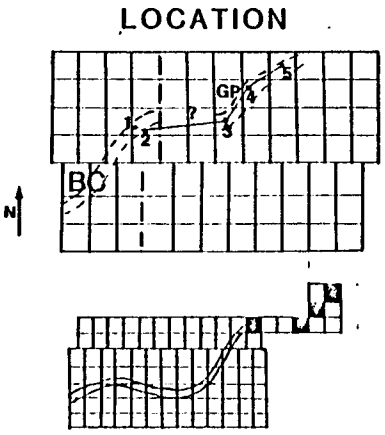

WELL NAMES

1 M. Parks No. 4
2 Craig No. 2
3 EM Byerley B99
4 HB Cox F3
5 Fuerborn No. 1

SCALE

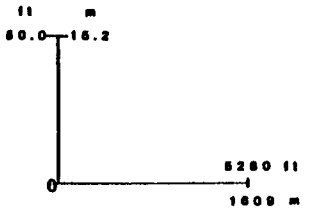

SEC 16-20-30 T20S R22E
SEC 27 T20S R21E

Figure 21

A portion of the Centerville oil and gas field is located south of the Bush City Shoestring (Figure 2). The main oil and gas production from this field is a "Bartlesville shoestring sand" (Jewett, 1954). Recent drilling in this field by a local operator penetrated the Lagonda interval. Drilling has established that this trend continues northward to the SE quarter of Sec. 4, T. 21 S., R. 21 E. Lack of control points in Secs. 15 and 10, T. 21 S., R. 21 E. prevented unequivocal delineation of the stratigraphic relationships between this channel and the Bush City Shoestring.

To evaluate the eastern portion of the Bush City trend, B-B' was constructed (Figure 22). Two important stratigraphic relationships are shown on this cross-section. First, the main body of the Centerville is not linked to the Bush City in the NE quarter of Sec. 4, T. 21 S., R. 21 E. Second, the cross-section displays three thin sandstones occurring in wells 6, 7, 8, and 13 in horizons B and C. (Figure 22). These sandstones coarsen upward in a similar manner and appear to be very continuous in this area. The main channel of the Bush City lies between wells 6 and 7, suggesting the Bush City sandstone has incised laterally continuous sandstone units. Although well-logs between wells 6 and 7 are not available, other well-log signatures from wells penetrating the main sandstone body of the field

Figure 22. Cross-section B-B' showing stratigraphic relationship between interchannel strata and Bush City-Centerville sandstones. Incisement of previously deposited sediments by channels is suggested.

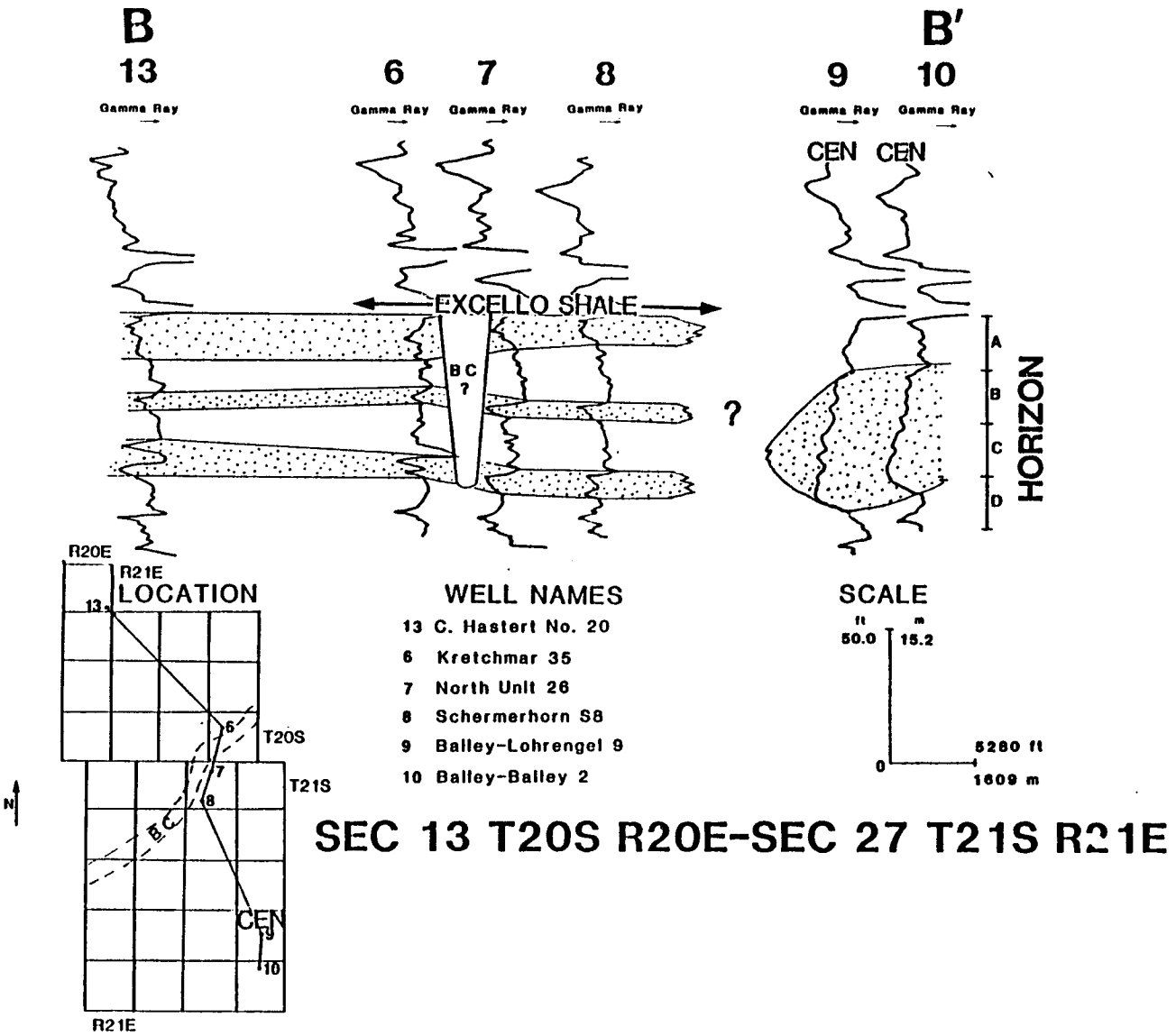

SEC 13 T20S R20E-SEC 27 T21S R21E

Figure 22

are dissimilar and do not display the three sandstone horizons. The genetic implications of this observation are discussed in the depositional environment section.

The continuity of four thin sandstone horizons and the persistence of thin coal is demonstrated in C-C' constructed across the southern half of Sec. 13, T. 20 S., R. 20 E. (Figure 23). The thin sandstones are also present in Sec. 4, T. 21 S., R. 20 E. (D-D')(Figure 24). The stratigraphic continuity of the thin sandstones in both of these areas support the correlations illustrated in Figure 22.

A NW-SE cross-section (E-E') oblique to the Bush City trend and extending to the Garnett field, shows several distinct sandstone bodies (Figure 25). In well 24, a fining-upward sandstone is present in horizons A and B. Laterally this sandstone becomes interstratified with finer grained sediments (Lithofacies C-E) of well 23. The sandstone dominated intervals in wells 21 and 22 have abundant shale interbeds (indicated by the serrated nature of the gamma-ray logs) and may not be physically connected to those of well 23 (as illustrated in Figure 25). In well 20 a basal sandstone in the C horizon is overlain by irregular thin beds of sandstone and shale (Lithofacies B-E). Without better well control between wells 20 and 21, it is difficult to interpret stratigraphic relationships between the two fields but, it is apparent that similar appearing sandstones occur in the two areas.

Figure 23. Cross-section C-C' located north of Bush City Shoestring showing Lagonda sandstones in Sec. 13, T20S, R20E. Nearly identical gamma-ray patterns and stratigraphic positions of the sandstone horizons suggest four sandstones and one coal that are laterally continuous.

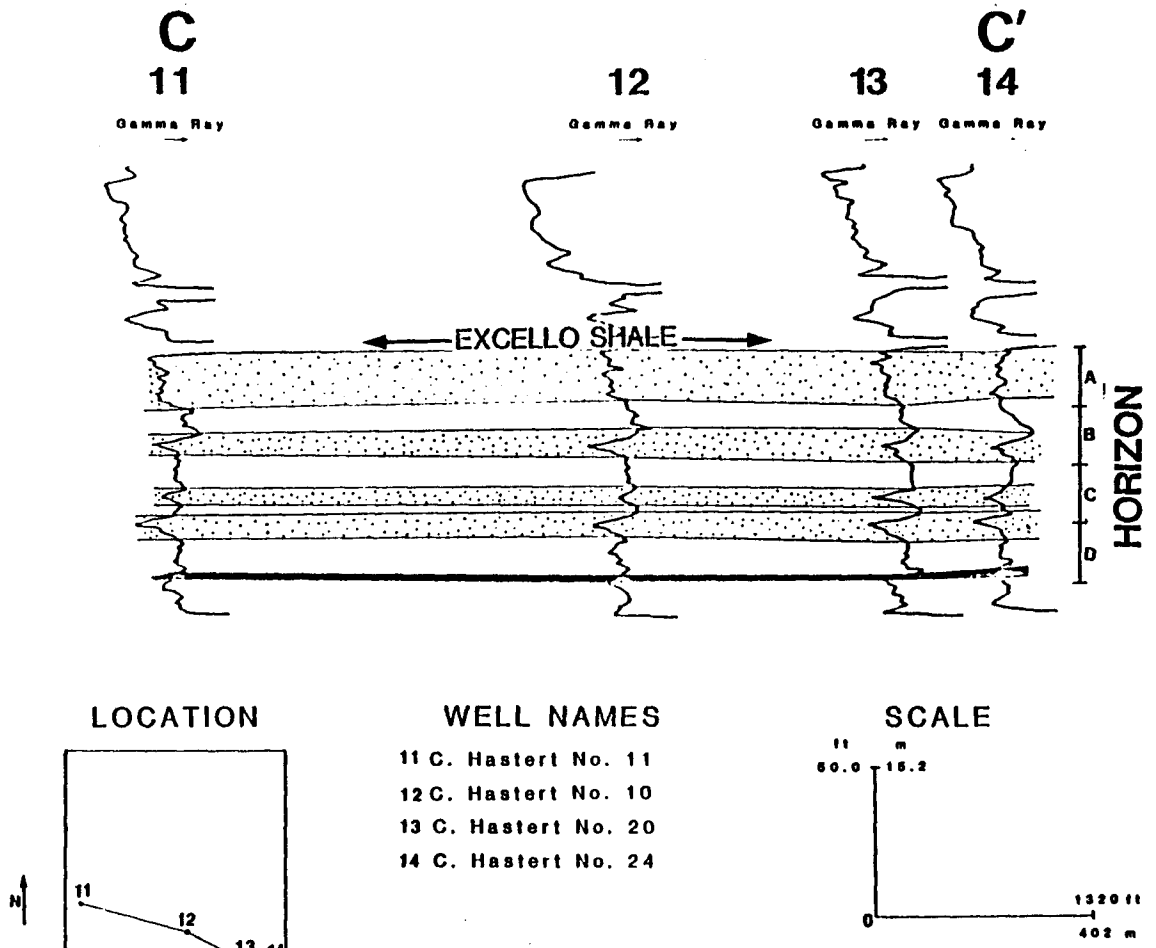
C
C'
11
12
13
14
Gamma Ray
Gamma Ray
Gamma Ray
Gamma Ray
EXCELLO SHALE
A
B
C
D
HORIZON
LOCATION
N
11
12
13
14
WELL NAMES
11 C. Hastert No. 11
12 C. Hastert No. 10
13 C. Hastert No. 20
14 C. Hastert No. 24
SCALE
ft
m
50.0
15.2
0
1320 ft
402 m
SEC 13 T20S R20E

Figure 23

Figure 24. Cross-section D-D' south of Bush City Shoestring showing Lagonda sandstones in Sec. 4, T21S, R20E. Stratigraphic positions of sandstones and coal are similar to those described in Sec. 13, T20S, R20E (Figure 23).

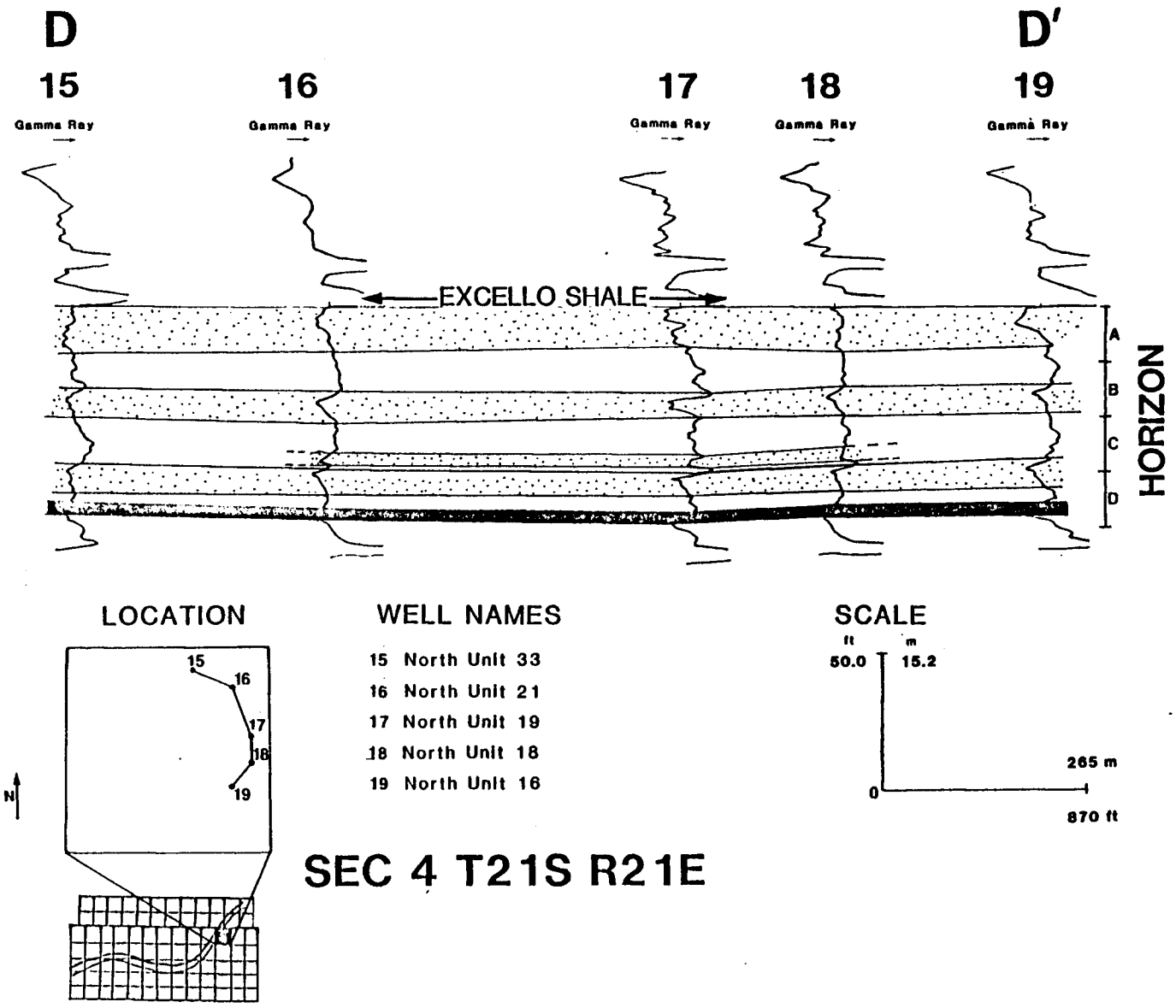
D
D'
15
16
17
18
19
Gamma Ray
EXCELLO SHALE
A
B
C
D
HORIZON
LOCATION
WELL NAMES
15 North Unit 33
16 North Unit 21
17 North Unit 19
18 North Unit 18
19 North Unit 16
SCALE
ft
m
50.0
15.2
265 m
0
870 ft
N
SEC 4 T21S R21E

Figure 24

Figure 25. Cross-section E-E' showing stratigraphic relationship between Bush City (Wells 21 to 24) and Garnett (Well 20) sandstone trends. Similar horizons of sandstone occurrence in two distinct shoestring sandstones.

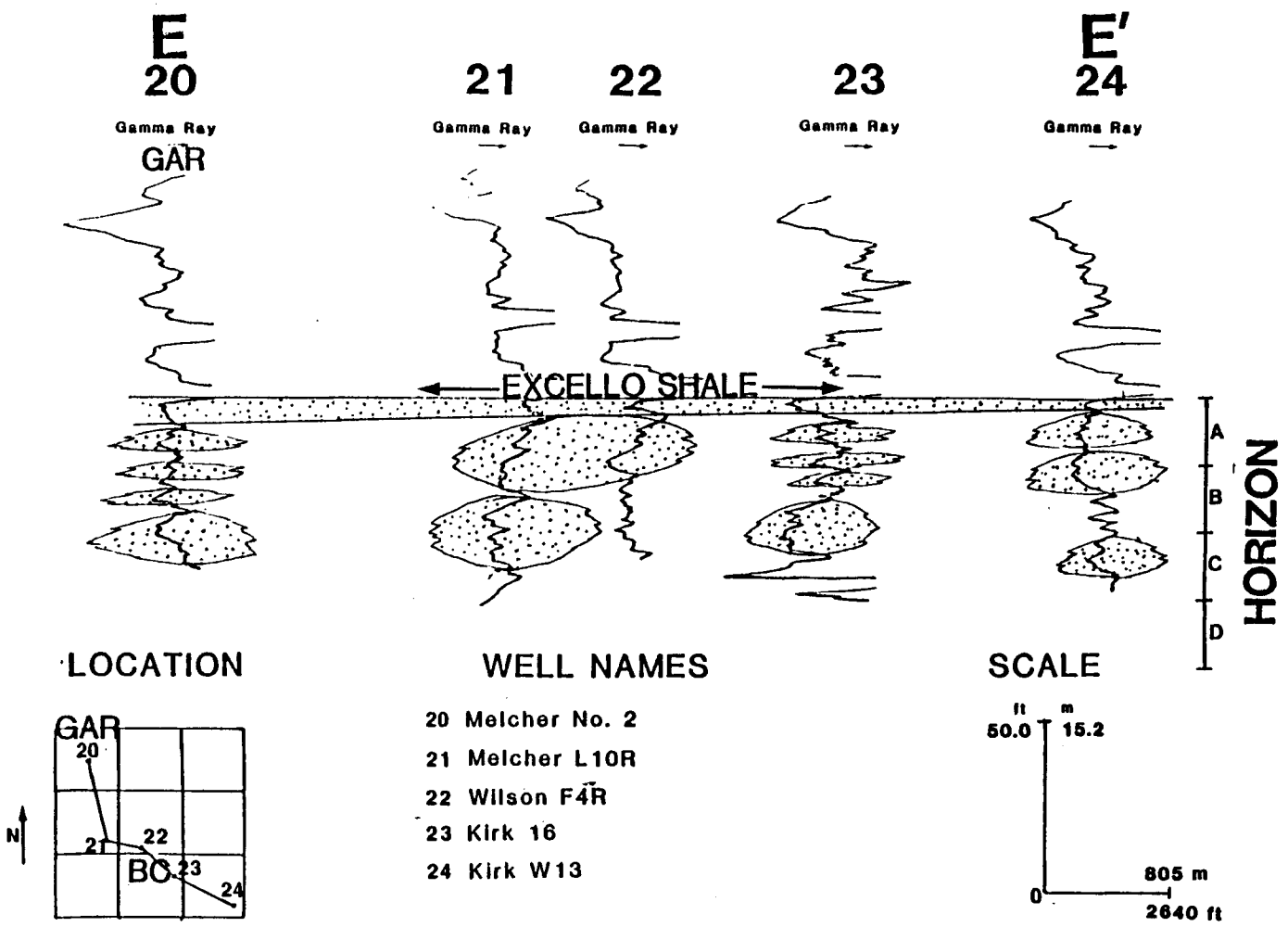

SEC 6 T21S R20E-SEC 16 T21S R20E

Figure 25

A more detailed picture of the geometry of the sand lenses within the Bush City Shoestring can be observed by looking at cross-sections constructed in Sec. 16, T. 21 S., R. 20 E. The east-west (F-F') (Figure 26) and north-south (G-G') (Figure 27) cross-sections display the apparent discontinuity of the sandstone bodies. A thick sandstone occurs in horizon C and the lower part of B. Examples are the basal sandstones of well 23 (Figure 26), 28 and 29 (Figure 27). Most sandstones fine upward in a irregular manner, as indicated by the very serrate gamma-ray log response, suggesting many thin interbeds of Lithofacies B-E. A second sandstone is present in the upper B and lower A horizons. This trend can be correlated between wells 25, 26, and 27 for approximately 790.0 meters (Figure 26). The log patterns of this sandstone are irregular but suggest a thickening of the sand to the west in well 25. A third sandstone occurs in horizon A. The uniform gamma-ray pattern suggests this sandstone can be correlated across the entire length of Figure 26 and in three of the four wells in Figure 27. Decreasing deflection of the gamma-ray logs up-section in horizon A of wells 23, 25, and 26 suggest a coarsening-upward sequence (Figure 26). This sandstone appears to be the most consistent of the three sandstone dominated intervals. In both cross-sections in Sec. 16, the interbedded nature of the sandstone and shale units is again

Figure 26. Cross-section F-F' showing irregular occurrence of sandstone dominated intervals in Sec. 16, T21S, R20E. Lateral discontinuity of the sandstones along depositional strike is suggested by serrate gamma-ray responses.

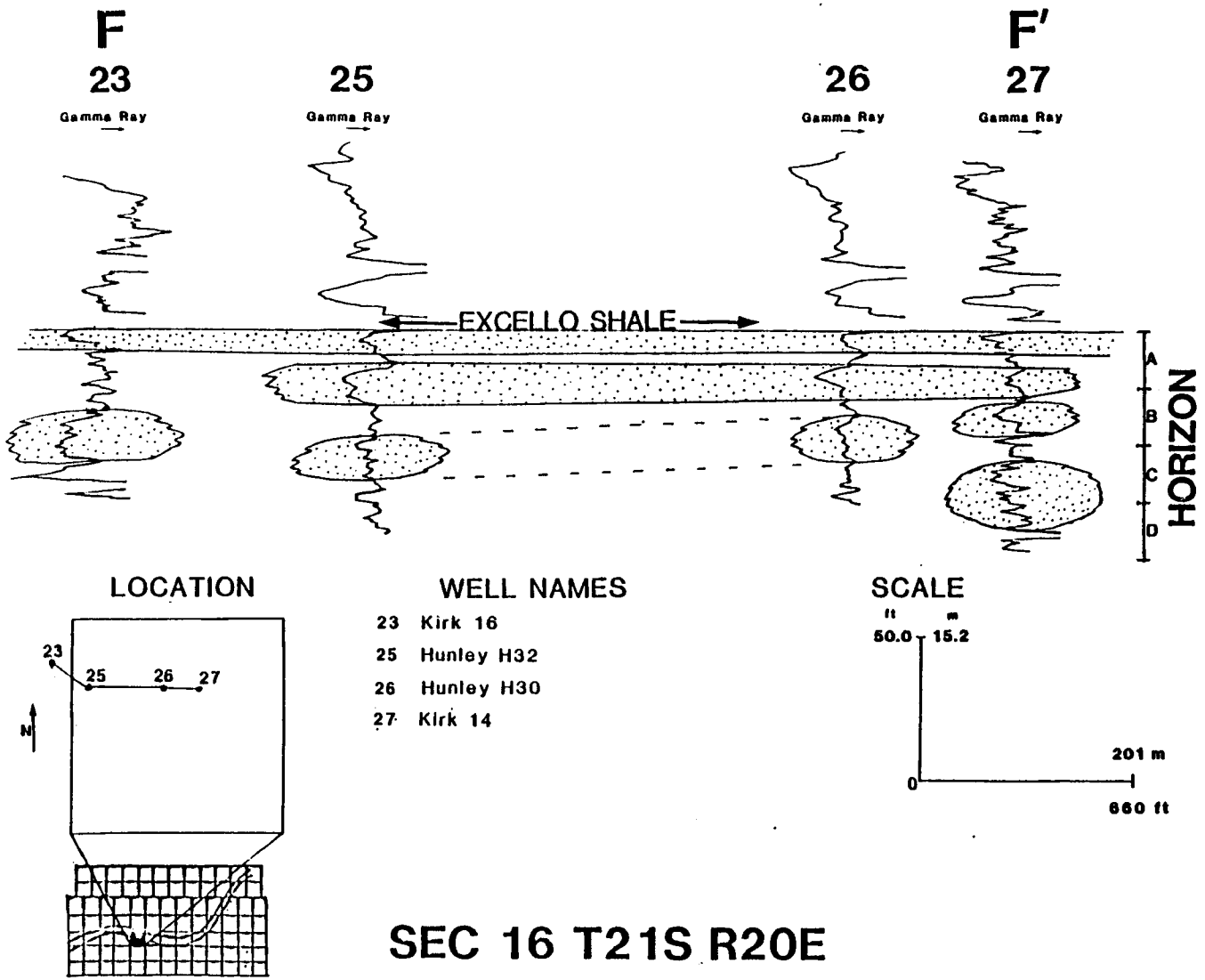
F
F'
23
25
26
27
Gamma Ray
Gamma Ray
Gamma Ray
Gamma Ray
EXCELLO SHALE
A
B
C
D
HORIZON
LOCATION
23
25
26
27
N
WELL NAMES
23 Kirk 16
25 Hunley H32
26 Hunley H30
27 Kirk 14
SCALE
ft
m
50.0
15.2
201 m
0
660 ft
SEC 16 T21S R20E

Figure 26

Figure 27. Cross-section G-G' constructed oblique to depositional strike in Sec. 16, T21S, R20E. Lower sandstone dominated horizons in wells 28 and 29 may represent basal point-bar sediments. Upsection irregular and thin interstratified sandstone-shale strata are suggestive of upper point-bar sedimentation.

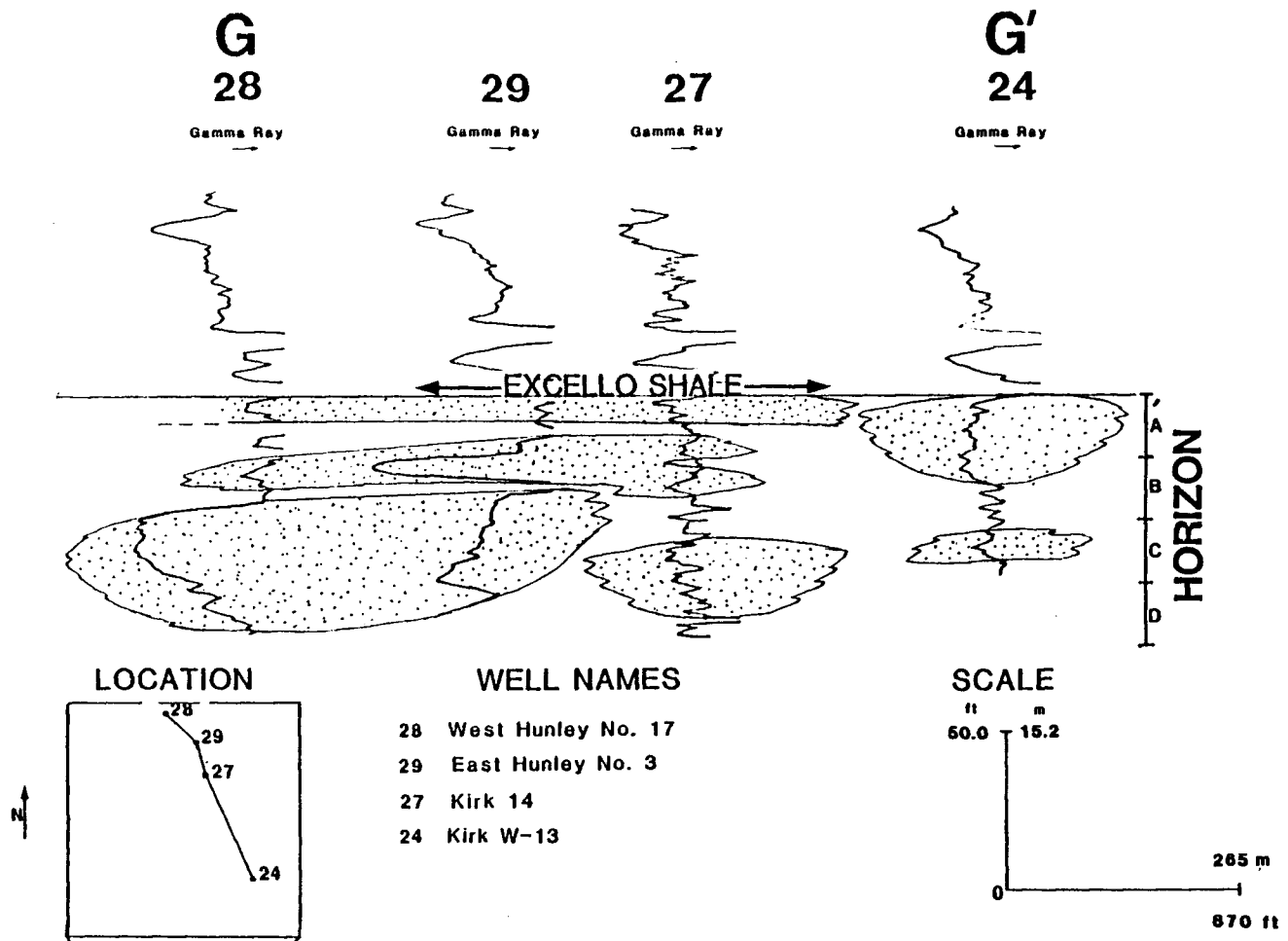

SEC 16 T21S R20E

Figure 27

characterized by the serrated nature of the gamma-ray deflections.

Sandstone occurrence and geometries in Sec. 15, T. 21 S., R. 20 E. (Figures 28 and 29) are very similar to those described in Sec. 16. A fining-upward sandstone body occurs at about the same depth in horizons C and B in wells 31, 32 (Figure 28) and well 37 (Figure 29).

In Figure 28 a stratigraphic relationship similar to that in Figure 22 is suggested. The thin but consistent sandstone horizons, described in Sec. 13, T. 21 S., R. 21 E. and Sec. 4, T. 21 S., R. 21 E., are present in well 34 which is located at the outer margin of the Bush City field. Localized sandstone bodies are again present in horizons B and C in wells 30 to 33 and have apparently incised previously deposited sediments.

The uppermost sandstones are present in wells 30 and 31 (Figure 28). These sandstones are fining-upward in nature in contrast to the upper sandstones in wells 32 and 33, which coarsen upward (Figure 28). These differences in sandstones in close proximity at the same horizon will be discussed in the depositional environment section.

At the extreme northeast end of the Bush City trend the middle and upper sandstones are present. The SW-NE cross-section (J-J') illustrates the inconsistancy along depositional strike for the sandstone that occurs in the

Figure 28. Cross-section H-H' showing stratigraphic relationship between Bush City channel and laterally adjacent strata in Sec. 15, T20S, R20E. Sandstone dominated interval with a convex-downward basal contact is present in the B and C horizons.

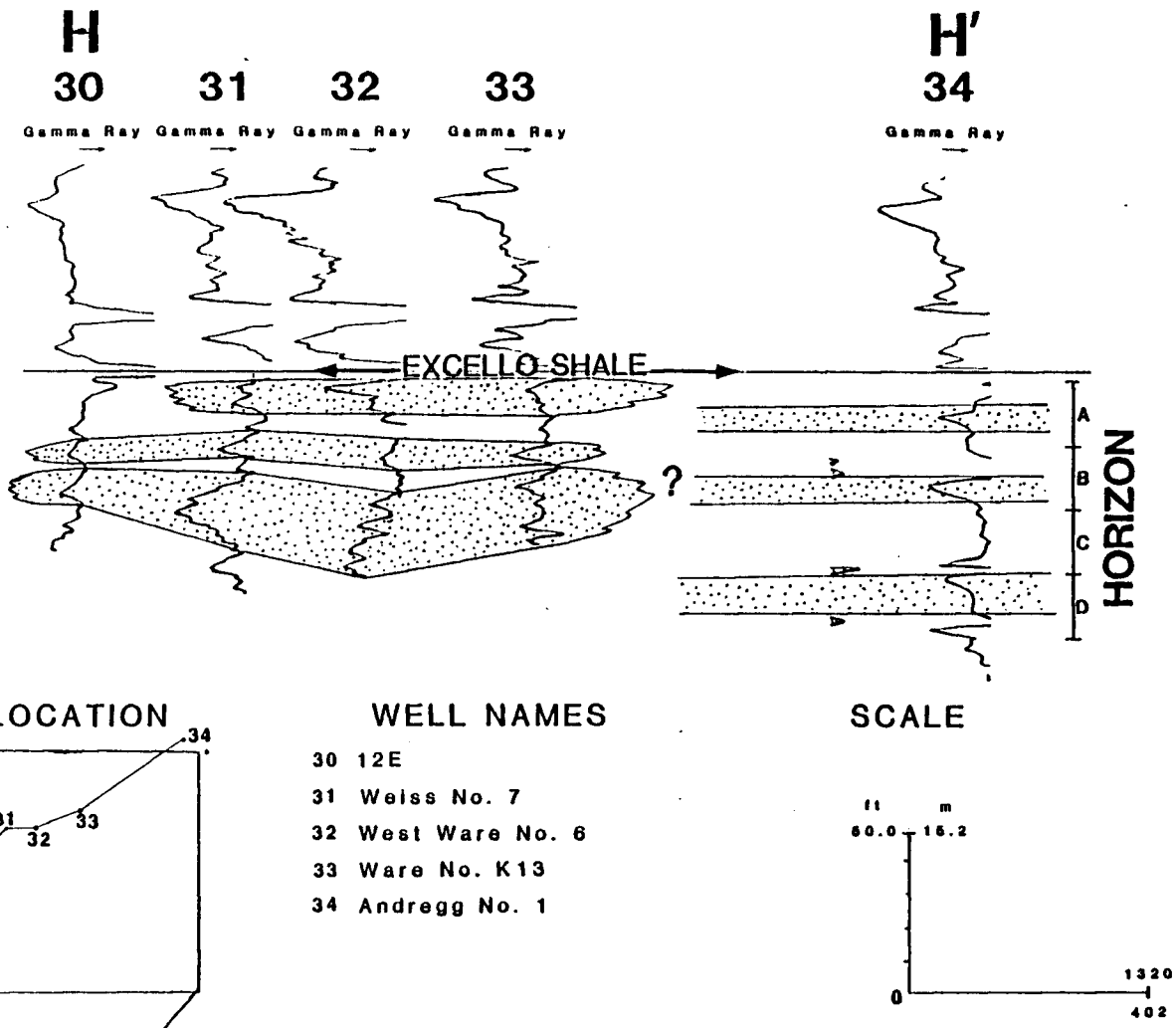
H
30
31
32
33
Gamma Ray
Gamma Ray
Gamma Ray
Gamma Ray
H'
34
Gamma Ray
EXCELLO SHALE
?
A
B
C
D
HORIZON
LOCATION
34
31
32
33
30
N
WELL NAMES
30 12E
31 Weiss No. 7
32 West Ware No. 6
33 Ware No. K13
34 Andregg No. 1
SCALE
ft
m
60.0
15.2
0
1320 ft
402 m
SEC 15 T21S R20E

Figure 28

Figure 29. Cross-section I-I' showing Lagonda stratigraphic relationships in Sec. 15, T20S, R20E. Thick basal sandstones present in wells 32, 36, and 37 are followed upsection by fine-grained sediments, suggesting a point-bar depositional environment.

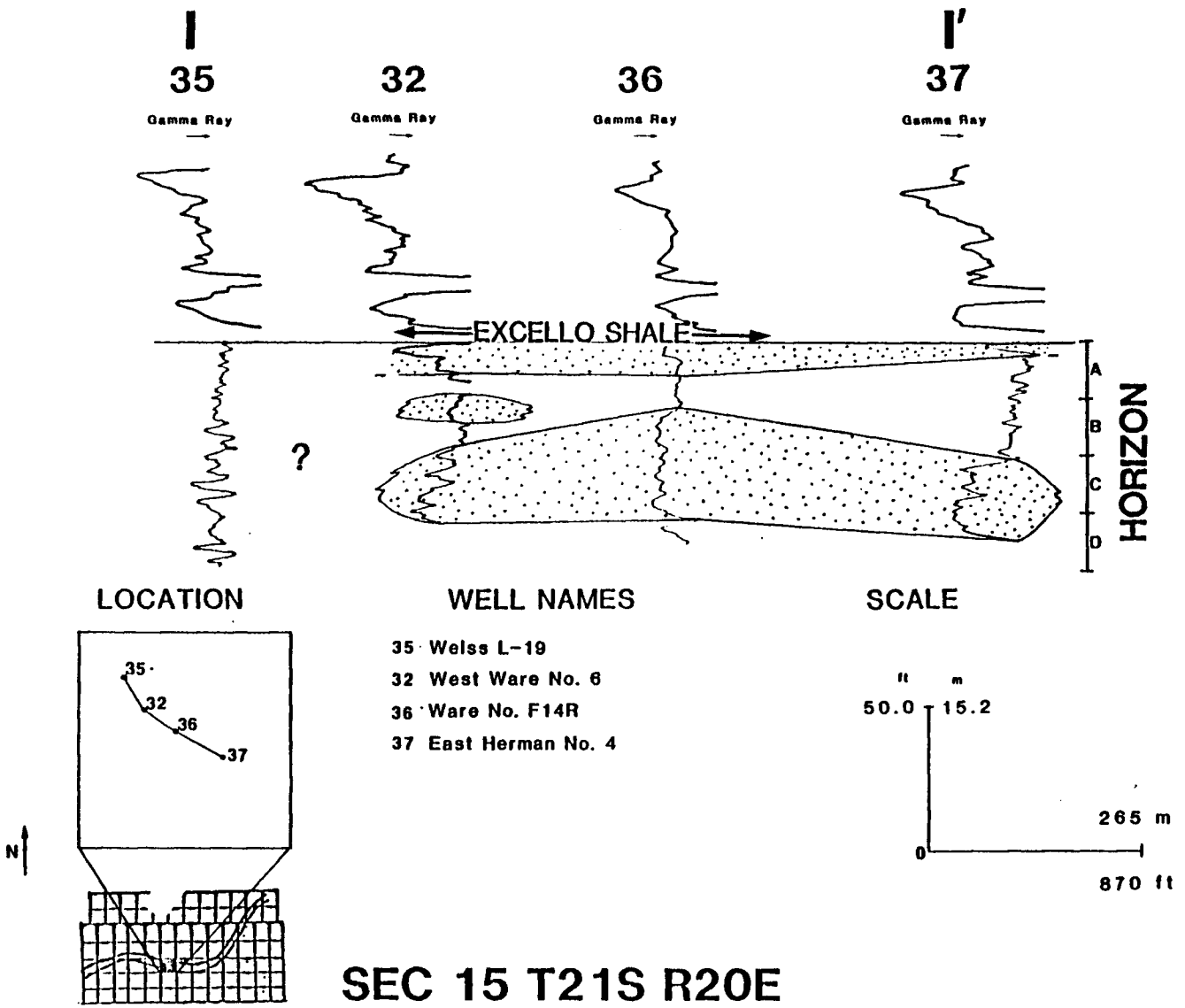
I
35
Gamma Ray
32
Gamma Ray
36
Gamma Ray
I'
37
Gamma Ray
EXCELLO SHALE
?
A
B
C
D
HORIZON
LOCATION
35
32
36
37
N
WELL NAMES
35 Welss L-19
32 West Ware No. 6
36 Ware No. F14R
37 East Herman No. 4
SCALE
ft
m
50.0
15.2
0
265 m
870 ft
SEC 15 T21S R20E

Figure 29

upper C, B and lower A horizons (Figure 30). The sandstone varies in thickness from approximately 6.0 meters (well 43) to 1.2 meters (well 42) (Figure 30). The middle sandstone can be easily correlated in cross-section K-K' (Figure 31). Basal contacts of this sandstone vary from abrupt as in wells 38, 46, and 47 (Figure 31) to more gradational as in wells 41 and 42 (Figure 30). As in the cross-sections discussed earlier, the upper sandstone is the most consistent sandstone in the trend.

The Colony-Welda Field is located southwest of the Bush City trend (Figure 2). L-L' was constructed to compare the characteristics of the two sandstone trends observed in well-logs (Figure 32). A lower basal sandstone occurs in horizon C as in the Bush City trend. The sandstone in horizon B is poorly defined in wells 50 and 51 in the center of the Welda field.

Summary

Gamma-ray well-log patterns of the Lagonda sandstones within the study area suggest four stratigraphic relationships: 1) The most distinct fining-upward sandstones are present in the D, C and lower B horizons. These sandstones are most clearly developed in the Centerville trend. 2) Two consistent sandstone horizons are present in the upper Lagonda, a highly variable sandstone in the lower

Figure 30. Cross-section J-J' constructed SW to NE across Sec. 27., T20S, R21E. Lens- like nature and pinch out of lower sandstones (Horizons C and B) are suggested by varying well log patterns and stratigraphic positions of the sand bodies. Lateral continuity of the upper sandstone is suggested by consistant gamma-ray response.

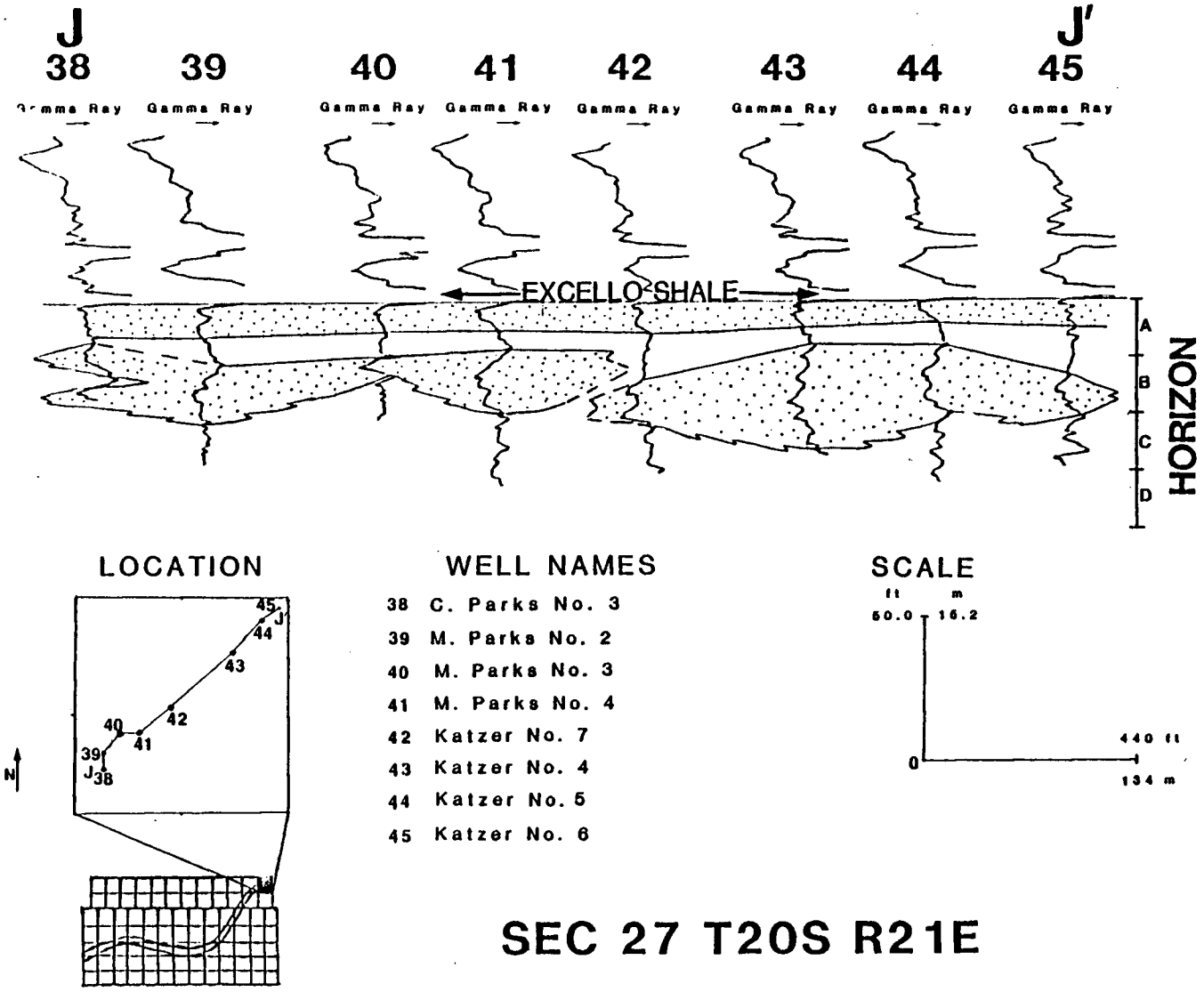
J
J'
38
39
40
41
42
43
44
45
Gamma Ray
EXCELLO SHALE
A
B
C
D
HORIZON
LOCATION
N
WELL NAMES
38 C. Parks No. 3
39 M. Parks No. 2
40 M. Parks No. 3
41 M. Parks No. 4
42 Katzer No. 7
43 Katzer No. 4
44 Katzer No. 5
45 Katzer No. 6
SCALE
ft
m
50.0
15.2
0
440 ft
134 m
SEC 27 T20S R21E

Figure 30

Figure 31. Cross-section K-K' constructed parallel to depositional strike of Bush City Shoestring in Sec. 27, T20S, R21E. Sandstones in A and B horizons are continuous across the area.

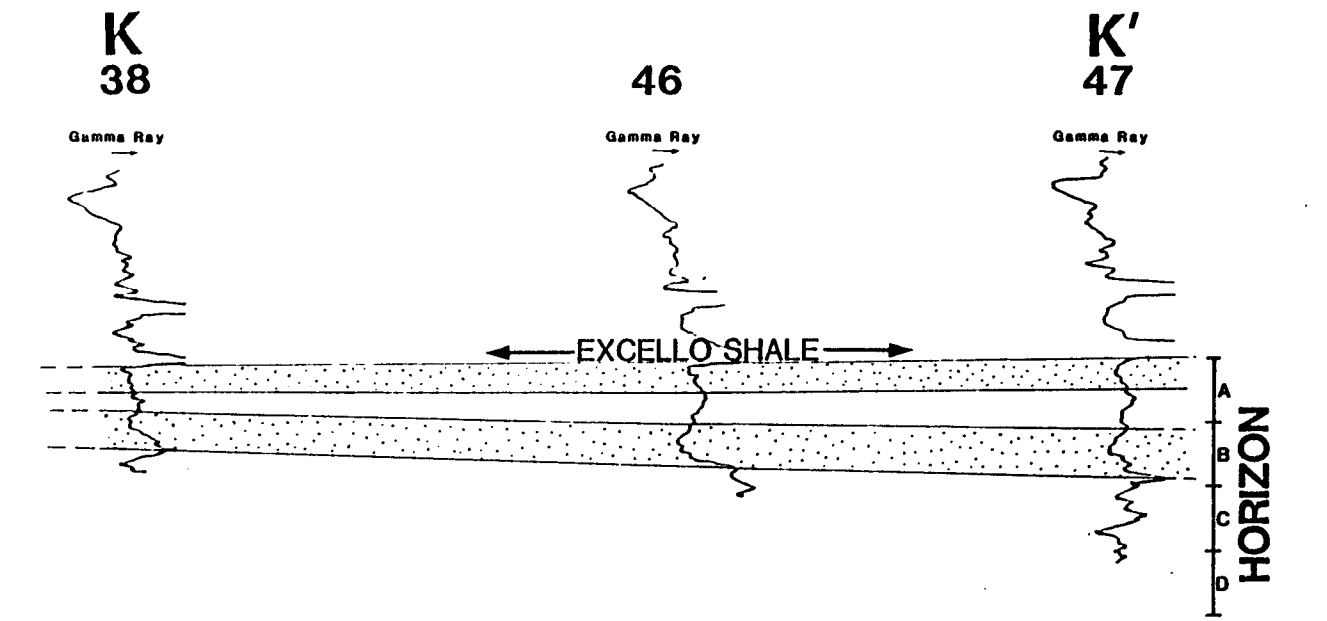

LOCATION

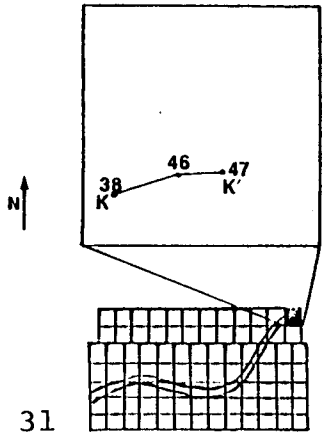

WELL NAMES

38 C. Parks No. 3

46 C. Park No. 3

47 Craig No. 2

SCALE

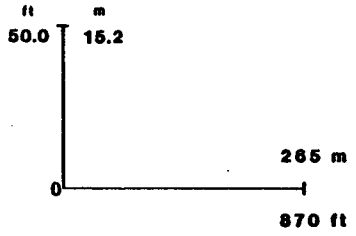

SEC 27 T20S R21E

Figure 31

Figure 32. Cross-section L-L' showing Bush City and Colony-Welda Lagonda sandstones. Similar occurring sandstone dominated horizons are illustrated.

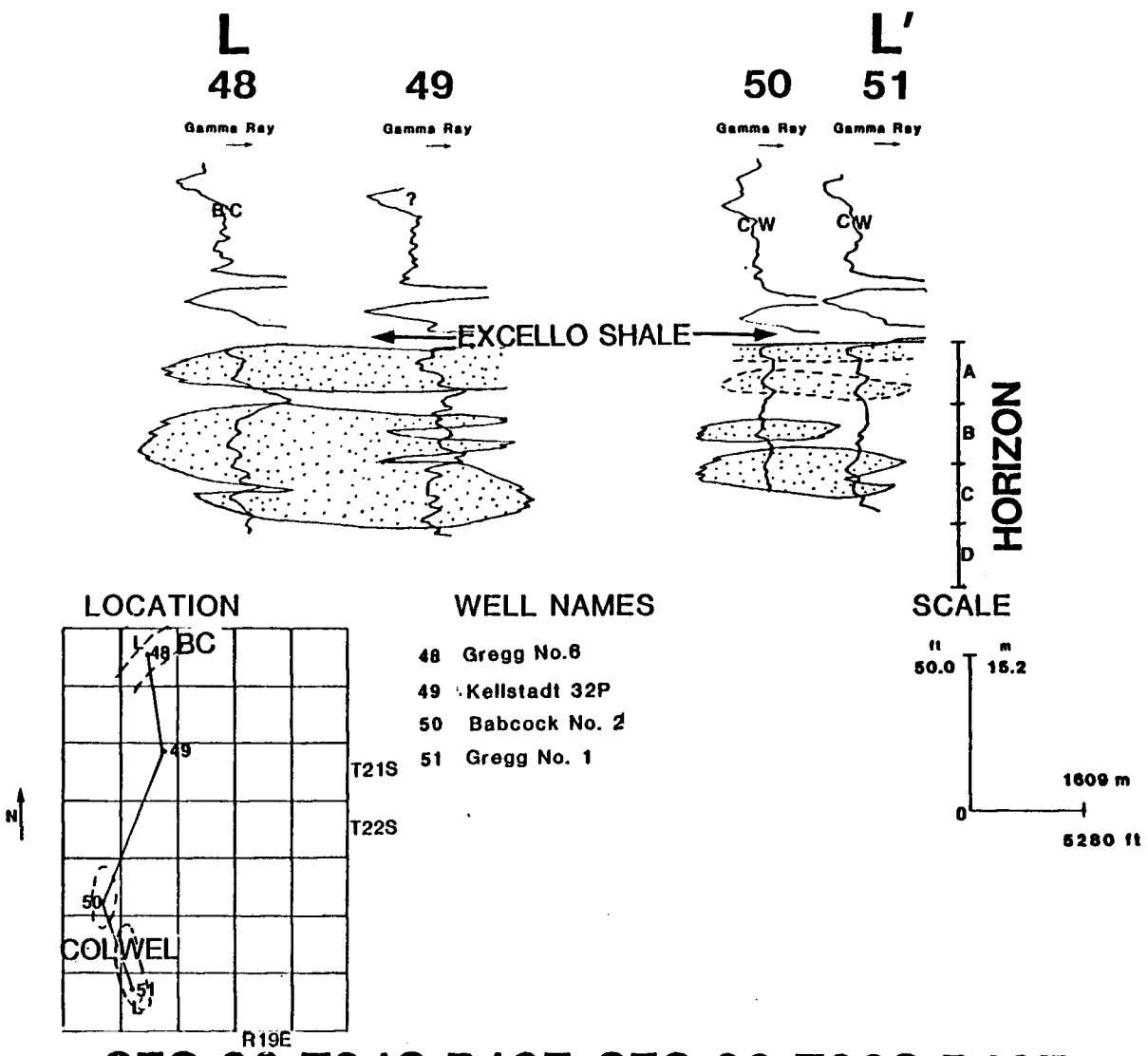

Figure 32

SEC 22 T21S R19E-SEC 22 T22S R19E

A and upper B horizons and a generally coarsening-upward sandstone in the A horizon. 3) Three laterally consistent coarsening-upward sandstones are present in the interchannel areas in the upper D, lower C, and B horizons. 4) The Bush City Shoestring is a channel complex consisting of interfingering and laterally discontinuous sandstone bodies.

DEPOSITIONAL ENVIRONMENTS

Interpretation of the depositional environments of the Bush City and Centerville sandstone trends was based on the geometries of the sandstone bodies, sedimentary structures, composition, and lithologic succession derived from core and well-log analyses.

Geometry

Correlation of the well-log signatures of the Bush City sandstone indicates the lenticular nature of the sandstone dominated bodies within the trend. The lower sandstones in the C and lower B horizons are thicker and more uniform in gamma-ray character. These sandstones are generally convex downward at the base and have sharp basal contacts as indicated by sharp gamma-ray deflections (Figure 28). In contrast, the sandstones located in the B and upper C horizons are irregular in their occurrence and well-log character (Figure 26). The most continuous sandstone in the Bush City area is located in the A horizon.

The lower boundary of the Centerville sandstone is also convex downward (Figure 22) and an erosive basal contact is again suggested by the gamma-ray response (Figure 22).

Three to four thin sandstones are located in horizons B and C in the areas between the main channel systems (Figures 23 and 24). Cross-sectional analyses suggest these deposits have been incised by the Bush City and Centerville channels (Figure 22).

Sedimentary Structures

Small-scale sedimentary structures are prevalent throughout the Bush City cored intervals which were examined in this study. Irregular laminae and thin beds displaying varying degrees of rippling and cross-stratification characterized the lower energy environments. Fining-upward sequences,as well as abrupt lithologic variations, are present in the cores.

The sandstones examined from the main channel of the Centerville are massive (Figure 9). A steady increase in gamma-ray radiation up-section suggests a fining-upward sequence of deposition. Clay-shale chip conglomerate is present in these sandstones.

Lithology

Very fine to fine-grained sandstone, siltstone, and silt to clay shales are the dominant lithologies of the Bush City cores. Glauconite pellets occur consistently in the sandstones in trace amounts. Plant fragments, including possible leaf imprints, are common in the Bush City cores.

Fine-grained sandstone dominated the lithology of the main channel of the Centerville trend. A core located outside the main channel (Bailey-Bailey No. 1) was similar in lithology and structure to the Bush City cores but the sandstones are slightly coarser.

Discussion - Interpretation

Evaluation of available data suggests that the Bush City and Centerville sandstones were deposited in fluvial channels on the lower coastal plain of a prograding delta lobe. This general interpretation is suggested by the following specific interpretations: 1) Strata bounding the Bush City and Centerville shoestring deposits are the result of sediment deposition in prodelta, delta front, interdistributary, and marsh environments as indicated by lithologies and well-log signatures. 2) Sharp contacts and a convex-downward base for the shoestring sands suggested from well-log signatures indicate channel form. The erosive nature of channel deposits on underlying sediments noted in this study has been noted by Bloomer (1977), Harms (1966), and Land and Dutton (1978). 3) Well-log signatures within the Bush City trend suggest the presence of a series of local sandstone bodies, which resulted from aggradation and switching of a fluvial channel. This type of chainlike pattern within a single sandstone trend was noted by Exum

and Harms (1968) in their study of a Cretaceous channel fill in Nebraska. 4) Sedimentary structures suggest deposition of point-bars. The massive bedding, clay-shale chip conglomerate, and decrease in grain size up-section within the Centerville trend suggests deposition of point-bar sediments (Figure 33). 5) Gamma-ray patterns indicate that a thin, widespread sandstone is present at the top of the "Lagonda" interval. This sandstone coarsens upward in most cases (Figures 30 and 25 , and represents the final phase of sediment deposition of the interval resulting from deltaic subsidence or transgression of the Cherokee Sea. In the Bush City trend, interstratification of finer sediments (Lithofacies B-E) increases in the upper half of the interval suggesting middle to upper point-bar and splay depositional environments.

Depositional Model

The existance of lowland marshes and swamps along a highly vegetated coastline is indicated by the presence of a thin coal below the sandstone intervals investigated. Subsequent transgression resulted in an eastward shift in the coastline and a return to shallow marine conditions in the east-central Anderson County area. A regional sandstone isolith of the Lagonda interval indicates influx of siliciclastic sediments from the east (Figure 34). This

Figure 33. Comparison of point-bar sediments and gamma-ray response that would be expected from borehole investigations. (Modified from Brown, 1979).

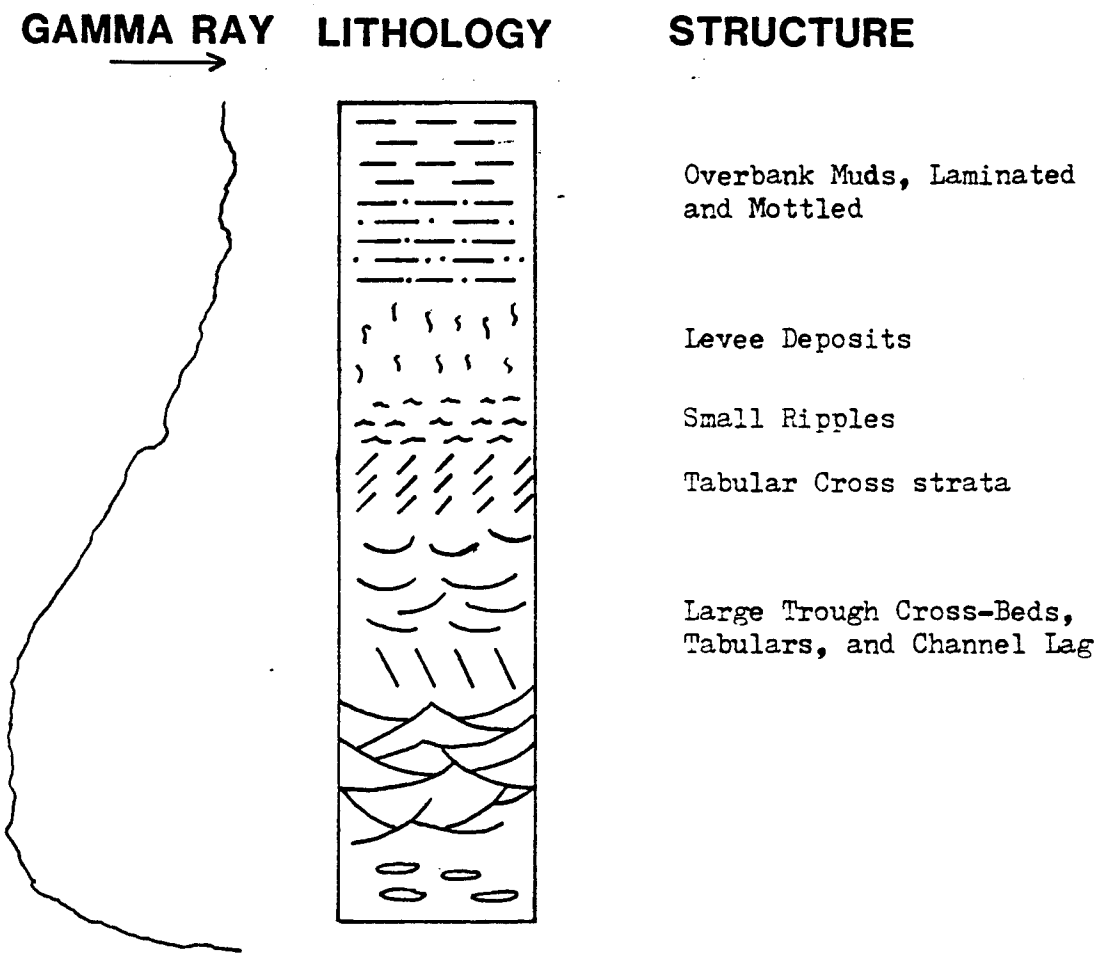
GAMMA RAY
LITHOLOGY
STRUCTURE
Overbank Muds, Laminated and Mottled
Levee Deposits
Small Ripples
Tabular Cross strata
Large Trough Cross-Beds, Tabulars, and Channel Lag

Figure 33

Figure 34. Sandstone isolith (feet) map of Lagonda interval in Anderson and surrounding counties, Kansas. (Unpublished work, R. L. Brenner, 1982).

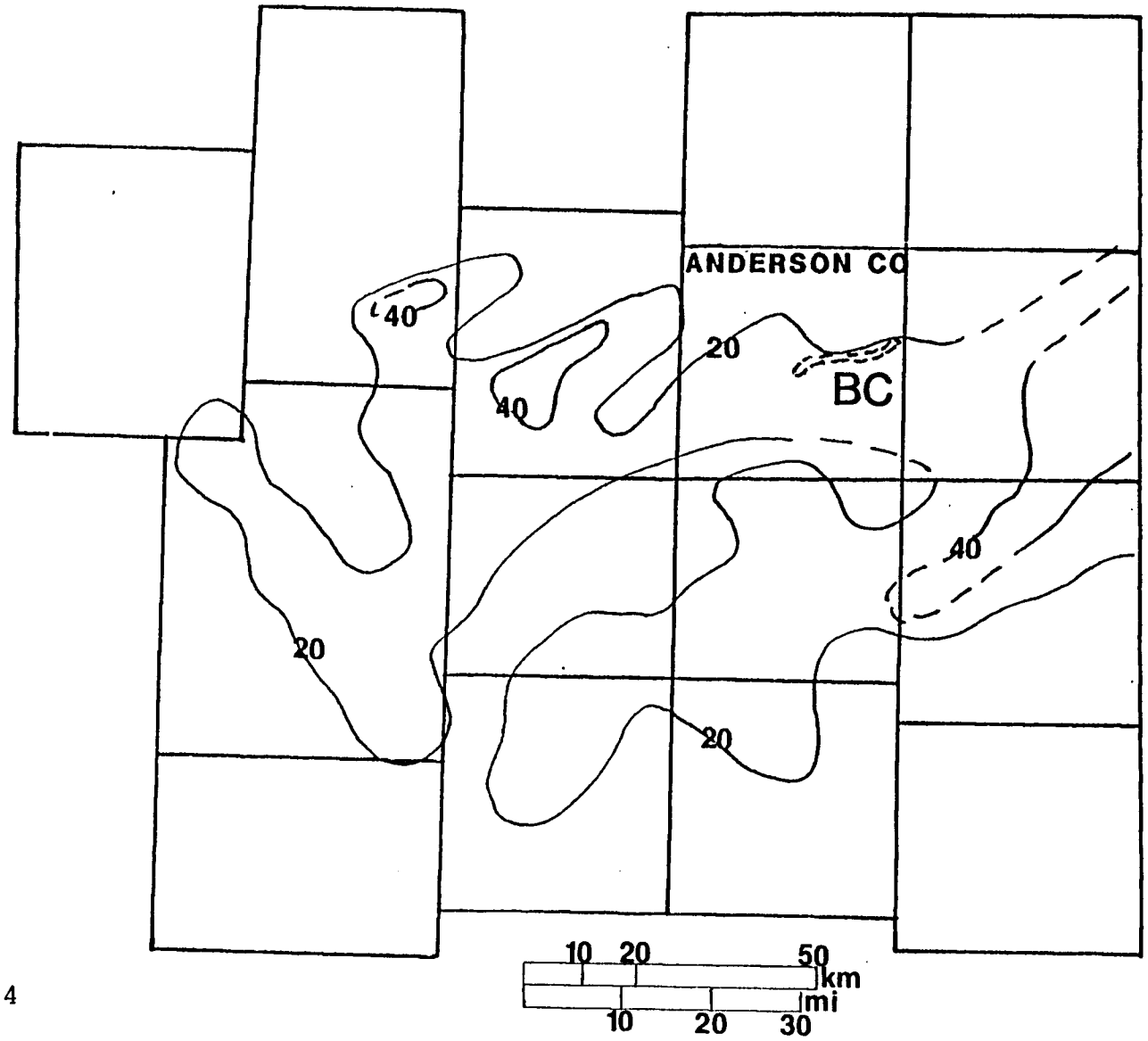

Figure 34

influx of siliciclastics resulted in prodelta, delta front, and interdistributary bay sedimentation (Figure 35). Thin coarsening-upward sandstones, suggesting coalescing distributary mouth bars, offshore barrier bars, or minor transgressive episodes, are interstratified with shale-dominated strata. Shale intervals adjacent to the Bush City channel reportedly contain brachiopods (Rich, 1923).

During subsequent sedimentation, establishment of the lower alluvial plain resulted in deposition of the Centerville Lagonda sandstone in a slightly meandering river system (Figure 36). Vegetation flourished in marsh and floodplain areas and resulting accumulation of plant material later became localized coal beds.

Regression of the Cherokee Sea led to a redirection of the main streams. The steeper gradient resulted in the incisement of the Bush City channel into previously deposited sediments (Rich, 1923) (Figure 37). This paleovalley was then gradually filled by a slightly meandering stream system. Encroachment of the Cherokee Sea probably influenced this channel filling process, causing sediment to be deposited increasingly upstream. Finally, as the seas transgressed east-central Anderson County, a thin delta-destructional sandstone was deposited as previously deposited sediments were reworked by wave action (Figure 38). Sedimentation during maximum transgression resulted in

Figure 35. Paleogeographic reconstruction illustrating initial siliciclastic influx into Anderson County, Kansas. Pro-delta, delta front, and lower delta plain sediments are deposited as delta lobe migrates westward.

Figure 36. Paleogeographic reconstruction illustrating deposition of Centerville sandstone. Continued progradation of delta lobe results in the modification of previously deposited sediments by a subsequent alluvial stream system.

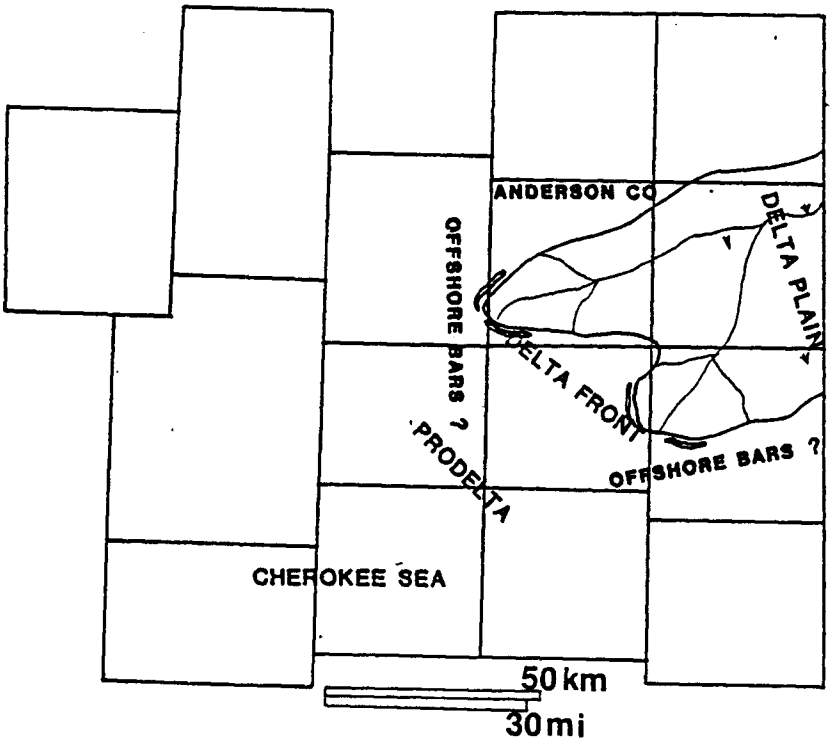

Figure 35

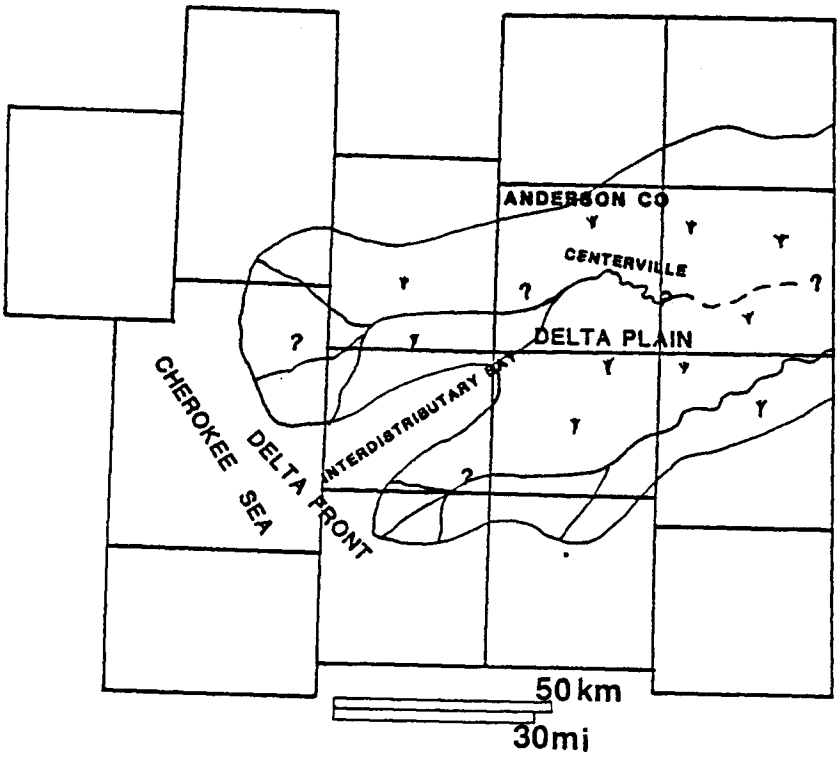

Figure 36

Figure 37. Paleogeographic reconstruction showing incisement of Bush City Channel. Cherokee Sea regression resulted in higher river gradients and subsequent channeling of previously deposited sediments.

Figure 38. Paleogeographic reconstruction showing transgression of the Cherokee Sea during final stages of Lagonda sedimentation. Rise in sea level causes river channels to fill with their sediment load. Reworking of previously deposited sediments by wave action results in thin, coarsening upward sandstone at top of Lagonda interval. The black Excello Shale represents deposition during maximum transgression.

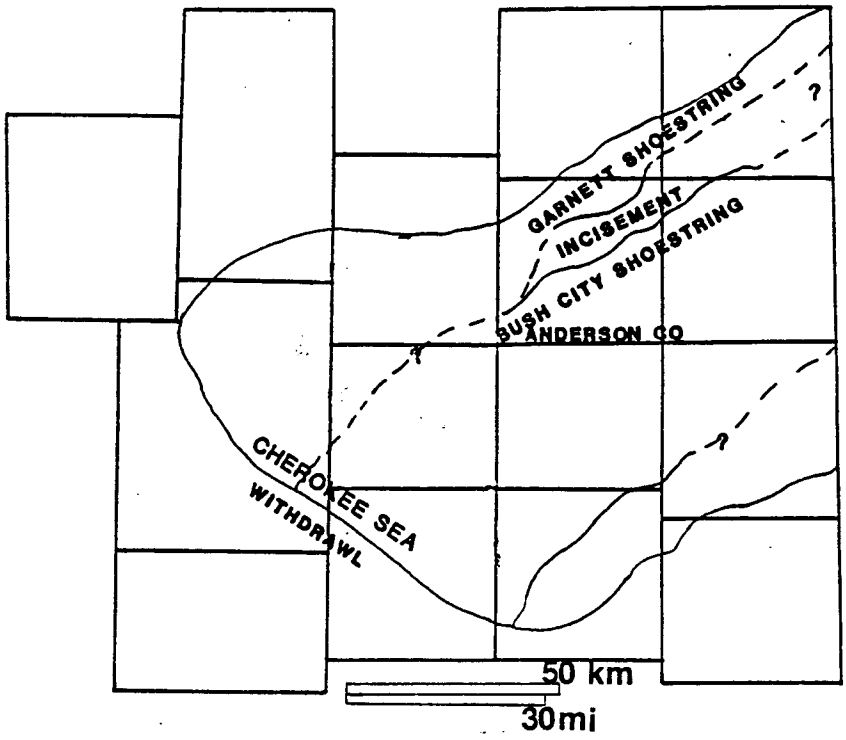

Figure 37

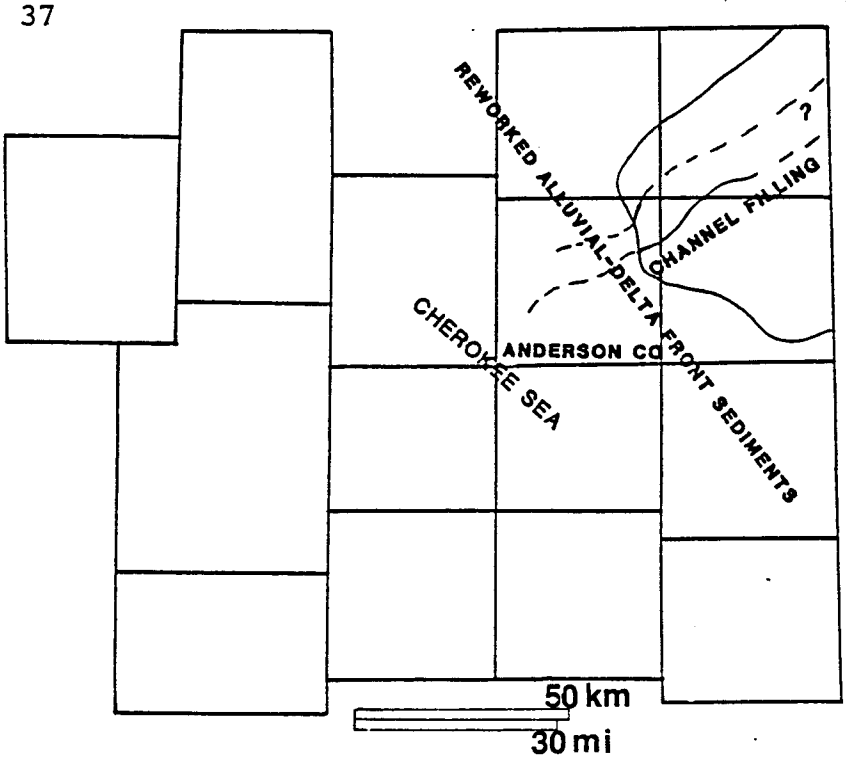

Figure 38

deposition of the widespread, black, phosphatic Excello Shale.

SANDSTONE PETROLOGY

The detrital and authigenic composition of the Bush City and Centerville sandstones is varied. Average percentages of these components are based on point counts of 39 thin-sections (Table 2).

Detrital Minerals

Monocrystalline Quartz

Monocrystalline quartz is the dominant mineral of the sandstones examined. The majority of monocrystalline quartz grains exhibit slight (1 to 5 degrees rotation of stage) to strong (5 to 10 degrees rotation of stage) undulose extinction. Blatt and others (1980) have found 80 to 90 percent of plutonic quartz possess this characteristic.

Size of the monocrystalline quartz grains ranges from .07 (very fine sand) to .28 mm (medium sand) in diameter. Average grain size in the Bush City trend is 0.16 mm and in the Centerville 0.23 mm. The very fine-grained quartz is angular to subrounded with low to moderate sphericity. The fine to medium sand fraction is subangular to subrounded with moderate to high sphericity. Original grain shape is often obscured because of interlocking quartz overgrowths,

Table 2. Detrital and authigenic composition of the Bush City and Centerville sandstones. Two columns at left represent percent of that component out of total composition. Comparison at right shows percent of that component out of main detrital minerals (Quartz, feldspar, and rock fragments).

	BUSH CITY	CENTERVILLE	BUSH CITY	CENTERVILLE
DETRITAL	(% of Detrital and Authigenic)		(% of Detrital) Q+F+RF	
Quartz	(17 Samples)	(22 Samples)	(17 Samples)	(22 Samples)
Monocrystalline	59.4	54.2	92.5	85.2
Polycrystalline	1.2	2.7	1.8	4.2
Feldspar				
Plagioclase	1.0	2.3	1.8	3.6
Orthoclase	1.9	2.8	2.9	4.4
Mica				
Muscovite	2.6	2.8		
Biotite	T	T		
Rock Fragments			0.0	2.4
Schist	0.3	0.2		
Shale	0.2	0.9		
Chert	T	T		
Matrix	12.2	6.6		
Phosphate	0.2	T		
Heavy Minerals	0.2	0.2		
AUTHIGENIC				
Carbonates				
Fe-Calcite	4.0	8.3		
Siderite	0.6	T		
Clays				
Kaolinite	0.4	1.7		
Sericite	3.9	3.7		
Chlorite	0.3	0.2		
Silica	3.6	1.9		
Pyrite	0.9	0.2		
FeO	1.8	2.8		
OTHER				
Pore Space	1.6	2.3		
Organics	3.0	5.3		

Table 2

unless early clay rims or "dust" coatings exist on the grains (Figure 39).

Inclusions in the monocrystalline quartz grains include tourmaline and rutile needles. Rutile inclusions are common in granitic quartz (Blatt and others, 1980). The quartz grains are largely unaffected by diagenesis except for a small percentage of those in the heavily carbonate-cemented sandstones, where slight corrosion of grain boundaries occurs (Figure 40).

Polycrystalline Quartz

Three types of polycrystalline quartz are present in the Bush City and Centerville sandstones: 1) schistose metamorphic, characterized by elongate grains often displaying straight borders and mica inclusions; 2) stretched metamorphic, composed of elongate grains that are irregularly sutured; 3) recrystallized metamorphic, exhibiting straight boundaries between interlocking, equant grains. Polycrystalline quartz grains exhibit strong undulose extinction.

Polycrystalline quartz grains are highly variable with respect to suturing characteristics, with the three types grading into one another, especially with regard to recrystallized and stretched metamorphic grain types. Polycrystalline quartz grains are subangular to subrounded

Figure 39. Photomicrograph showing "dust" coating on detrital quartz grain. Fe-calcite (c) postdates syntaxial quartz overgrowths (q). Crossed polarizers. Sample K-12. Bar scale equals 0.1 mm.

Figure 40. Photomicrograph showing heavily carbonate-cemented sandstone of Centerville trend. Calcite cement partially replaces detrital grains (arrows). Crossed polarizers. Sample BB3. Bar scale equals 0.5 mm.

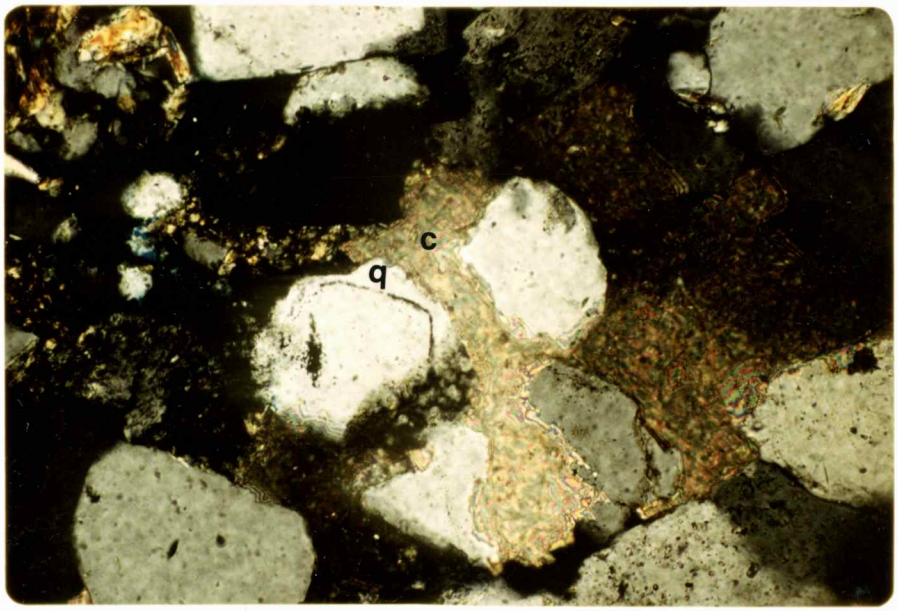

Figure 39

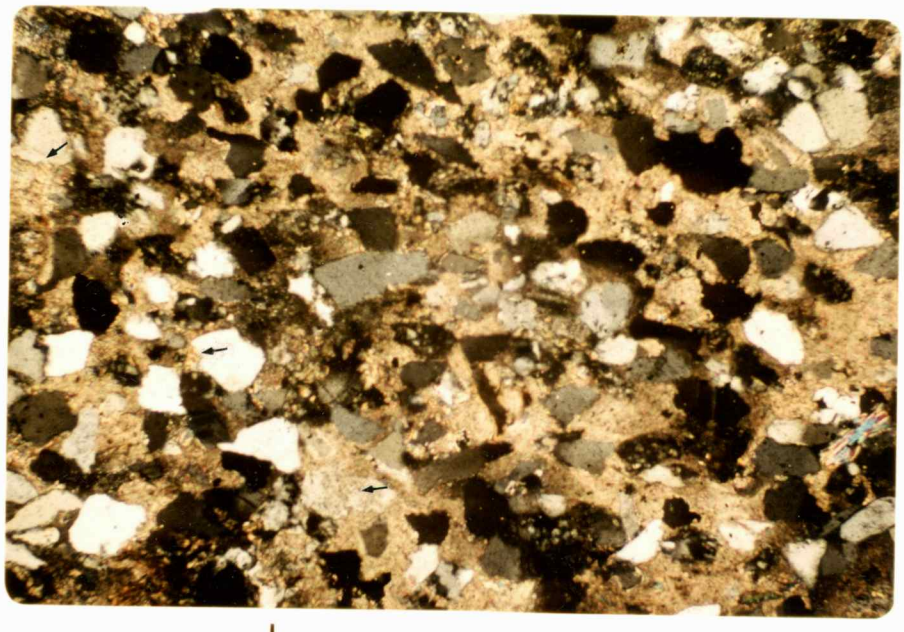

Figure 40

and are moderately spherical. Size of these quartz grains ranges from 0.15 to 0.25 mm.

Feldspars

Potassium Feldspar

Orthoclase is the major feldspar in the Bush City and Centerville sandstones, identified on the basis of optical properties, including cleavage and Carlsbad twins. Minor sericitization is common among cleavage traces of orthoclase grains (Figure 41). The size range of orthoclase grains varies from approximately 0.10 to 0.23 mm, and degree of rounding ranges from angular to subrounded. Microcline with characteristic grid twinning also is present.

Plagioclase Feldspar

Plagioclase feldspar grains were identified on the basis of multiple (albite) twinning. These plagioclase grains are of albite composition as identified on the basis of the maximum extinction angles between adjacent twinned laminae (Michael-Levy method), which vary from 15 to 19 degrees.

A majority of the plagioclase grains are angular and exhibit few noticeable effects of weathering. Size range of the plagioclase is comparable to that of monocrystalline quartz grains.

Thin-section analyses indicate potassium to plagioclase feldspar ratios range from a maximum of 6:1 to a ratio of 1:2 in the Bush City Shoestring, and from 4:1 to 1:2 in the Centerville trend.

Rock Fragments

Rock fragments compose a small percentage of the detrital component of the sandstones. Rock fragment types include schist, silty shale, chert, and a trace of volcanics.

Schistose Rock Fragments

Schistose rock fragments are composed of elongated quartz grains set a micaceous framework and were differentiated from schistose metamorphic quartz on the basis of their higher percentage of platy minerals and smaller component grain size. Compaction of these fragments between more resistant quartz grains resulted in some difficulty at times in distinguishing them from matrix detritus. Size of the fragments varies from 0.20 to 0.25 mm.

Silty Shale Rock Fragments

Silty-shale fragments are present as fine-grained constituents as well as large rip-up clasts up to 5 cm long and 2 cm wide, which occur in the massive units within the

Centerville trend. The smaller fragments are identified by their coherent fine-grained texture of aligned fine micas and clays, which distinguishes them from matrix material. This grain type is also deformed between other detrital grains.

Volcanic Rock Fragments

One possible volcanic rock fragment was observed. If other such rock fragments were present in the samples studied, then they have been diagenetically altered beyond recognition.

Chert Rock Fragments

Microcrystalline chert fragments are minor constituents in the sandstones. The chert is subangular to subrounded and ranges from 0.15 to 0.25 mm in diameter.

Muscovite

Muscovite is a persistant accessory mineral in The Lagonda sandstones. It occurs as colorless euhedral laths in a size range of 0.1 to 0.3 mm. The mica is often aligned parallel to stratification, resulting in conspicuous micaceous partings. Deformation of muscovite between more resistant detrital grains by compactional forces is common (Figure 42). Crystallization of carbonate cement also results in deformation of mica by splitting the laths along

Figure 41. Photomicrograph showing partial sericitization of K-feldspar. Sericite congregates along cleavage planes. Crossed polarizers. Sample BB 11. Bar scale equals 0.1 mm.

Figure 42. Photomicrograph showing muscovite displaying compaction features. Elongate muscovite grain has been compressed between more resistant detrital grains. Crossed polarizers. Sample BB 3. Bar scale equals 0.1 mm.

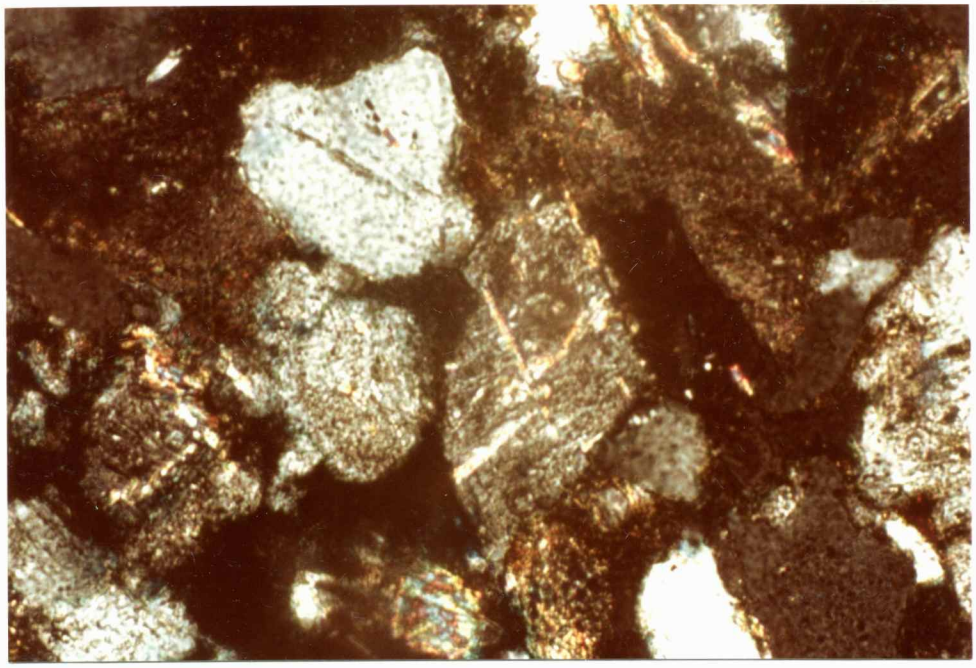

Figure 41

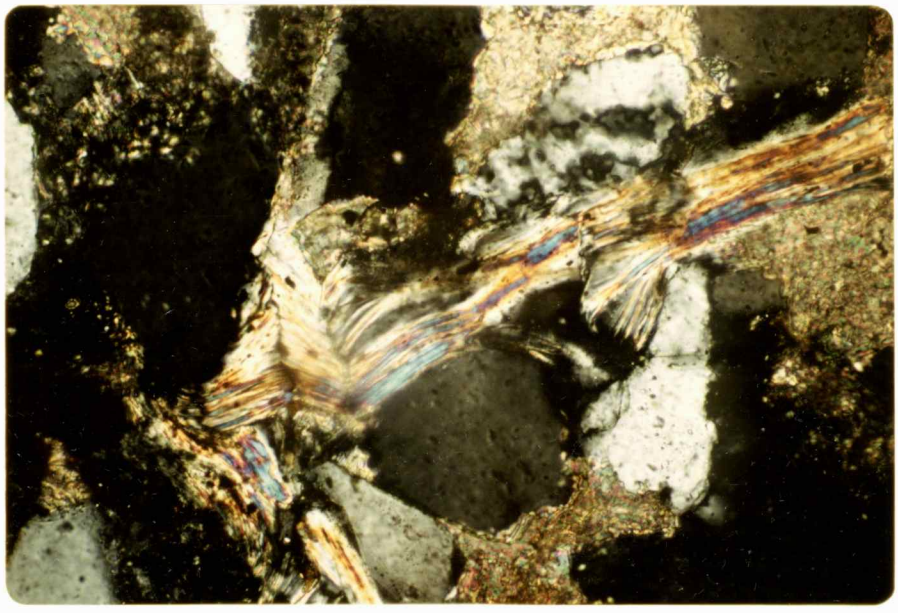

Figure 42

the prominent cleavage planes. Petrographic observations suggest kaolinite is a frequent alteration product of the muscovite (Figure 43), a relationship previously observed and described in Cherokee sandstones by Woody (1982).

Biotite

A small amount of biotite is present in the Lagonda sandstones. This mica occurs as euhedral laths that are 0.15 to 0.25 mm in length and are brown to reddish-brown in color and display strong pleochroism. Oxidation of Fe to hematite is a common alteration of the biotite.

Heavy Minerals

Zircon, ilmenite, and tourmaline are present in trace amounts in a majority of the thin sections. The zircon is colorless, rounded, and 0.10 to 0.20 mm in size. Tourmaline occurs in green and gold varieties. The grains are subrounded to rounded. Ilmenite grains are opaque, and were identified on the basis of their grey-black color, which differentiates them from pyrite.

Phosphate

Detrital phosphate is present in trace amounts in the Bush City trend. The structure of the phosphate is finely lamellar, suggesting a skeletal origin (Figure 44).

Figure 43. Photomicrograph showing muscovite (m) altering to kaolinite (k). Crossed polarizers. Sample 16-6. Bar scale equals 0.05 mm.

Figure 44. Photomicrograph showing detrital phosphate (p). A curved morphology displays fine lamellar structure. Plane polarized light. Sample K 6U. Bar scale equals 0.5 mm.

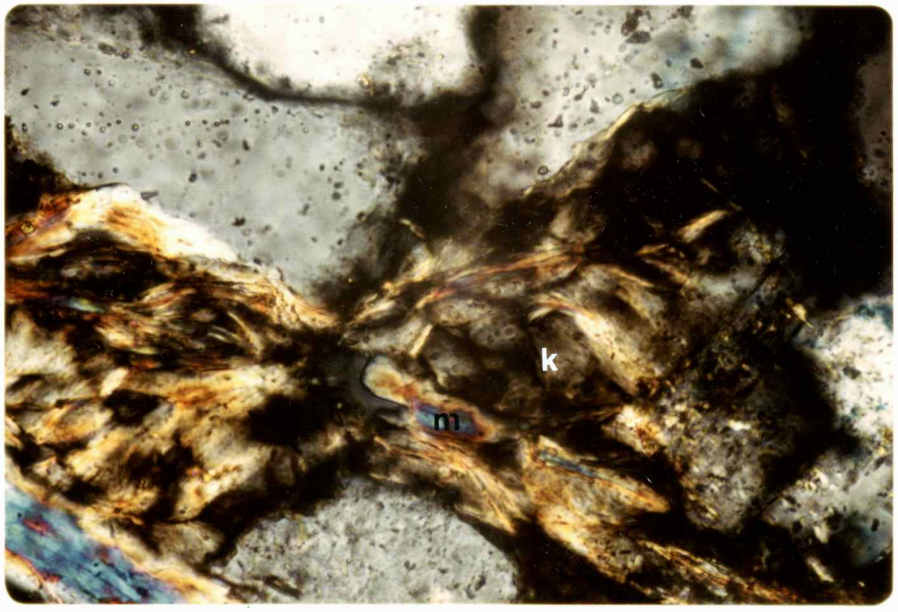

Figure 43

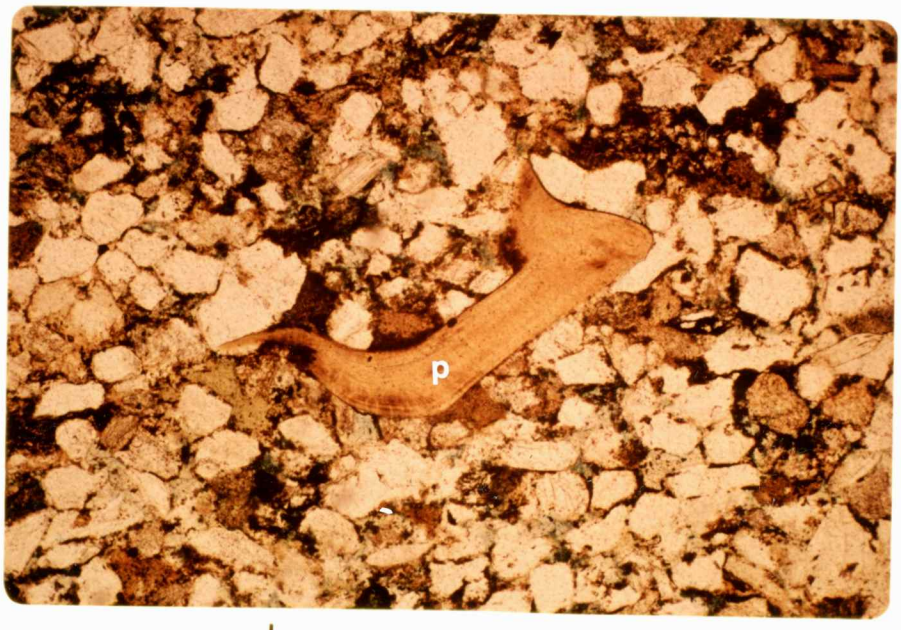

Figure 44

Organic Matter

Organic matter occurs as fine-grained, light to dark brown "clotted" material within many pore spaces and along laminations. This material represents the more resistant waxes and lignins left after decay, where burial is fast and bacteria is lacking (Folk, 1974). In the sandstone thin sections that were not cleaned by the soxhlet process (Bush City trend), a small percent of the organic component may be attributable to residual hydrocarbons (Table 2).

Glauconite

Detrital glauconite occurs in trace amounts in the Bush City trend. The grains are often slightly deformed between other detrital grains (Figure 45).

Authigenic Minerals

A variety of authigenic minerals are found within the Bush City and Centerville Lagonda sandstones. They include Fe-calcite, quartz overgrowths, siderite, pyrite, kaolinite, smectite-illite, illite, sericite, gypsum, hematite, and chlorite. The characteristics of these minerals are discussed in the diagenesis section.

Composition of Bush City Trend

The sandstones in the Bush City trend were recovered from approximately 6.0 to 16.8 meters below the Excello

Figure 45. Photomicrograph showing detrital glauconite (G). Grain has been slightly deformed between more resistant detrital minerals. Plane polarized light. Sample K-8.

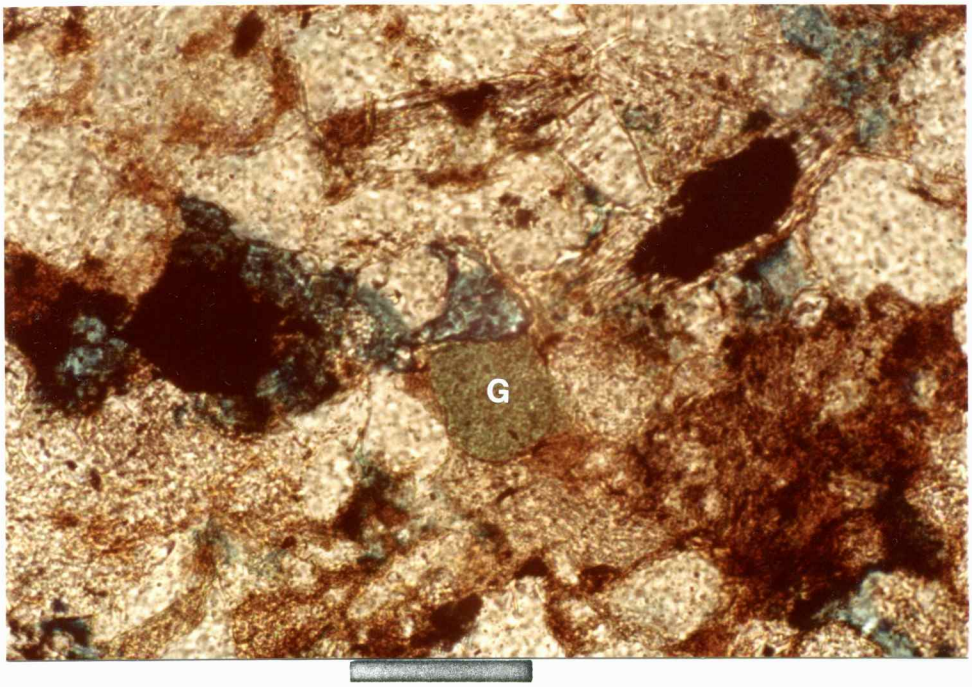

Figure 45

Figure 46. Classification of Bush City (A-B) and Centerville (C-D) sandstones using Folk's (1974) (See Figure 5) classification scheme. Quartz field includes monocrystalline quartz, polycrystalline quartz, and chert. Rock fragments included metamorphic and sedimentary grains. Potassium and plagioclase feldspar were included in feldspar field.

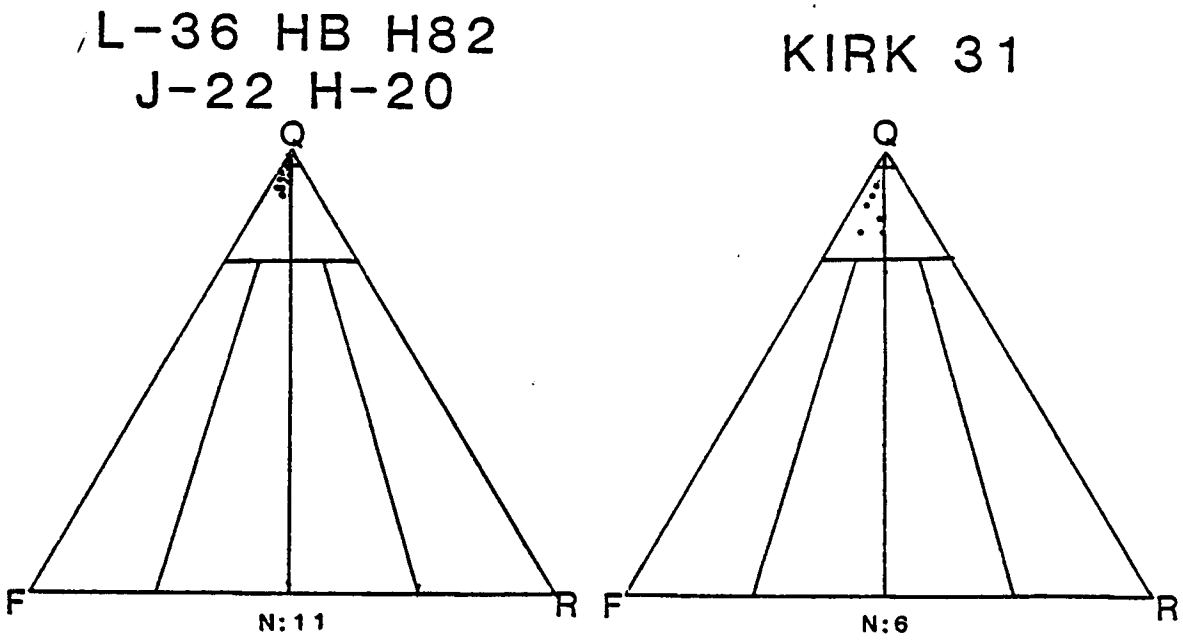

BUSH CITY TREND

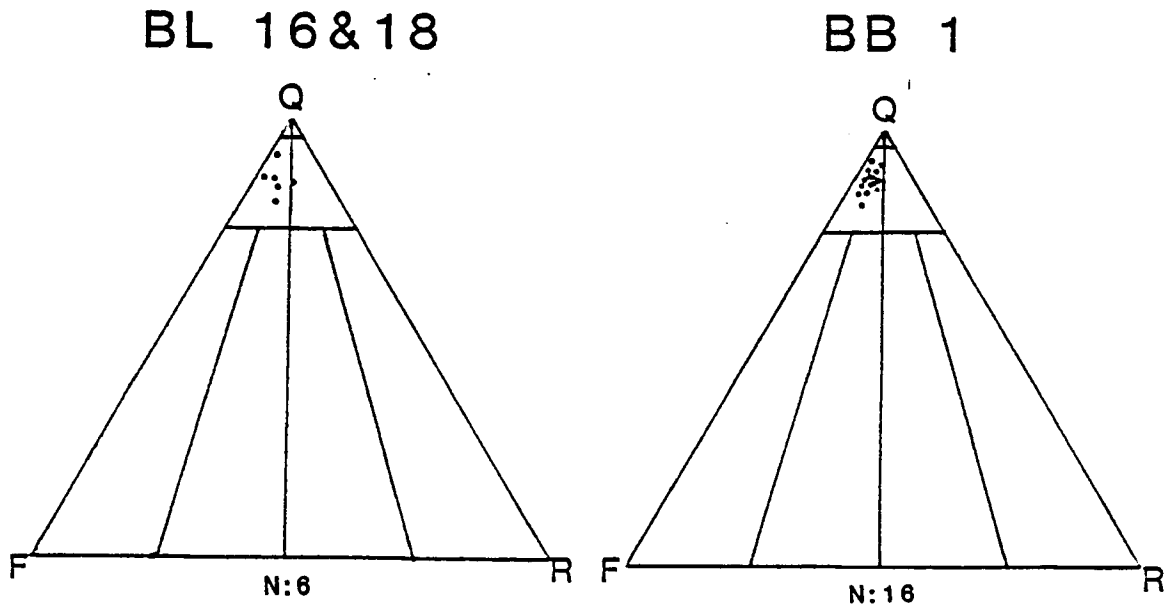

CENTERVILLE TREND

Figure 46

Shale. On a triangular diagram, these sandstones plot mainly in the quartz arenite field with minor subarkoses (Figure 46). High matrix percentages place many of these sandstones into the wacke category. Quartz percentage is as high as 93% with matrix averaging 12%. The lithofacies represented by these cores are dominantly D and E with thinner intervals of C. The sandstones from well Kirk 31 are predominantly subarkosic in composition. (Figure 46). Quartz arenites and subarkoses that are wackes because of high matrix content are minor. The more variable composition in Kirk 31 is related to a lithofacies change to dominantly B with minor A.

Composition of Centerville Trend

The Centerville sandstones are predominantly subarkoses (Figure 46), but display a greater range in composition due to the increase in feldspar and introduction of rock fragments. Lithofacies A and B are dominant in these sandstones. The stratigraphic position in the Lagonda section of these sandstones is approximately equivalent to that of the other cored intervals (Table 1).

Summary

Two distinct trends are developed in the Bush City and Centerville sandstones: 1) The finer sandstones of the Bush City are higher in matrix and quartz content due to the

finer grain size of the sandstone. 2) The Centerville sandstones and the coarser sandstones in the Bush City trend (Kirk 31) are more variable in composition.

Provenance

The sandstones of the Bush City and Centerville trends are uniformly fine-grained. The absence of coarse sand grains and larger pebbles in the sandstones of the higher energy depositional environments suggests that the incoming sediments had undergone an extensive history of deposition and reworking, or several cycles of transportation and deposition.

Using the criteria of Folk (1974) many of the sandstones of the Bush City are immature, possessing a detrital clay matrix content of 5% or more. Mineralogically the sandstones are mature because of a high stable mineral content (Pettijohn and others, 1973). Monocrystalline quartz is the dominant grain type with feldspar present in low amounts (Table 2). Less resistant grains such as hornblende are absent, and rock fragments and biotite are low in abundance (Table 2).

Several grain types indicate source rock composition. A plutonic source is suggested by albite plagioclase and quartz with rutile inclusions. Schistose rock fragments indicate a metamorphic source for a portion of the sediments.

Both distant and local sources have been suggested for Pennsylvanian deltaic deposits. Visher and others (1971) point out that the Desmoinesian was a time of general emergence. Hayes (1963) proposed the Canadian Shield as a source of sediments, which were transported along a shelf extending southwesterly into the western interior basin, and he also cited the Nemaha Uplift as a probable local source. Mississippian dolomites in the Ozark region as well as cherty carbonates eroded from the Nemaha Uplift may have supplied chert detritus to the mid-continent area. Mineralogical criteria suggest that the Lagonda sandstones of the Bush City and Centerville trends in Anderson County, Kansas were derived primarily from the distant Canadian Shield.

DIAGENESIS

Major processes of diagenesis that altered the sandstones in the Bush City and Centerville trends include authigenic crystallization of mineral cements, and dissolution, replacement, and alteration of detrital components and cements.

Authigenic Minerals

Pyrite

Pyrite is the dominant opaque mineral of the Lagonda interval under investigation. The pyrite occurs as small isolated irregular cubes and clusters of small crystals among matrix material, replacement of organic fragments, and as elongated to spherical nodules, which may reach 20 mm in size (Figure 47).

Pyrite often replaces organic matter identifiable as plant fragments. The pyrite indicates that reducing conditions and high dissolved sulfur content were present in the local environment. The bacterial decay of organic matter is a likely source of sulfur in pyrite (Bucke and Mankin, 1971).

Pyrite may be the result of diagenesis within "micro-environments". Local "micro-environments" of diagenesis in the immediate vicinity of altering components of a sedimentary rock create high ionic concentrations, which may cause precipitation or replacement of mineral species (Keller, 1970). The proximity of pyrite to organic fragments in the sandstones is suggestive of such a diagenetic event. Low permeability restricting the movement of pore fluids may also favor the establishment of localized high concentrations of ions.

The boundary relations between pyrite and the other constituents suggest that it precipitated early. Pyrite nodules often encompass detrital grains, and where this occurs, cements such as calcite and silica are not observed (Figure 47). Calcite void filling in fractures within a pyrite nodule also suggests early formation of the pyrite (Figure 47).

Siderite

Siderite occurs as a minor pore-filling cement in the finer-grained sandstones of the Bush City trend. The siderite is microcrystalline and is commonly iron-oxide stained. When formed soon after deposition, siderite is often microcrystalline (Jonas and McBride, 1977).

Reducing conditions, low sulfur concentrations, and ferrous iron are required for the formation of siderite (Blatt and others, 1980). Woody (1982) suggested that early formation of pyrite would cause the low sulfur environment needed for siderite crystallization.

Fe-Calcite

Fe-calcite is the most abundant cementing agent in the Bush City and Centerville sandstones (Table 2) and occurs in two main habits: 1) poikilotopic cement (Friedman, 1965) surrounding one or more detrital grains (Figure 48); 2) irregular subhedral pore fillings (Figure 49). The pore fillings range in size from 0.05 to 0.25 mm in cross-section. Examined under crossed polarizers, the Fe-calcite is characterized by sweeping extinction, indicating strained crystal lattices. X-ray analyses of selected samples did not detect dolomite.

The highest percentage of Fe-calcite cementation occurs in the basal 0.6 meters of Bailey-Bailey No. 1 (Figure 40). In this interval approximately 40% of the rock total is Fe-calcite poikilotopic cement. The sandstone is fine-grained and appears to be loosely packed, but deformed muscovite demonstrates that some compaction did occur before complete cementation.

Figure 47. Photomicrograph showing pyrite nodule. Early fractures contain calcite spar (s). Calcite cement is absent from remainder of the nodule. Crossed polarizers. Sample H-20 696.9. Bar scale equals 3 mm.

Figure 48. Photomicrograph showing poikilotopic calcite cement. Porosity and permeability nearly eliminated by the cementation (c). Detrital grains are partially replaced by calcite (arrows). Sample BB 3. Bar scale equals 0.1 mm.

Figure 47

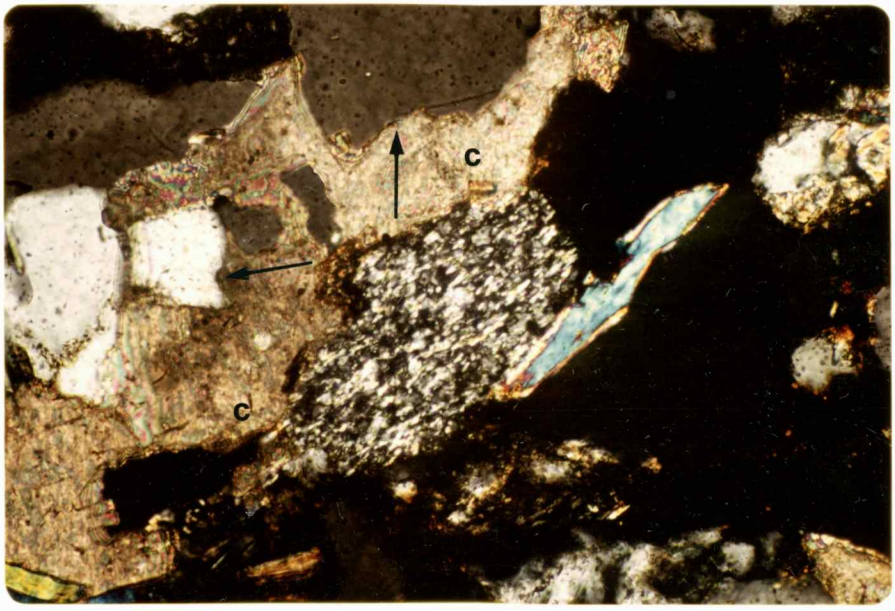

Figure 48

Fe-calcite partially replaces feldspar grains (Figure 50) and to a lesser extent quartz grains (Figure 48). Two stages of Fe-calcite are present in the sandstones of Bailey-Bailey No. 1. Cathodoluminoscope investigations demonstrated that approximately half the carbonate does not luminesce but the remainder did. Microprobe analyses have shown that the iron-manganese ratios vary among these two calcites in the following manner. In the luminescing Fe-calcite, the K/Fe-K/Mn ratio is approximately 7. The non-luminescing Fe-calcite has a K/Fe-K/Mn ratio of approximately 14. Frank (1981) has shown that the Fe/Mn ratio in dolomites affects luminescence characteristics. He found that dolomites with Fe/Mn ratios less than 7.5 did luminesce while those with ratios greater than 7.5 did not. Limited microprobe analyses suggest that in the Fe-calcite of this study, the Fe/Mn ratio is the controlling factor of luminescence. The sequence of crystallization of the two Fe-calcites was not determinable in thin section.

The precipitation of calcite requires an increase in the product of Ca^{++} and CO_3^{--} in solution (Bucke and Mankin, 1971). Rise in temperature has been suggested as playing an important role in carbonate cementation by raising the solubility of quartz and lowering that of calcite. Clay diagenesis may also be a factor in calcium carbonate precipitation. During smectite-illite alteration,

Figure 49. Photomicrograph showing irregular (subhedral to euhedral) Fe-calcite pore-filling cement (c). Crossed polarizers. Sample K-17. Bar scale equals 0.1 mm.

Figure 50. Photomicrograph showing carbonate replacement of feldspar (arrows). Crossed polarizers. Sample 16-5. Bar scale equals 0.1 mm.

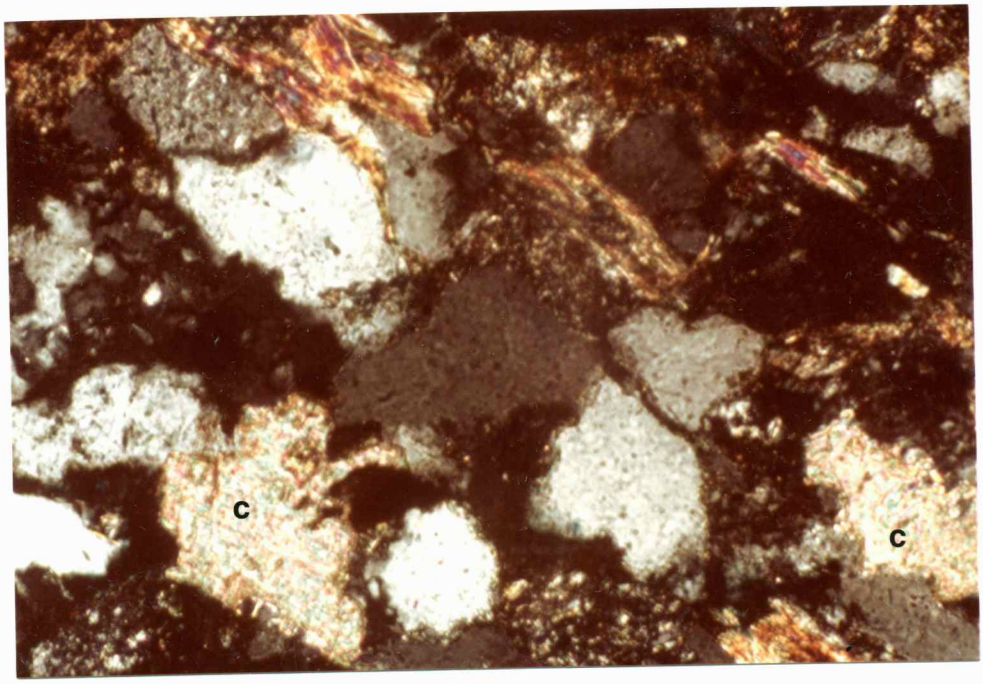

Figure 49

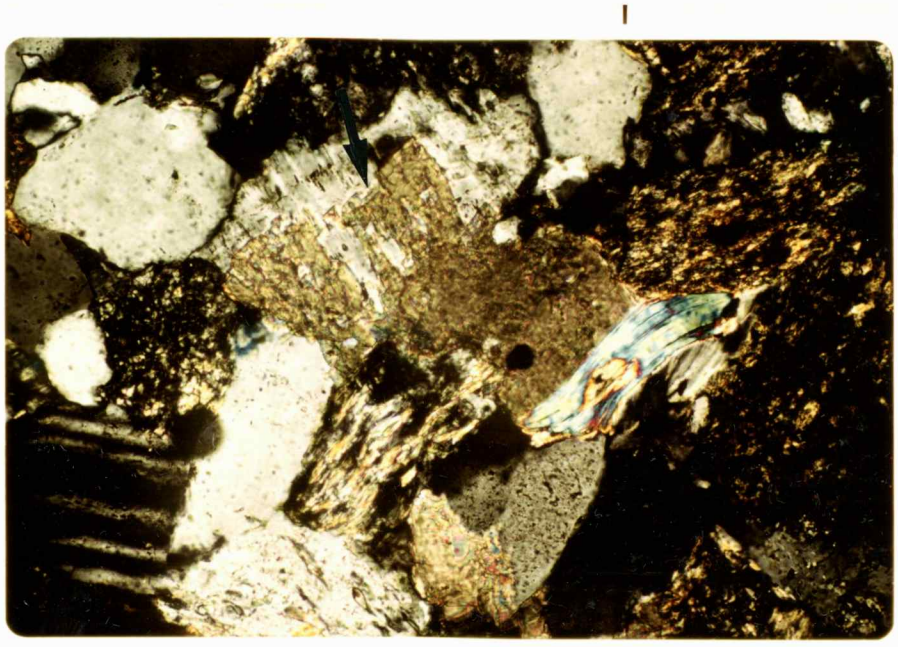

Figure 50

interlayer Ca ions are released as K fixation takes place in the illite structure (Boles and Franks, 1979). The combination of CO 2 from the decomposition of organic matter in shales, with the Ca released from clays, has been proposed as a possible mechanism of calcium carbonate crystallization (Boles and Franks, 1979).

Carbonate cement is more prevalent in the coarser sandstones. In general, the amount of matrix decreases as pore space increases in these sandstones. This relationship suggests that more original porosity along with the easier migration of the interstitial fluids in coarse sediments promoted more calcium carbonate precipitation.

Authigenic Clays

Authigenic clays within the Bush City and Centerville sandstones include kaolinite, smectite-illite, illite, sericite, and possibly chlorite.

Kaolinite is present as fine to very fine-grained authigenic pore fillings (Figure 51) and as apparent alterations of muscovite (Figure 43). S.E.M. examination reveals the characteristic hexagonal crystal shape of the booklets (Figure 52) and indicates some of the kaolinite may also be the result of the alteration of feldspar (Figure 53).

Figure 51. Photomicrograph showing kaolinite pore filling. Crossed polarizers. Sample 16-10. Bar scale equals 0.5 mm.

Figure 52. Scanning electron micrograph showing hexagonal kaolinite booklets. Delicate morphology indicates authigenic origin. Sample BB 1. Bar scale equals 1.0 micron.

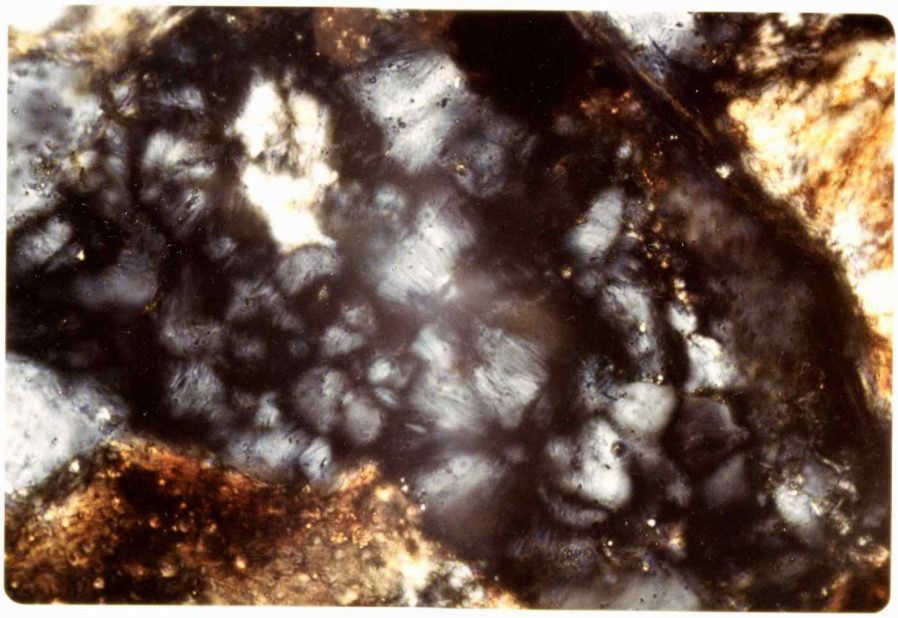

Figure 51

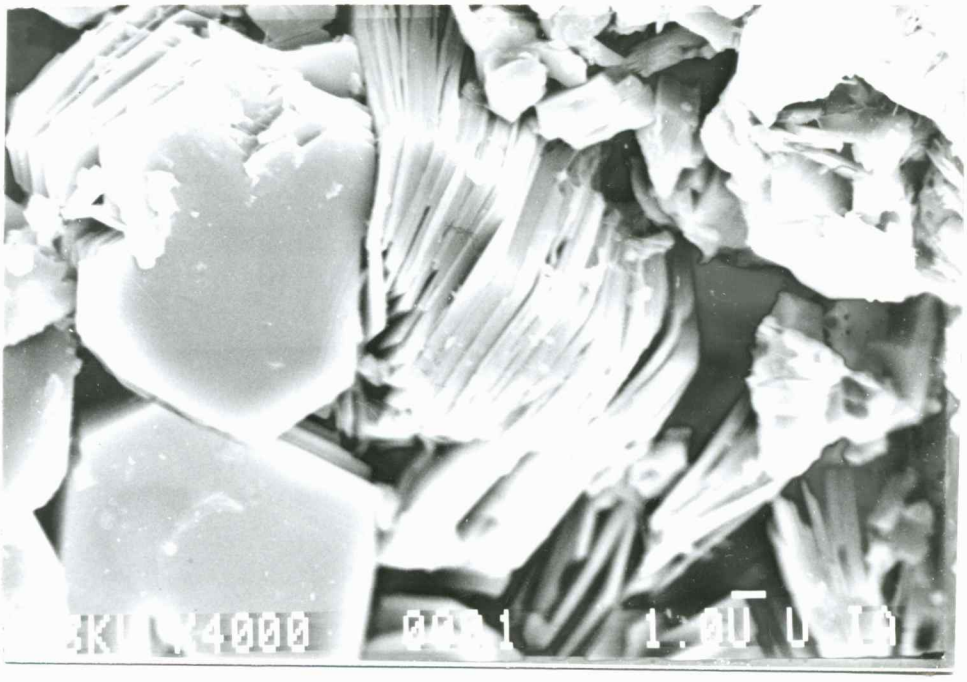

Figure 52

Four factors contributed to the formation of kaolinite in Pennsylvanian sandstones in Oklahoma (Bucke and Mankin, 1971): 1) permeability; 2) K-feldspar as a Al-Si source; 3) partly degraded illite, which serves as a K^+ acceptor, creating a low KCL-HCL ratio; 4) organic material to maintain a low pH. In addition to K-feldspar, smectite-illite diagenesis may also contribute Si for the formation of kaolinite. (Boles and Franks, 1979).

Authigenic mixed-layer smectite-illite occurs as a pore lining (Figure 54). These clays were observed under the S.E.M. but their minute size prevented petrographic examination and amount determination. L. Aden (personal communication, 1982) found illite to be the most abundant clay within the shales of the Lagonda interval.

Sericite is an impure K-deficient muscovite or illite (Folk, 1974). This mineral is a common feldspar alteration product in these sandstones.

Clay coatings are present on a small number of detrital quartz grains. These coatings are often preserved by subsequent crystallization of quartz overgrowths (Figure 55) but definite identification of the type of clay mineral was not possible. Woody (1982) reported similar clay coatings to be chlorite in composition.

Figure 53. Scanning electron micrograph showing possible feldspar alteration to kaolinite(arrows). Sample BB 30. Bar scale equals 1.0 micron.

Figure 54. Scanning electron micrograph showing authigenic mixed-layer clay mineral pore lining (c). Sample K-2. Bar scale equals 10.0 microns.

Figure 53

Figure 54

Quartz Overgrowths

Syntaxial quartz overgrowths post-dated the clay coatings (Figure 55) and are an important cementing agent. The overgrowths precipitated in a well defined fashion, which often extend into open pores and terminate with euhedral crystal form, and as interlocking syntaxial overgrowths (Figure 56). Irregular overgrowths are the result of two or more separate overgrowths competing for the same pore space (Jonas and McBride, 1977) and are prevalent in the fine-grained sandstones of the Bush City trend. Determination of the amount of silica cement was difficult unless early "dust" or clay rims were visible. Irregular growth patterns, suggesting that quartz overgrowths crystallized in stages rather than continuously, were revealed under the S.E.M. (Figure 57).

The origin of the silica in authigenic quartz overgrowths has been attributed to several mechanisms: 1) pressure solution; 2) clay mineral diagenesis; 3) replacement of quartz and silica grains by carbonates; 4) dissolution of quartz grains; 5) percolation of ground water through the sediments; 6) dissolution of siliceous organisms (McBride, 1977). The quartz grains in the Lagonda sandstones studied often exhibit slight to moderate compaction, but definite suturing (pressure solution) of the grains is not apparent. This suggests that pressure

Figure 55. Photomicrograph showing clay coatings (arrow) on detrital quartz grain. Sample 16-3. Plane polarized light. Bar scale equals 0.1 mm.

Figure 56. Photomicrograph showing interlocking quartz overgrowths. Crossed polarizers. Sample HB 742.1. Bar scale equals 0.1 mm.

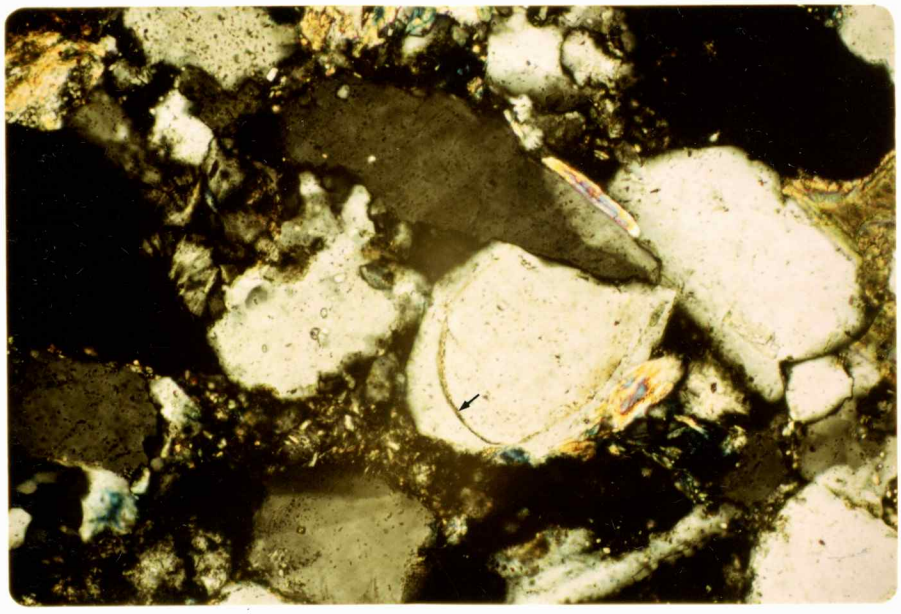

Figure 55

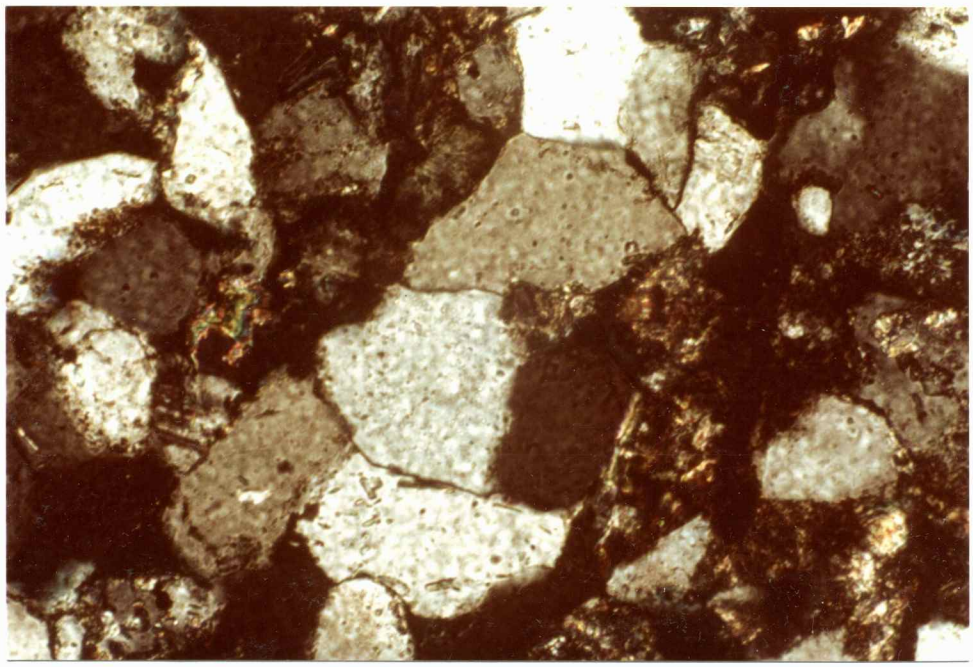

Figure 56

solution within the interval studied was not a source for silica. Percolation of ground water has been cited as an important transport medium of silica (Sibley and Blatt, 1977). However, the large number of pore volumes of connate water that would have to pass through the sandstone in order to precipitate silica has been pointed out by Blatt (1979).

Of the remaining mechanisms, feldspar clay-mineral diagenesis appears to be the most probable source of silica incorporated into quartz overgrowths. The alteration of smectite to illite has been suggested as an important source of silica in sandstone cementation by Boles and Franks (1979). They cited several important relationships in this clay conversion. K-feldspar in the shales provided the mecessary K for illite formation, and for each mole of illite formed, 24 moles of Si would be theoretically be released to become available for incorporation into quartz overgrowths and kaolinite formation. This reaction begins to occur at approximately 50 degrees C and will proceed at a moderate rate at 70 degrees C (Boles and Franks, 1979). Lahann (1980) has shown that when illitization reactions occur at or slightly above the initiation temperature of illitization (50 degrees C), the distance of migration of the released silica is increased. The interstratification of the sandstones and illite-rich shales of the Lagonda interval suggests that clay diagenesis was a source of Si, Al, and Ca found in authigenic cements.

Gypsum

A trace of gypsum is present in the Kirk 31 core of the Bush City trend as poikilotopic cement (Figure 58). Gypsum in sedimentary rocks is often the product of sulfuric acid from weathering of sulfides reacting with calcium in the sediments (Deer and others, 1978).

Hematite

Hematite occurs as small irregular blebs within the matrix of the sandstones. Conditions that favor the formation of hematite include: 1) presence of iron-bearing minerals; 2) post-depositional conditions favoring intrastratal alteration of the iron-bearing minerals; 3) favorable Eh-pH environment; 4) absence of subsequent reduction of the ferric iron; 5) elevated temperatures (Walker, 1967). When the Eh-pH conditions lie in the Fe (OH)3 field (Figure 59) the iron will precipitate. Initially ferric hydrate may precipitate, but it eventually alters to hematite both in the vadose zone and below the water table (Walker, 1967).

Feldspar Dissolution

The dissolution of feldspar resulted in the establishment of a small percentage of secondary porosity in the Bush City and Centerville sandstones (Figure 60). Feldspar dissolution has been previously recognized in the

Figure 57. Scanning electron micrograph showing regular (center) and irregular growth pattern of quartz overgrowth (arrows). Sample K-2. Bar scale equals 10.0 microns.

Figure 58. Photomicrograph showing poikilotopic gypsum cement (arrows). Crossed polarizers. Sample K-2L. Bar scale equals 0.1 mm.

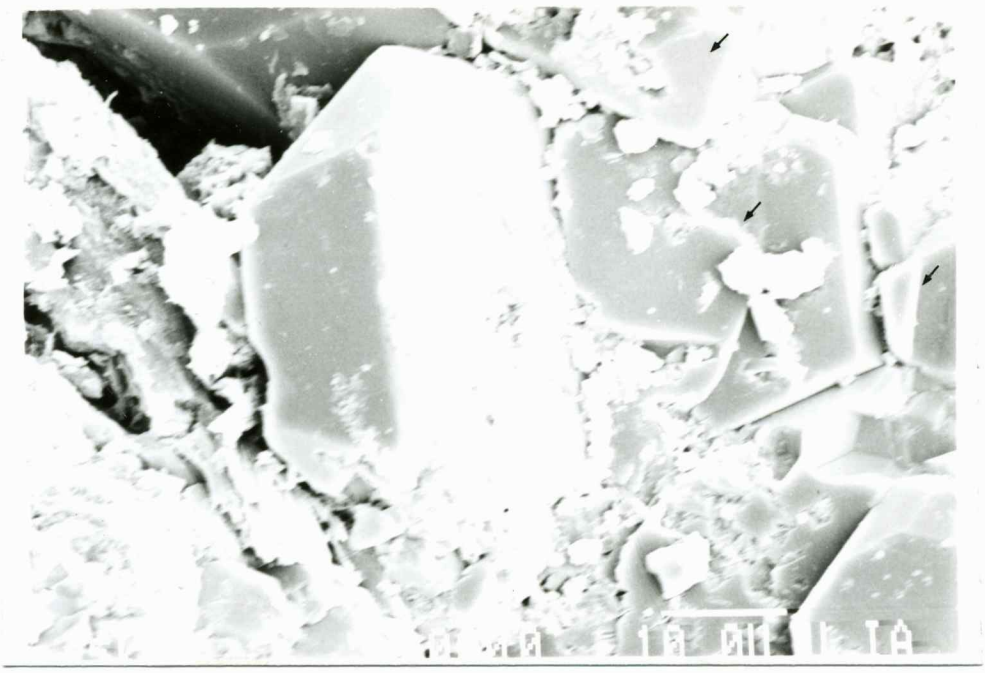

Figure 57

Figure 58

Figure 59. Stability fields of some solids and ions as functions of Eh and pH in the Fe-H_2O system at 25 degrees C. Dashed lines show positions of field boundaries at different activities of total iron in solution. Circled area outlines groundwater Eh-pH limits. (Modified from J. D. Ham, 1972).

Figure 60. Photomicrograph showing secondary porosity resulting from feldspar dissolution (arrows). Plane polarized light. Sample 16-6. Bar scale equals 0.1 mm.

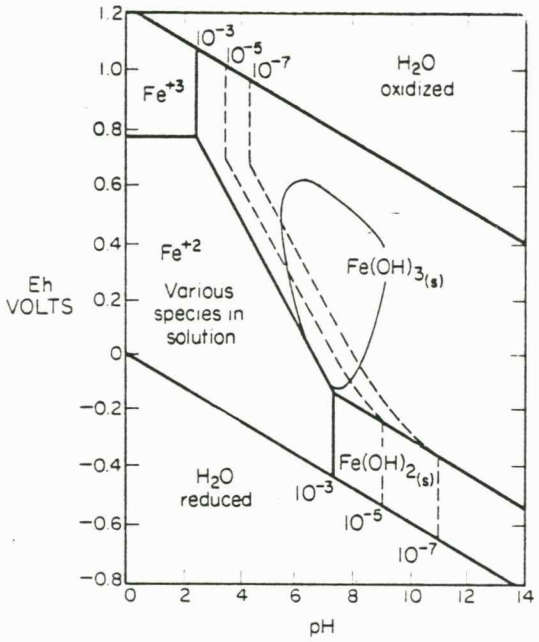

Figure 59

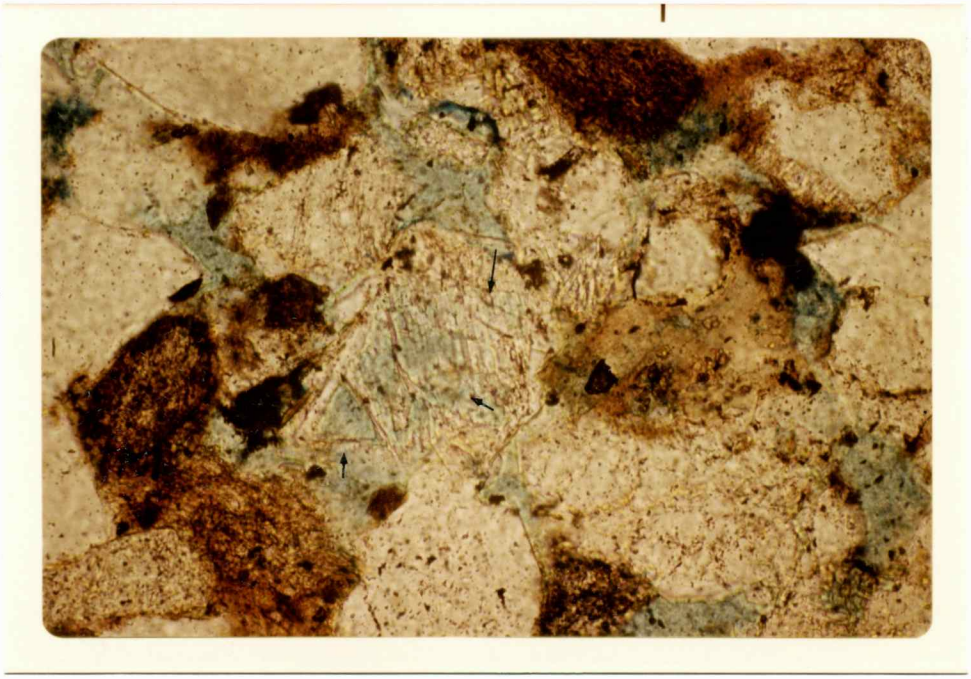

Figure 60

Cherokee sandstones of Kansas by Woody (1982). Boles and Franks (1979) reported that the decrease in the amount of K-feldspar corresponds to the addition of illite layers in smectite-illite clays, the K-feldspar providing the source of K in the illite. The dissolution of carbonate cement, that previously replaced the feldspar, may have caused part of the observed secondary porosity.

Paragenetic Sequence

Interpretation of grain-cement relationships suggest the following diagenetic sequence in the sandstones of the study area: 1) initial compaction of sediments; 2) formation of pyrite as a replacement of organic matter; 3) formation of microcrystalline siderite; 4) formation of minor amounts of authigenic clay coatings on detrital quartz grains; 5) precipitation of syntaxial quartz overgrowths; 6) crystallization of poikilotopic and pore filling Fe-calcite cement with partial replacement of feldspar and quartz grains; 7) authigenic formation of minor poikilotopic gypsum; 8) formation of kaolinite and sericite (white micas); 9) oxidation of iron (Figure 61).

Cherokee sandstones display diagenetic trends similar to those of Gulf Coast Tertiary sediments (Woody, 1982). Tertiary sediments of the Frio formation have been subjected to temperatures up to 180 degrees C and burial depths up to

Figure 61. Diagenetic sequence of Bush City and Centerville Lagonda sandstones. Dashed lines indicate exact timing of event was not determinable and may substantially overlap.

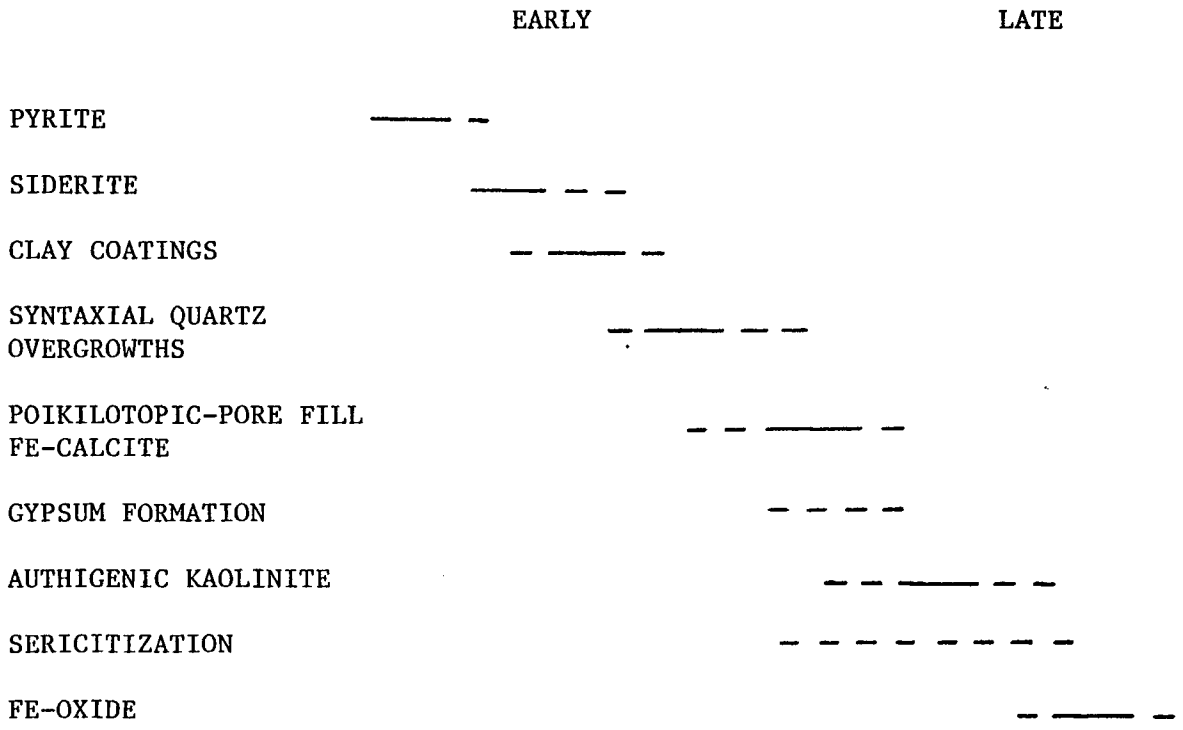
EARLY
LATE
PYRITE
SIDERITE
CLAY COATINGS
SYNTAXIAL QUARTZ OVERGROWTHS
POIKILOTOPIC-PORE FILL FE-CALCITE
GYPSUM FORMATION
AUTHIGENIC KAOLINITE
SERICITIZATION
FE-OXIDE

Figure 61

3,600 meters (Loucks and others, 1977). In contrast, the temperature in the Cherokee probably never exceeded 70 degrees C (Land and Dutton, 1978), and overlying sediments were a maximum of 1,000 to 1,200 meters thick (Ebanks, 1979). Petrographic evidence suggests that low-temperature diagenesis significantly affected the Cherokee Lagonda sandstones, and that the components (Al, Si, Fe, Mg, S) that are required for the formation of authigenic cements and mineral alterations were derived locally.

CONCLUSIONS

Information from well-log and core analyses has led to the following conclusions:

1) The Bush City Shoestring is a highly variable channel complex composed of three main sandstone horizons.

2) The Bush City and Centerville sandstones were the result of deposition by aggrading alluvial streams.

3) The Canadian Shield is the probable source for siliciclastic detritus deposited in the Anderson County, Kansas Lagonda sandstones.

4) Despite relatively low temperatures and shallow burial depths, diagenesis has been active in the Bush City and Centerville Lagonda sandstones. Smectite-illite clay diagenesis is suggested as a source for Si, Ca, Fe, and Mg ions, which become incorporated into authigenic kaolinite, quartz overgrowths, and calcite present in the sandstones.

5) Porosity and permeability have been significantly affected by diagenetic alterations. Reduction of pore space accompanies authigenic mineral crystallization. Secondary porosity was developed through the dissolution of feldspars.

REFERENCES

Bass, N. W., 1934, Origin of the Bartlesville shoestring sands of Greenwood and Butler Counties, Kansas: Am. Assoc. Petr. Geol. Bull., Vol. 18, p. 1313-1345.

Blatt, H., 1979, Diagenetic processes in sandstones: S.E.P.M. Special Pub. No. 26. p. 141-157.

Blatt, H., Middleton, G., and Murray, R., 1980, Origin of Sedimentary Rocks, 2nd ed.: Prentice-Hall, Inc., New Jersey, 782 p.

Bloomer, R., 1977, Depositional environments of a reservoir sandstone in west-central Texas: Am. Assoc. Petr. Geol. Bull., Vol. 61, p. 344-359.

Boles, J. R., and Franks, S. G., 1979, Clay diagenesis in Wilcox sandstones of southwest Texas: Implications of smectite diagenesis on sandstone cementation: J. Sed. Pet., v. 49, p. 55-70.

Brown, L. F. Jr., 1979, Deltaic sandstone facies of the mid-continent, in Hyne, N. D., ed., Pennsylvanian Sandstones of the Mid-Continent: Tulsa Geological Society Special Publication No. 1, p. 35-63.

Bucke, D. P., Jr., and Mankin, C. J., 1971, Clay-mineral diagenesis within interlaminated shales and sandstones: J. Sed. Pet., v. 41, p. 971-981.

Busch, D. A., 1971, Genetic units in delta prospecting: Am. Assoc. Petr. Geol. Bull., v. 55, p. 1137-1154.

Charles, H. H., 1927, Oil and gas resources of Kansas; Anderson County: Kans. Geol. Surv. Bull. 6, Part 7, 95 p.

Charles, H. H., 1941, Bush City oil field, Anderson County, Kansas, p. 43-56, in Levorsen, A. I. (ed.), Stratigraphic Type Oil Fields: Am. Assoc. Petr. Geol., 902 p.

Deer, F. R., Howie, R. A., and Zussman, J., 1978, An Introduction to the Rock-forming Minerals, 11th ed.: John Wiley and Sons, Inc., 528 p.

Dickson, J. A., 1965, Carbonate identification and genesis as revealed by staining: J. Sed. Pet., v. 36, p. 491-505.

Ebanks, W. J., Jr., 1979, Correlation of Cherokee (Desmoinesian) sandstones of the Missouri-Kansas-Oklahoma Tri-State Area, in Hyne, N. J., ed., Pennsylvanian Sandstones of the Mid-Continent: Tulsa Geological Society Special Publication No. 1, p.295-312.

Exum, F. A., and Harms, J. C., 1968, Comparison of marine-bar with valley-fill stratigraphic traps, western Nebraska: Am. Assoc. Petr. Geol. Bull., v. 52, p. 1851-1868.

Folk, R. L., 1974, Petrology of Sedimentary Rocks: Hemphill Pub. Co., 182 p.

Frank, J. R., 1981, Dedolotomization in the Taum Sauk Limestone (Upper Cambrian) Southeast Missouri, J. Sed. Pet., v. 51, p. 7-17.

Friedman, G. M., 1965, Terminology of crystallization textures and fabrics in sedimentary rocks: J. Sed. Pet., v. 35, p. 643-655.

Gordon, G. H. 1893, A report on the Bevier sheet: in Reports on Areal Geology: Missouri Geol. Survey Bull. 9, 66 p.

Ham, W. E., and Wilson, J. L., 1967, Paleozoic epeirogeny and orogeny in the central United States, Am. Jour. Sci., v. 265, p. 332-407.

Harms, J. C., 1966, Stratigraphic traps in a valley fill, western Nebraska: Am. Assoc. Petr. Geol. Bull., v. 50, p. 2119-2149.

Hayes, M. O., 1963, Petrology of Krebs subgroup (Pennsylvanian, Desmoinesian) of Western Missouri: Am. Assoc. Petr. Geol. Bull., v. 47, p. 1537-1551.

Heckel, P. H., 1977, Origin of phosphatic black shale facies in Pennsylvanian cyclothems of mid-continent North America: Am. Assoc. Petr. Geol. Bull., v. 61, p. 1045-1068.

Heckel, P. H., 1980, Paleogeography of eustatic model for deposition of mid-continent upper Pennsylvanian cyclothems: Rocky Mountain Section, S.E.D.M.; West-Central United States, ed. by Fouch, T. D., and Magathan, E. R., p. 197-215.

Howe, W. B., 1956, Stratigraphy of pre-Marmaton Desmoinesian (Cherokee) rocks in southeastern Kansas: Kans. Geol. Survey Bull. 123, 132 p.

James, G. W., 1970, Stratigraphic geochemistry of a Pennsylvanian black shale (Excello) in the mid-continent and Illinois basin: Unpublished Ph.D. thesis, Rice University, 92 p.

Jewett, J. M., 1954, Oil and gas in eastern Kansas: Kans. Geol. Survey Bull. 104, 397 p.

Jonas, E. C., and McBride, E. F., 1977, Diagenesis of sandstone and shale: application to exploration for hydrocarbons, Univ. of Texas, 120 p.

Keller, W. D., 1970, Environmental aspects of clay minerals: J. Sed. Pet., v. 40, p. 788-813.

Kluth, C. F., and Coney, P. J., 1981, Plate tectonics of the ancestral Rocky Mountains: Geology, v. 9, p. 10-15.

Lahann, R. W., 1980, Smectite diagenesis and sandstone cement: the effect of reaction temperature: J. Sed. Pet., v. 50, p. 755-760.

Land, L. S., and Dutton, S. P., 1978, Cementation of a Pennsylvanian deltaic sandstone: isotopic data: J. Sed. Pet., v. 48, p. 1167-1176.

Lee, W., 1943, The stratigraphy and structural development of the Forest City Basin in Kansas: Kans. Geol. Survey Bull. 51, 142 p.

Loucks, R. G., Bebout, D. G., and Galloway, W. E., 1977, Relationships of porosity formation and preservation to sandstone consolidation history-Gulf coast lower Tertiary Frio Formation: Texas Univ. Bur. Econ. Geol. Circ. 77-5, p. 109-120.

Merriam, D. F., 1963, The geologic history of Kansas: Kans. Geol. Survey Bull. 162, 317 p.

Moore, D. G., and Scruton, P. C., 1957, Minor internal structures of some recent unconsolidated sediments: Am. Assoc. Petr. Geol. Bull., v. 41, p. 2723-2751.

Moore, G. E., 1979, Pennsylvanian paleogeography of the southern mid-continent, in Hyne, N. D., ed., Pennsylvanian Sandstones of the Mid-continent: Tulsa Geological Society Special Publication No. 1, p. 2-12.

Moore, R. C., 1931, Pennsylvanian cycles in the northern Mid-continent region: Ill. Geol. Survey Bull. 60, p. 247-257.

Moore, R. C., 1936, Stratigraphic classification of the Pennsylvanian rocks of Kansas: Kans. Geol. Survey Bull. 22, 256 p.

Moore, R. C., 1964, Paleoecological aspects of Kansas Pennsylvanian and Permian cyclothems: in Symposium on cyclic sedimentation, Kans. Geol. Survey Bull. 169, Vol. 1, p 287-380.

Oakes, M. C., 1953, Krebs and Cabaniss Groups of Pennsylvanian age of Oklahoma: Am. Assoc. Petr. Geol. Bull., v. 37, p. 1523-1526.

Pettijohn, F. J., Potter, P. E., and Siever, R., 1973, Sand and sandstone, Springer-Verlag, Heidelberg, Germany, 618 p.

Powell, J. P., and Eakin, J. L., 1953, Water flooding in the oil fields of Anderson, Franklin, Linn, and Miami Counties, Kansas: U. S. Bureau of Mines, Rept. of Invest. 4991.

Rich, J. L., 1923, Shoestring sands of eastern Kansas: Am. Assoc. Petr. Geol. Bull., v. 7, p. 103-113.

Rich, J. L., 1926, Further observations on shoestring oil pools of eastern Kansas: Am. Assoc. Petr. Geol. Bull., v. 10, p. 568-580.

Searight, W. V., Howe, W. B., Moore, R. C., Jewett, J. M., Condra, G. E., Oakes, M. C., and Branson, C. C., 1953, Classification of Desmoinesian (Pennsylvanian) of northern mid-continent: Am. Assoc. Petr. Geol. Bull., v. 37, p. 2747-2749.

Sibley, D. F., and Blatt, H., 1977, Quantitative evaluation of intergranular pressure solution as a source of silica in the Tuscarora Orthoquartzite, Central Appalachians: G. S. A. Ann. Mtgs., 6: p. 954.

Van Dyke,R. J., 1975, Geology and depositional environments of the reservoir sandstone, Kincaid oil field, Anderson County, Kansas: Unpublished M. S. thesis, Kansas University, 81 p.

Visher, G. S., 1968, Depositional framework of the Bluejacket-Bartlesville sandstone, in Geology of the Bluejacket Bartlesville sandstone of Oklahoma: Oklahoma City Geol. Soc., p. 32-51.

Visher, G. S., Saitta, B., and Phares, R. S., 1971, Pennsylvanian delta patterns and petroleum occurrences in eastern Oklahoma: Am. Assoc. Petr. Geol. Bull., v. 55, p. 1206-1230.

Walker, T. R., 1967, Formation of red beds in ancient and modern deserts, Geol. Soc. America Bull., v. 78, p. 353-368.

Wanless, H. R., Gednetz, D. E., Tubbs, J. B., and Weiner, J. L., 1963, Mapping sedimentary environments of Pennsylvanian cycles: Geol. Soc. America Bull., v. 74, p. 437-486.

Weirich, T. E., 1953, Shelf principles of oil origin, migration, and accumulation: Am. Assoc. Petr. Geol. Bull., v. 37, p. 2027-2045.

Wells, J. S., and Anderson, K. H., 1968, Heavy oil in western Missouri: Am. Assoc. Petr. Geol. Bull., v. 52, p. 1720-1731.

Woody, M. D., 1982, Sedimentary diagenesis, and petrophysics of selected Cherokee Group (Desmoinsian) sandstones in southeastern Kansas: Unpublished M. S. thesis, Univ. of Kansas, 129 p.

Zeller, D. E. (ed.), 1968, The stratigraphic succession in Kansas: Kans. Geol. Survey Bull. 189, 81p.

APPENDIX A

DESCRIPTIONS OF CORES USED IN STUDY

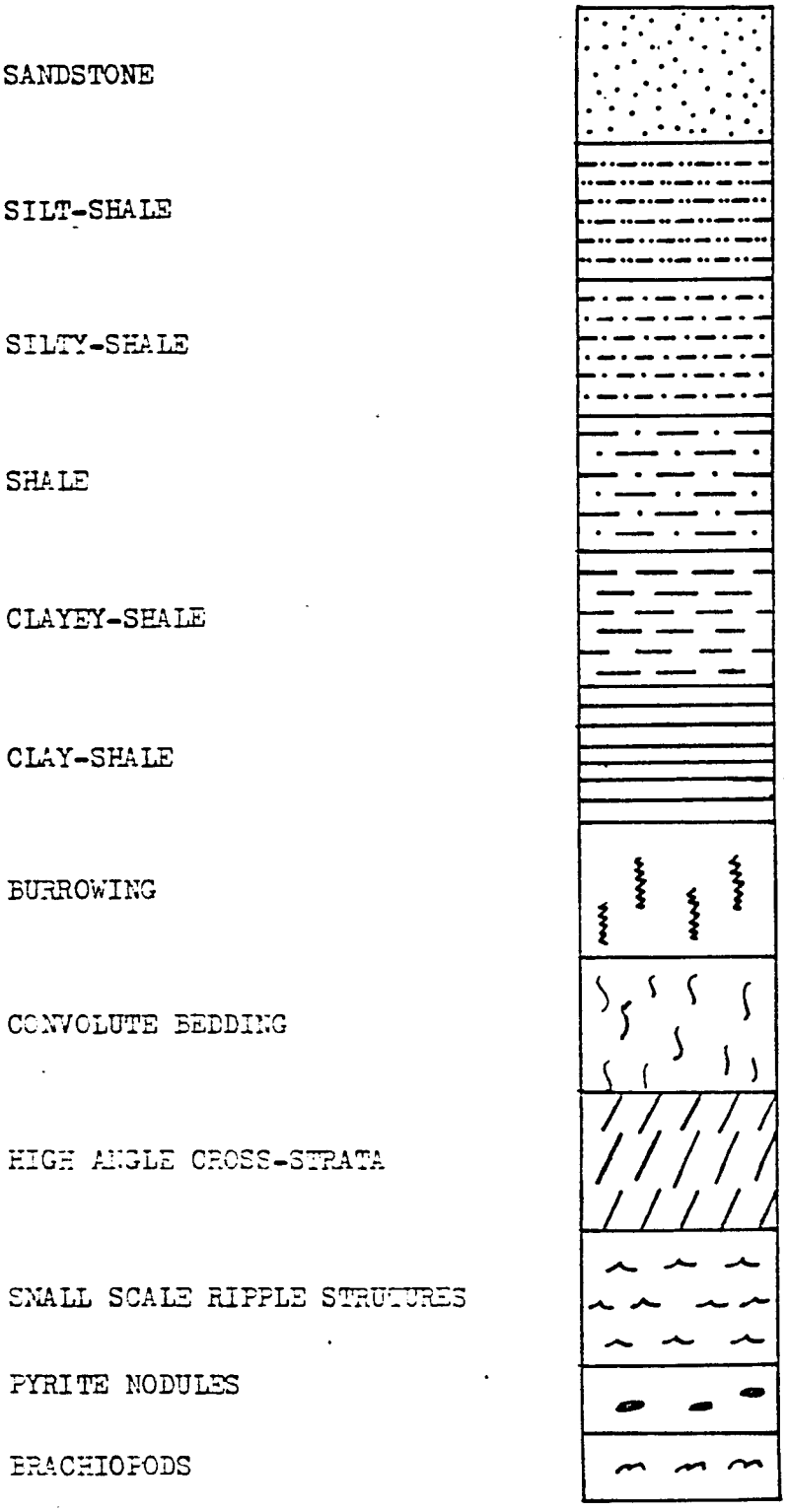

Figure 62. Lithologic symbols used in core descriptions.

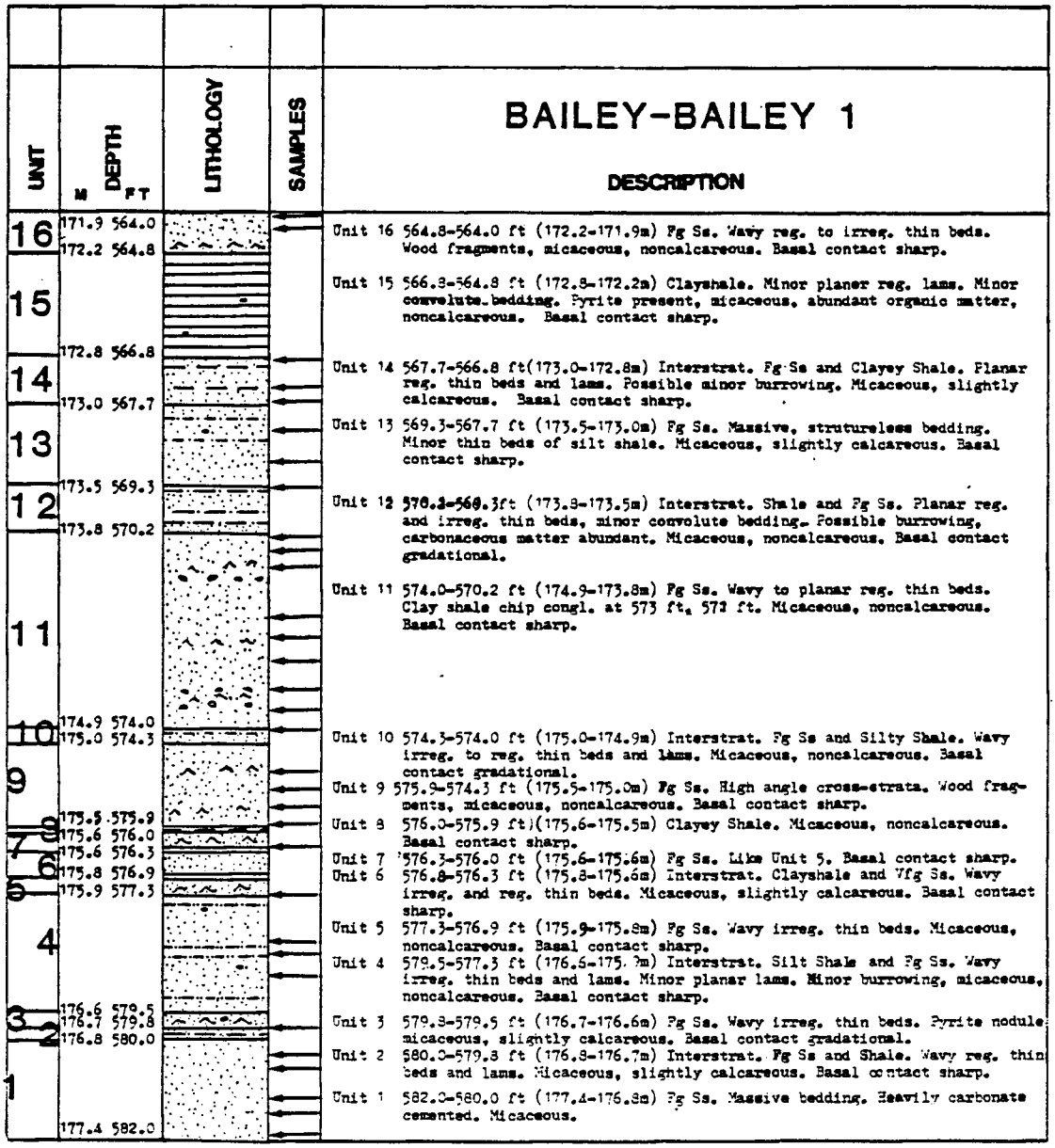

Figure 63. Lithologic log and description for well Bailey-Bailey No. 1. Centerville trend.

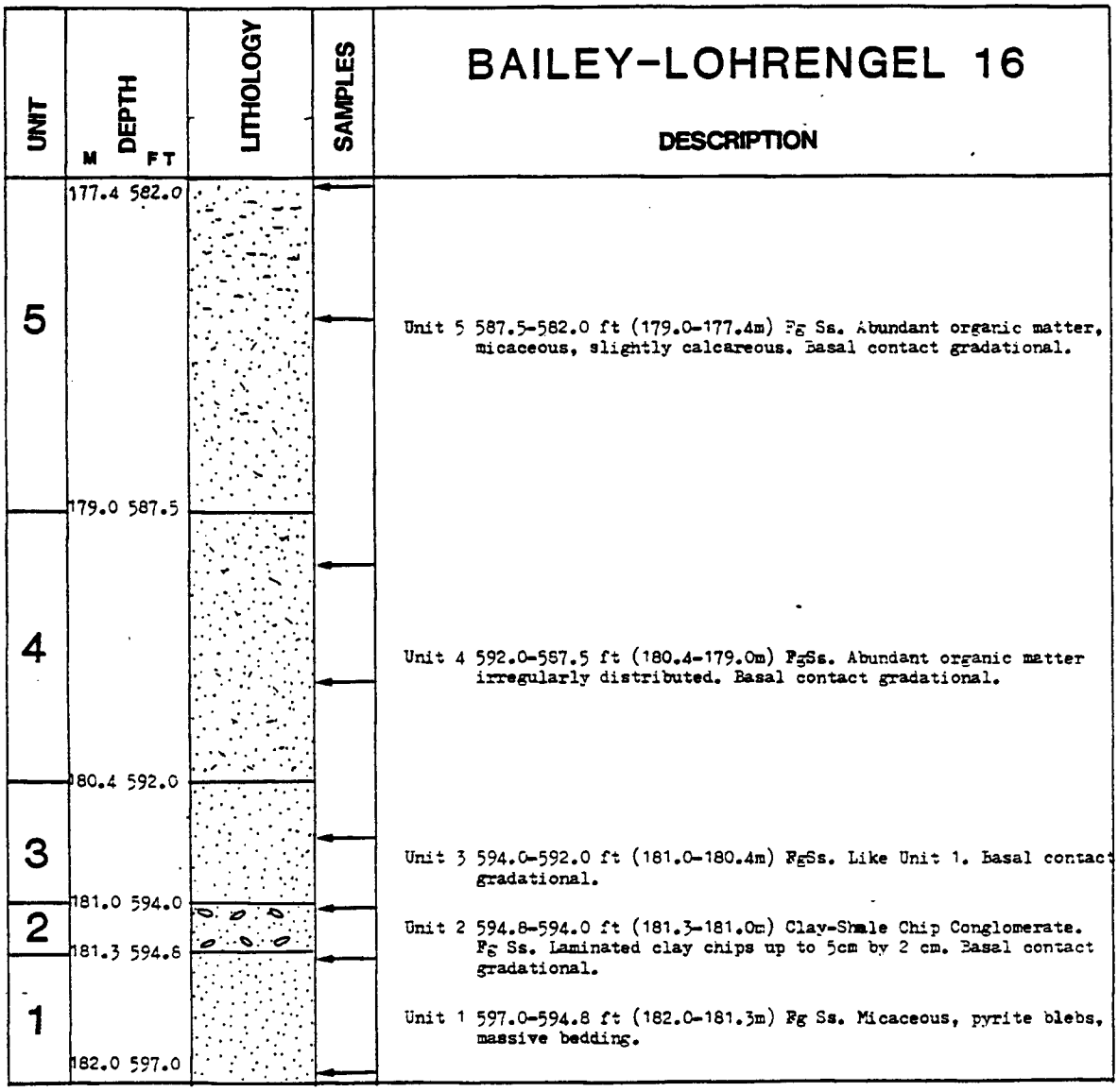

Figure 64. Lithologic log and description for well Bailey-Lohrengel 16. Centerville trend.

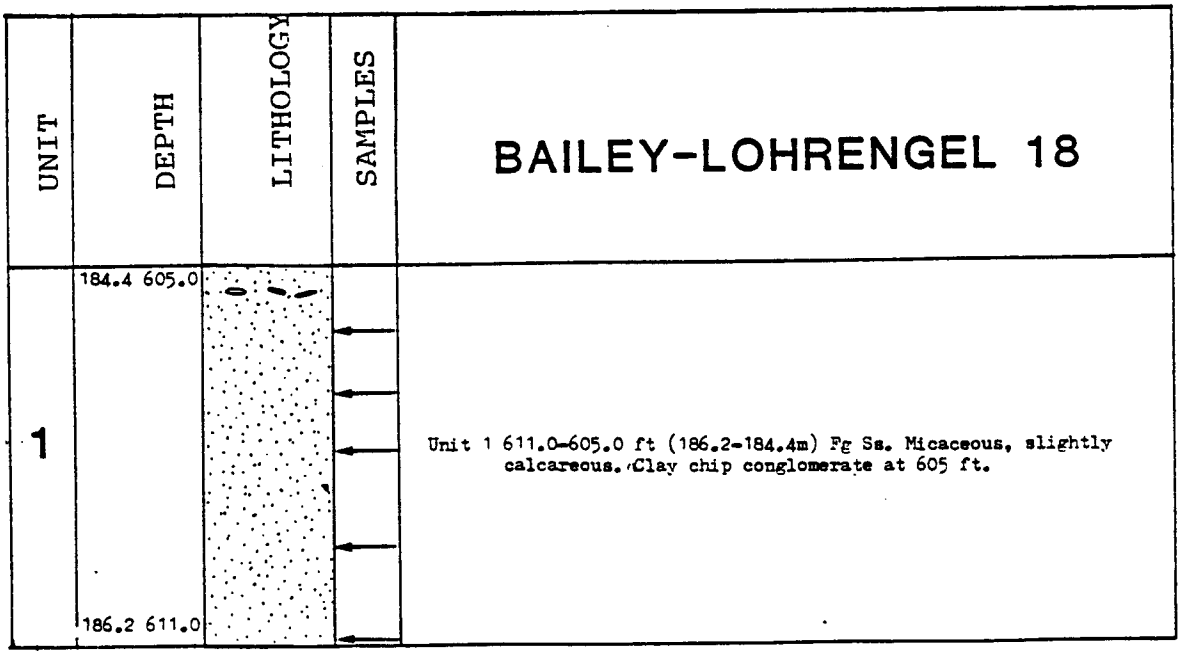

Figure 65. Lithologic log and description for well Bailey-Lohrengel 18. Centerville trend.

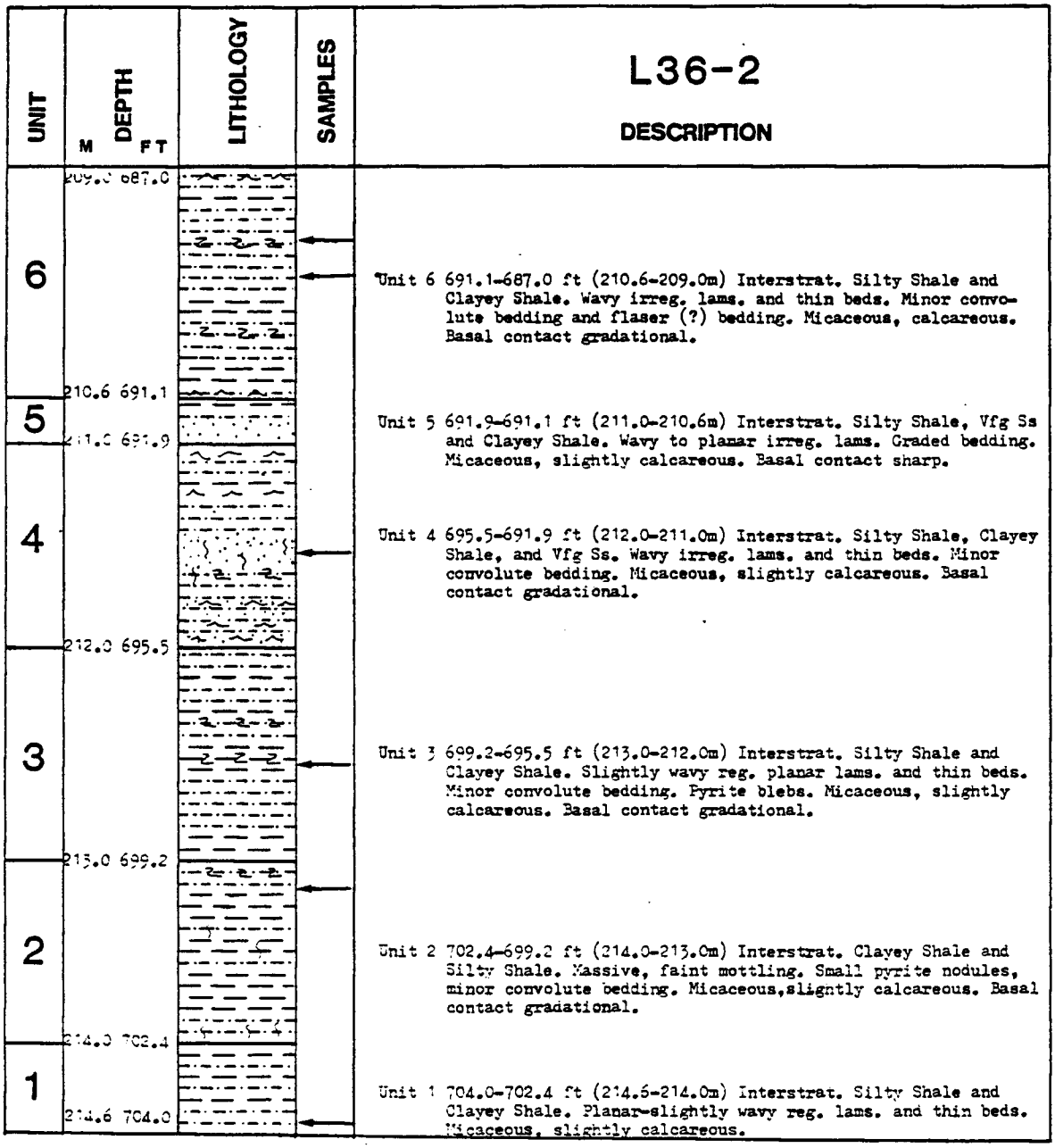

Figure 66. Lithologic log and description for well L-36. Bush City trend.

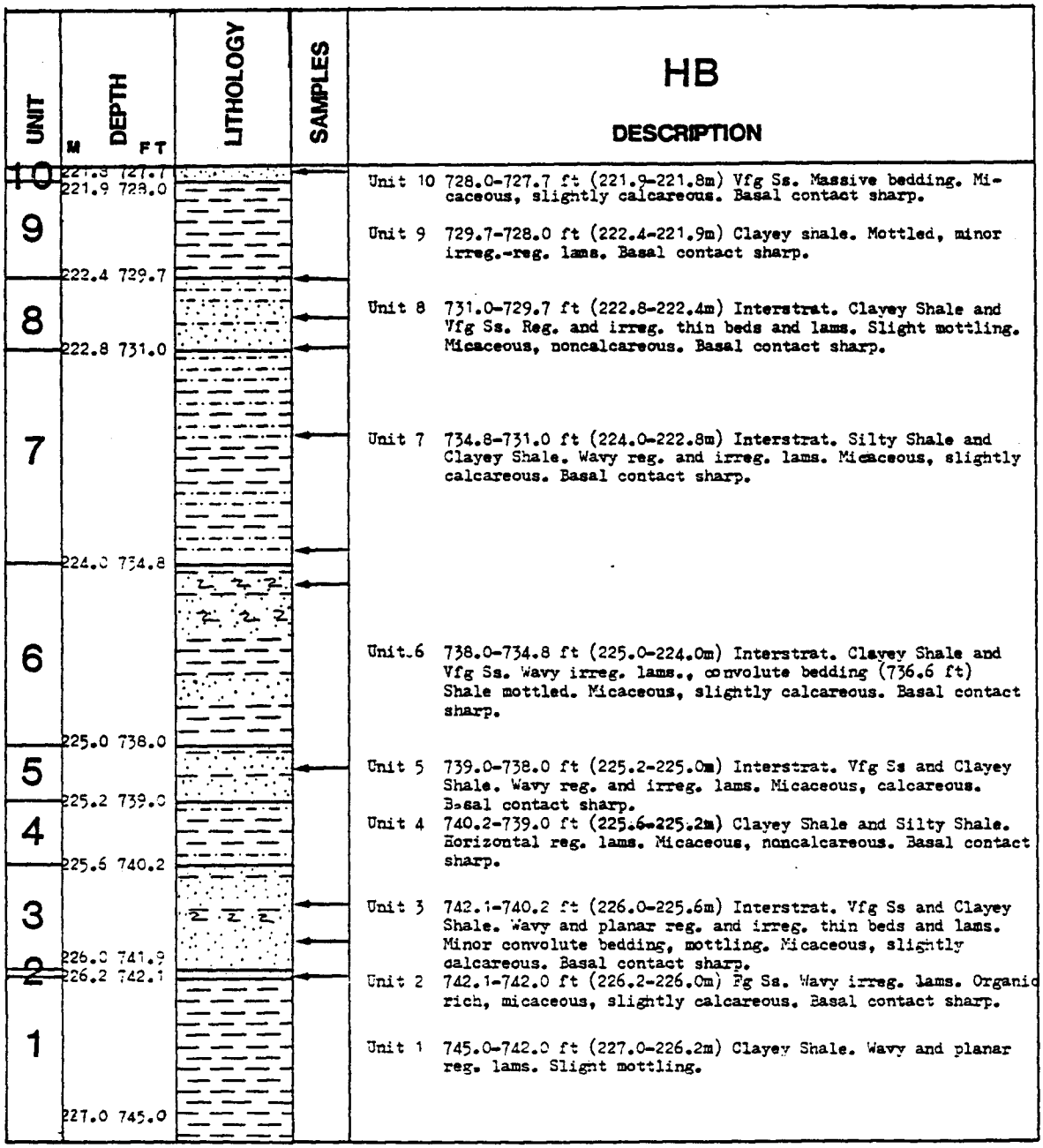

Figure 67. Lithologic log and description for well HB. Bush City trend.

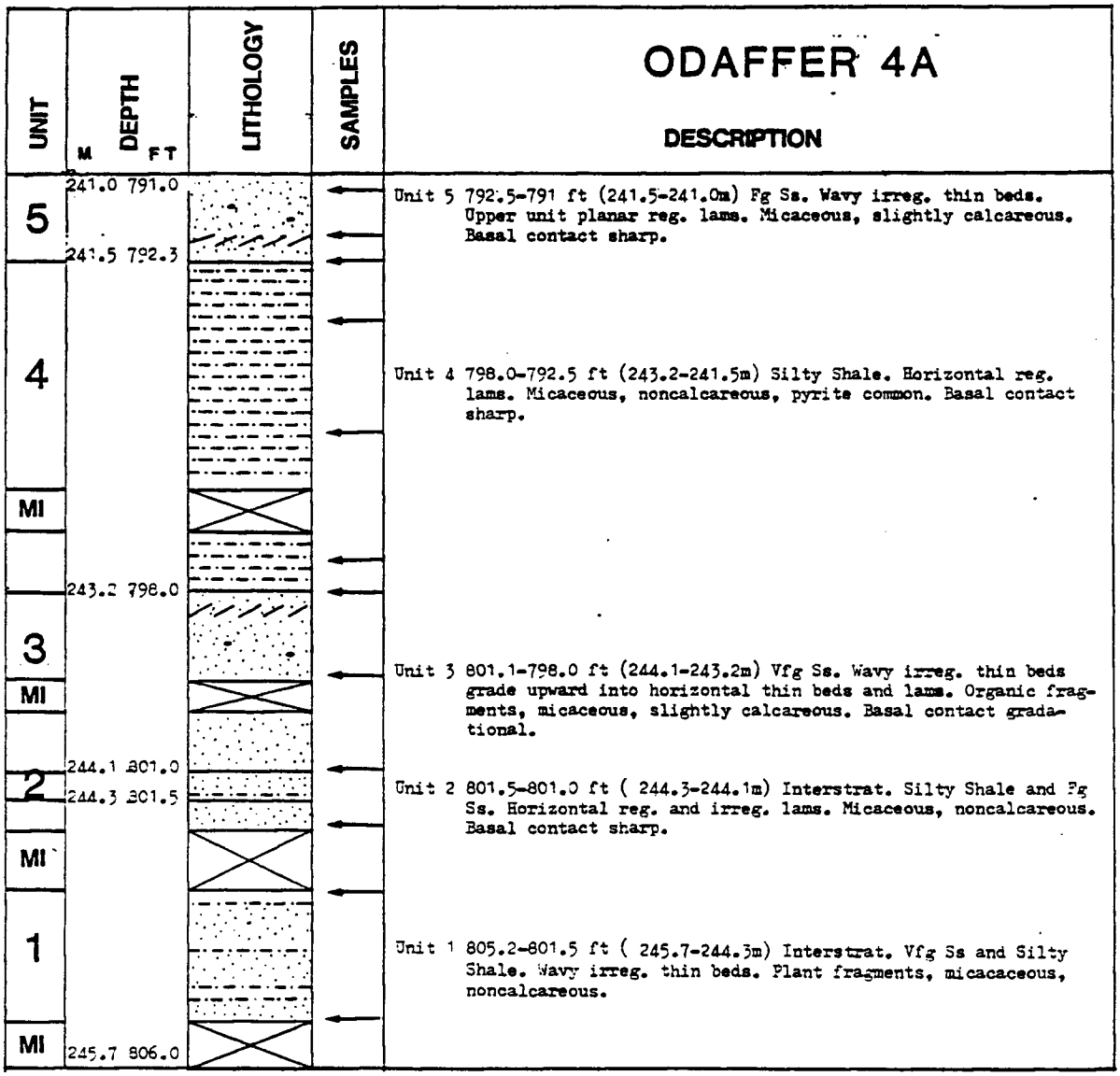

Figure 68. Lithologic log and description for well Odaffer 4A. Bush City trend.

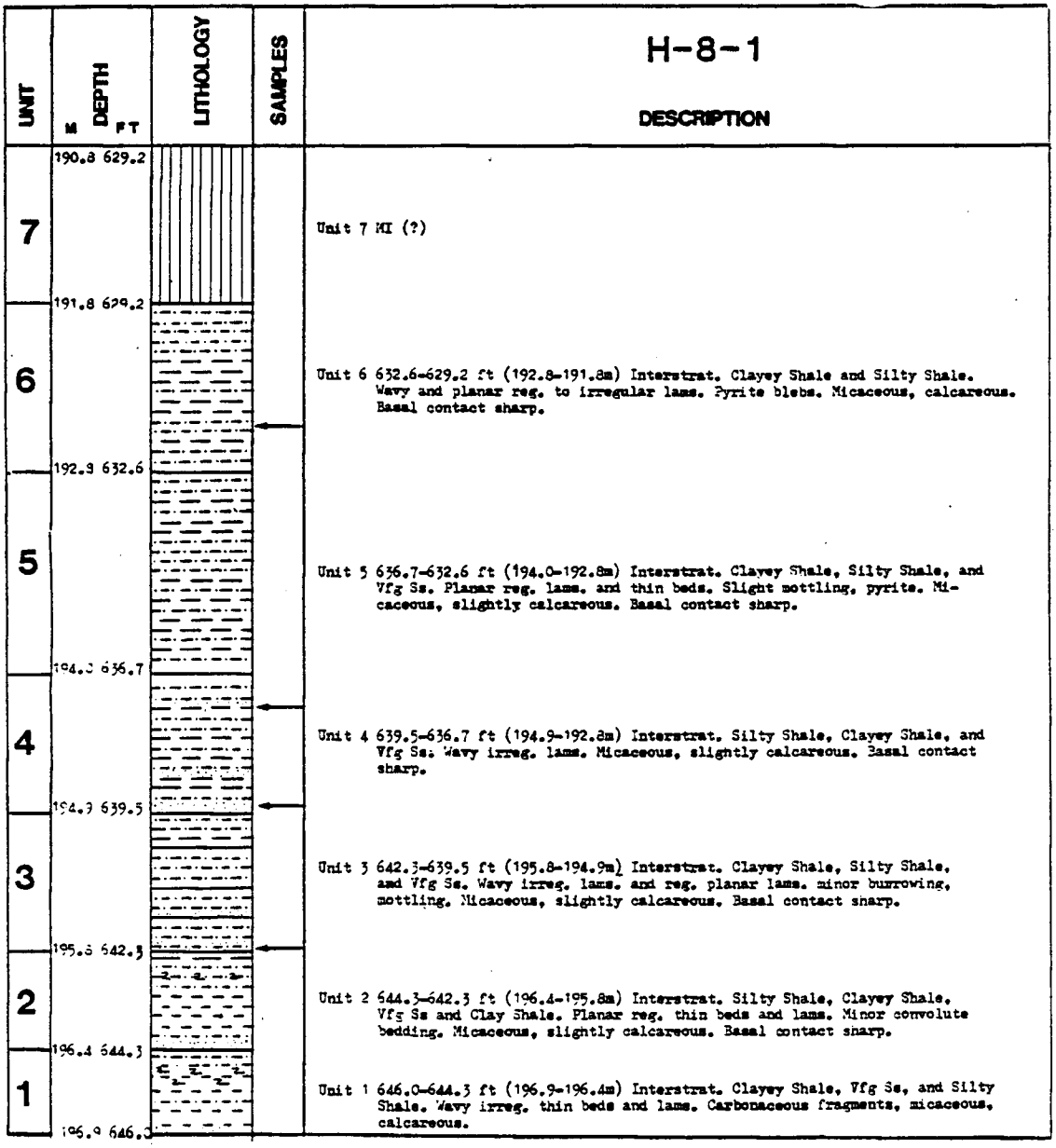

Figure 69. Lithologic log and description for well H-8-1. Bush City trend.

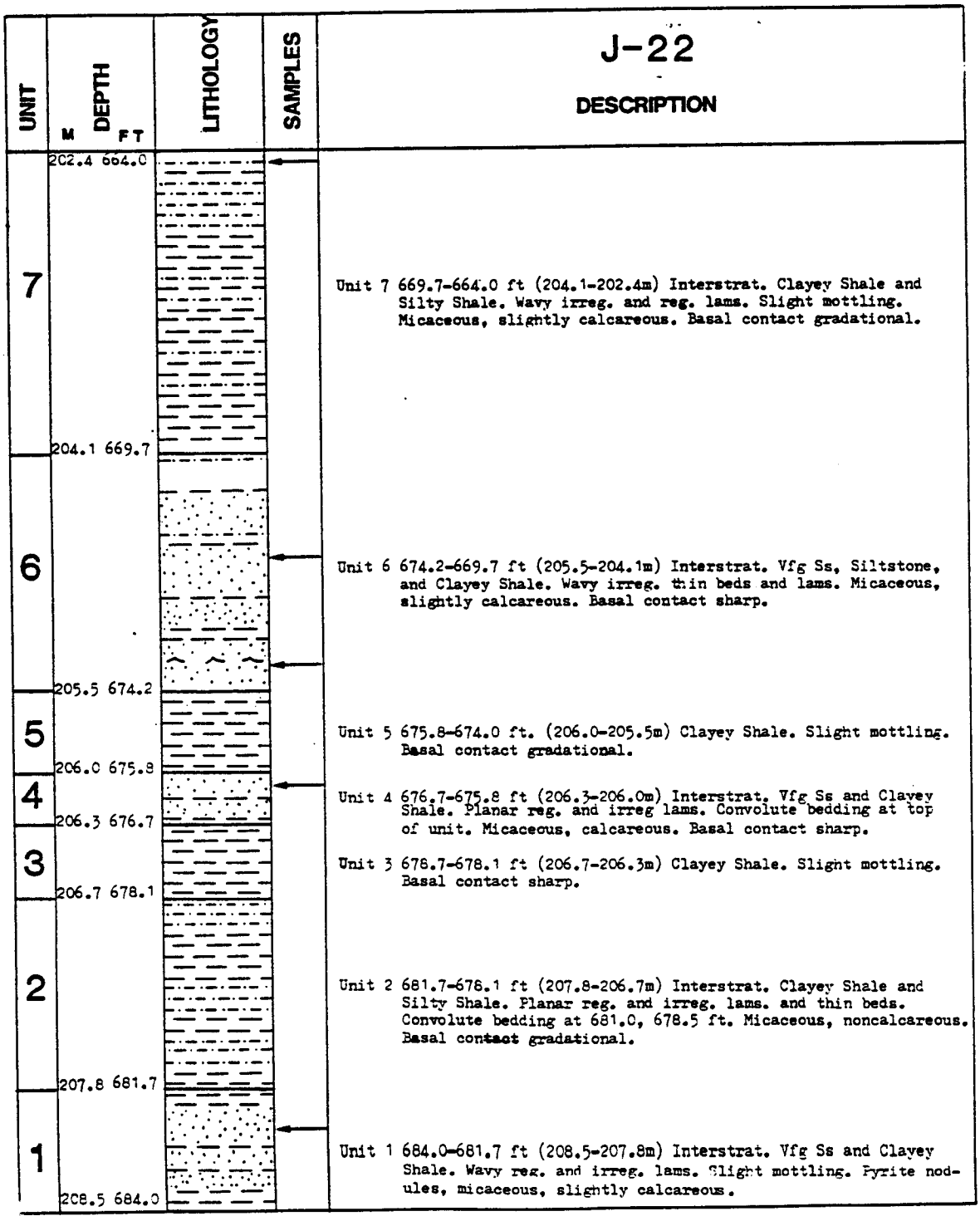

Figure 70. Lithologic log and description for well J-22. Bush City trend.

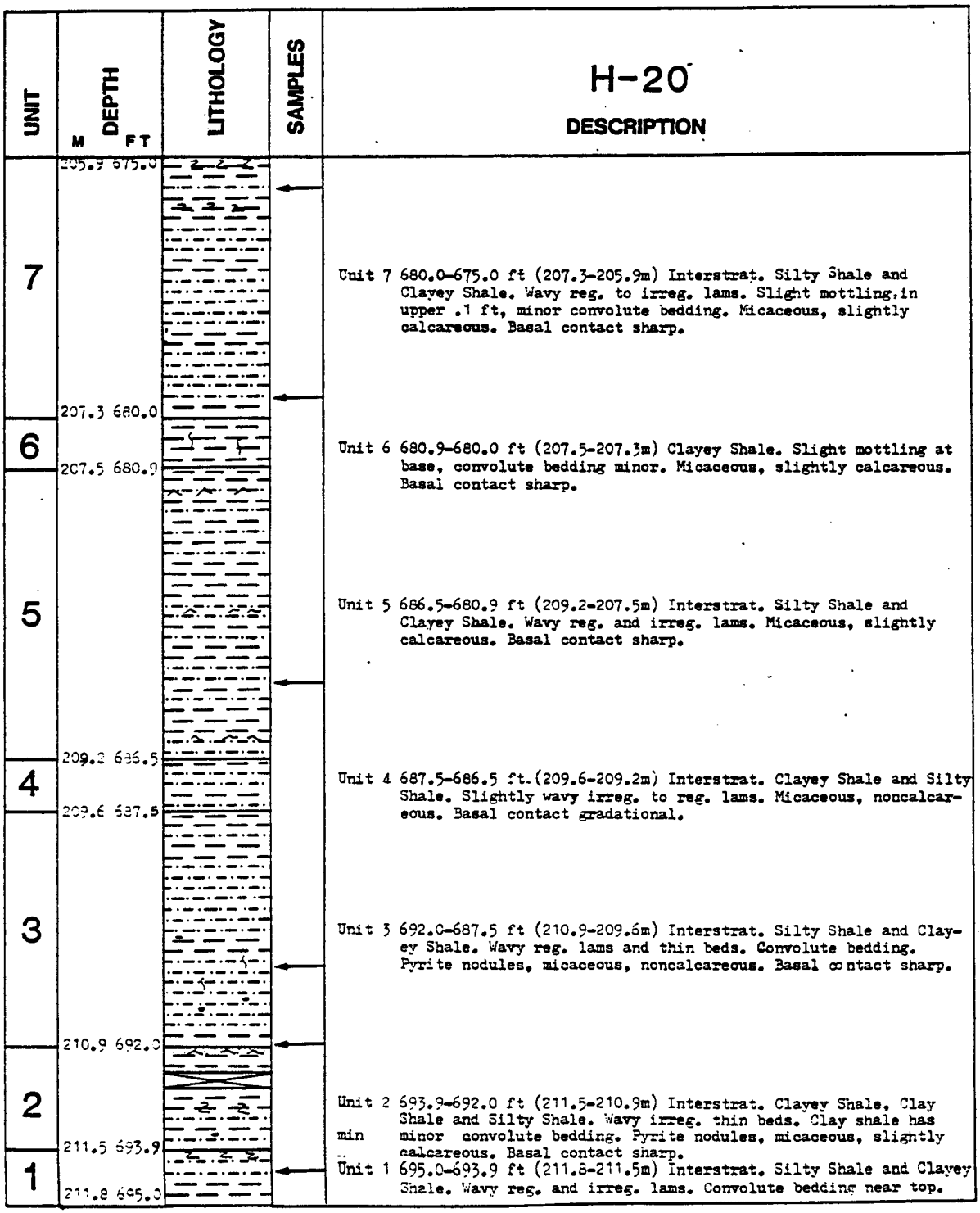

Figure 71. Lithologic log and description for well H-20. Bush City trend.

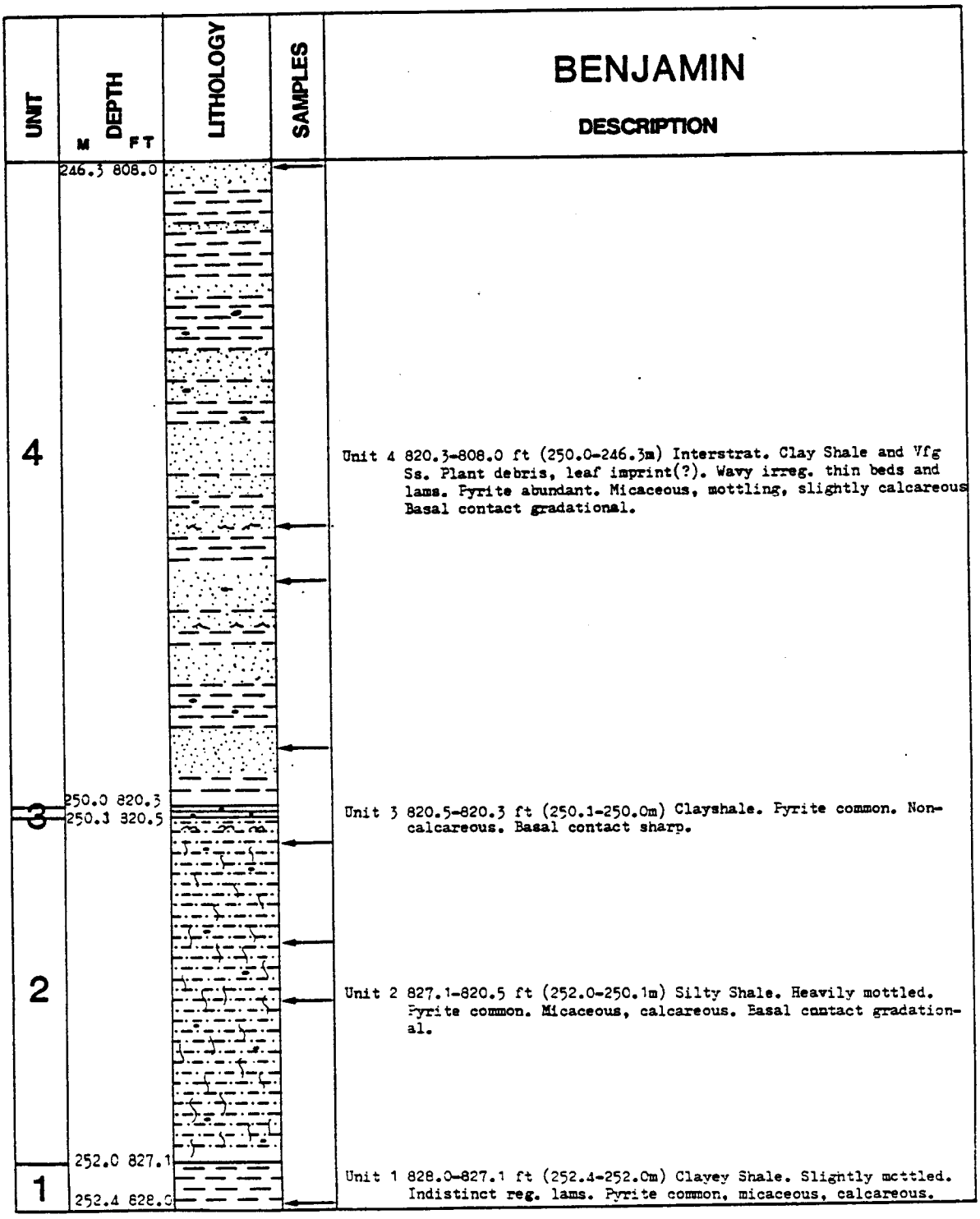

Figure 72. Lithologic log and description for well Benjamin (1). Bush City trend.

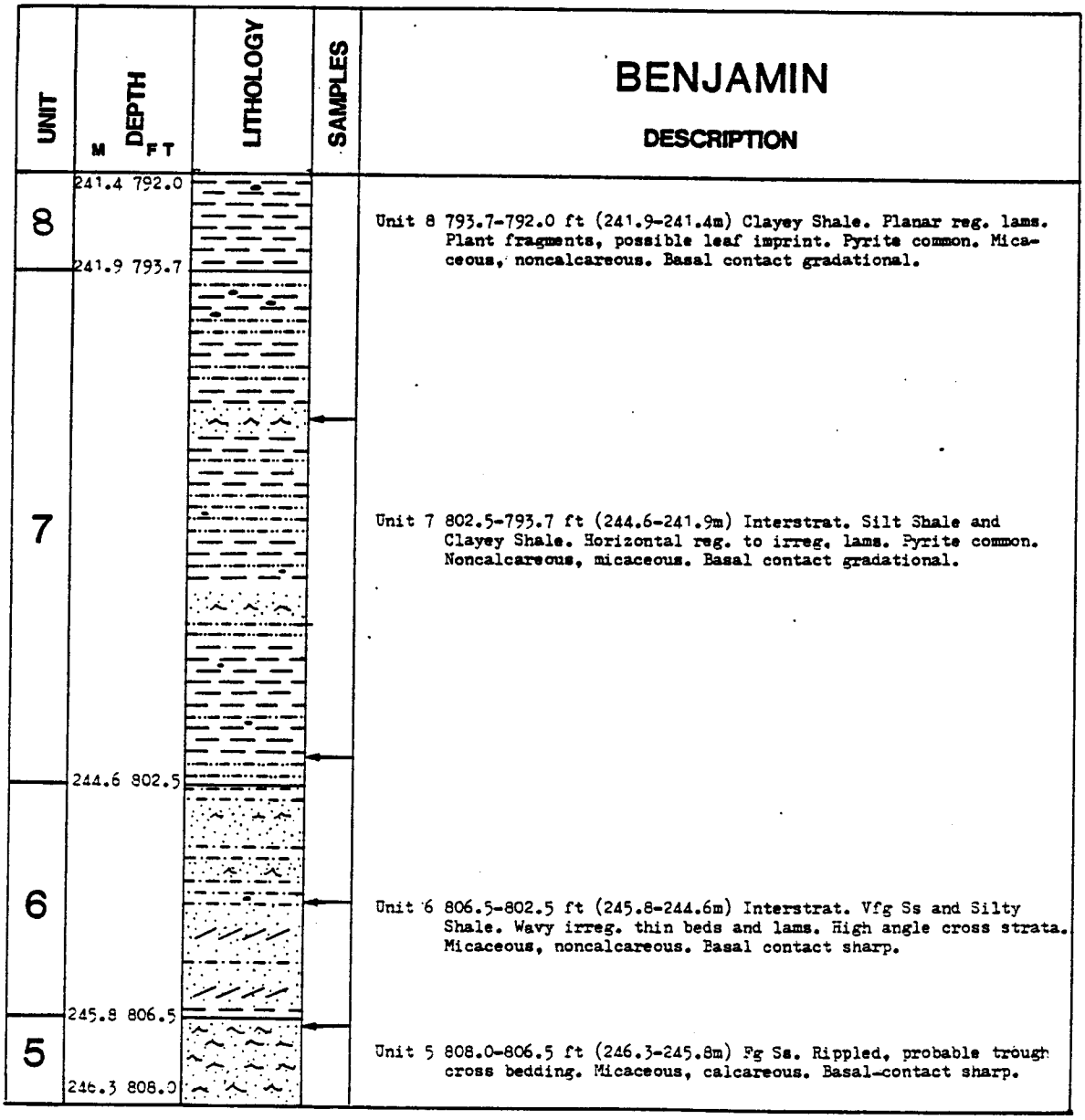

Figure 73. Lithologic log and description for well Benjamin (2). Bush City trend.

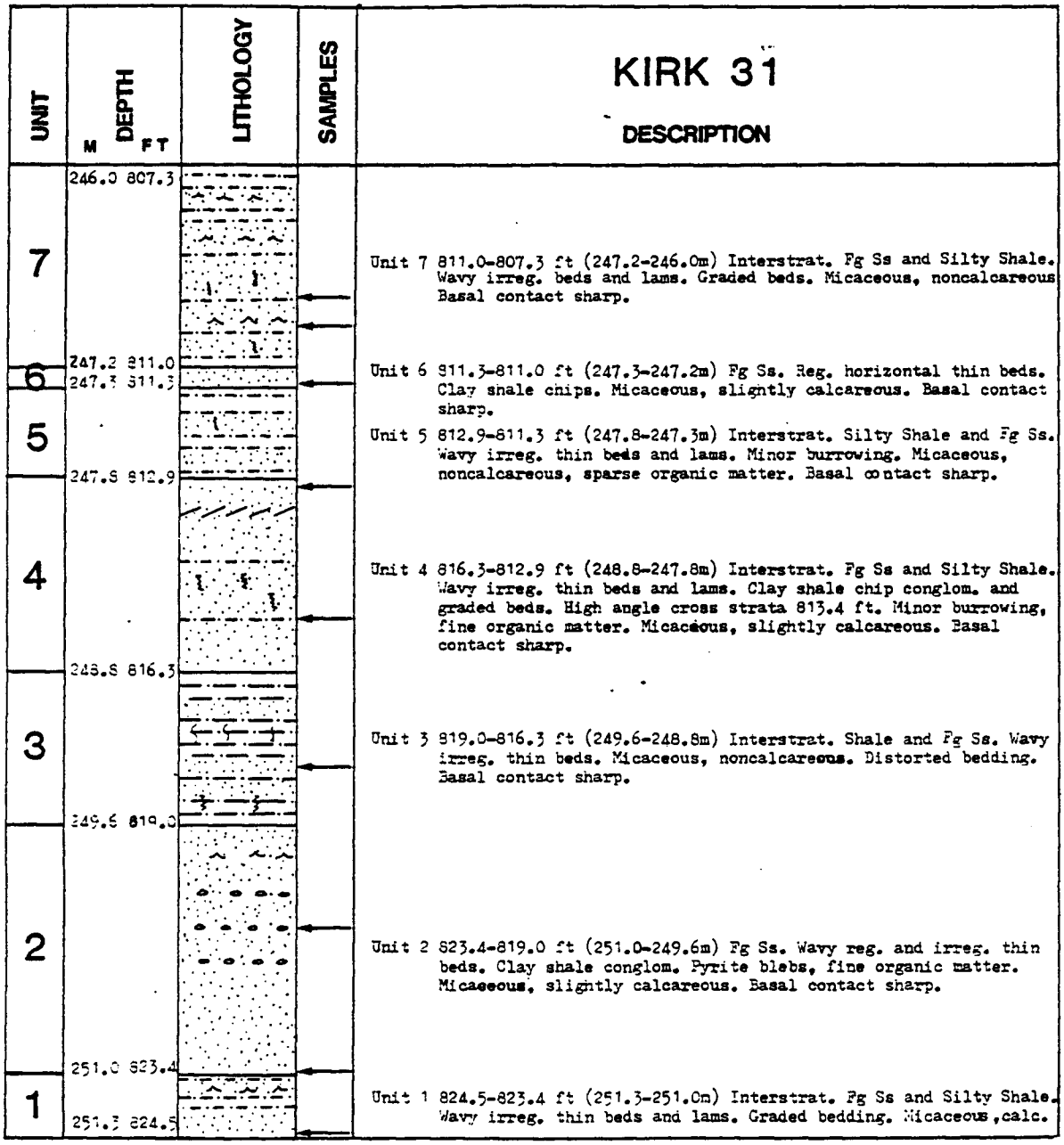

Figure 74. Lithologic log and description for well Kirk 31 (1). Bush City trend.

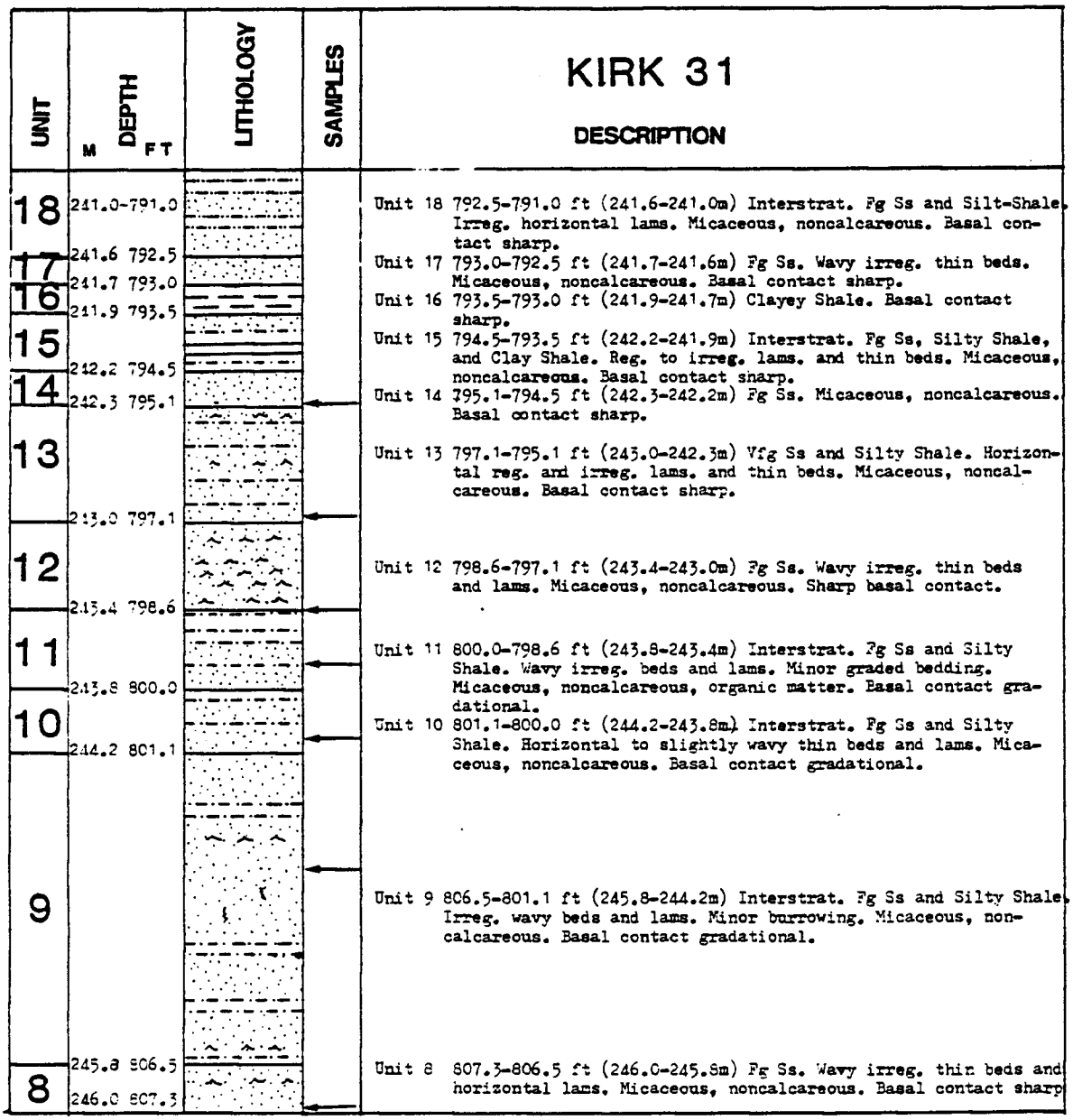

Figure 75. Lithologic log and description for well Kirk 31 (2). Bush City trend.

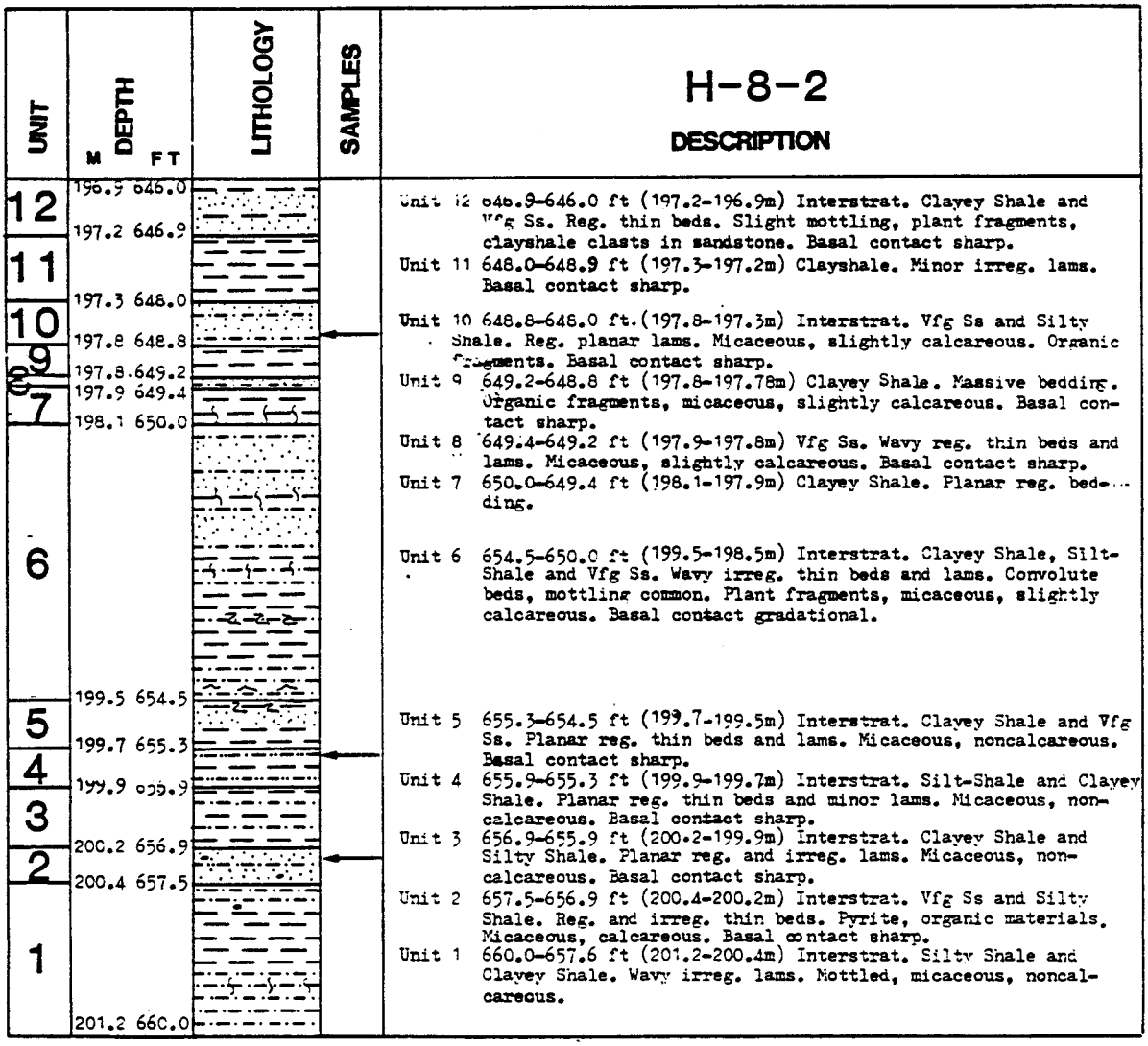

Figure 69. Lithologic log and description for well H-8-2. Bush City trend.

APPENDIX B

POINT COUNT DATA

Meters Below Excello Shale	21.5	21.2	21.0	20.5	20.2	19.8	19.6	19.0	18.7
Sample No.	BB3	BB5	BB7	BB9	BB11	BB13	BB15	BB17	BB20
DETRITAL									
Quartz									
Monocrystalline	86	110	110	117	103	96	123	98	108
Polycrystalline	2	3	8	7	5	9	8	7	1
Feldspar									
Plagioclase feldspare	1	2	6	6	6	5	2	8	2
Potassium	2	5	7	6	4	6	5	7	9
Mica									
Muscovite	6	2	11	2	8	8	7	4	10
Biotite									1
Rock Fragments									
Schist	3	3				3		3	
Shale			1		1			2	1
Chert									
Matrix	2	2	12	14	8	16	10	28	12
Phosphate									
Heavy Minerals			1						
Organic Material	4	1	6	15	20	23	10	5	8
AUTHIGENIC									
Carbonates									
Fe-calcite	87	60	12	2	9	6	6	2	27
Siderite									
Clays									
Kaolinite		1	4	4	4	3	3	4	4
Serecite		6	6	11	15	6	8	7	5
Chlorite	1	1				2	1		
Silica	4	4	5	3	4	2	3	8	1
Pyrite							2	2	1
Illmenite	2			1					
Feo	1		6	10	10	10	9	9	1
			5	2	3	5	3	6	9

18.6	18.0	17.9	17.6	17.3	17.0	16.5	16.3	15.2	19.8	18.4	17.2
BB22	BB24	BB26	BB28	BB30	BB32	BB34	18-2	18-5	16-2	16-6	16-8
118	106	116	117	102	99	110	94	121	104	124	105
2	5	3	8	5	6	8	4	5	8	5	4
4	3	2	4	10	4	5	7	5	6	8	2
6	7	4	4	5	8	5	6	3	6	5	9
1	6	9	3	6	5	5	4	5	3	3	8
						1			1		1
2	2				2	2	1		3	2	1
4	1		2	2		2	6	10		3	2
1			1		2					1	
14	9	18	14	5	13	10	31	17	5	15	25
			1		1		1	1	2		
14	12	14	7	15	11	16	12	5	7	8	12
10	20	14	14	23	18	11	5	8	21	2	6
3	4	1	6	5	8	6	1	1	6	2	3
6	7	9	9	10	7	8	11	6	8	7	5
2	1	-					1				
2	5	5	4	3	6	4	3	1	6	2	5
		1			1	2					
1						1					
4	6	2	3	3	5	-	6	5	9	6	5
6	6	1	4	5	5	4	7	7	6	7	7

15.8	18.5	18.1	17.3	14.4	13.2	10.4	?	?	15.8	13.3	?
16-10	K-1	K-3	K-5	K-9	K-11	K-17	HB742.1	HB729.7	H82657	H82648.6	L36-694.1
118	97	111	103	119	128	124	128	129	103	131	120
6	5	5	5	3	-	-	4	1	5	1	2
4	3	3	5	4	2	1	1	3	3	1	4
4	4	2	8	3	2	2	5	4	3	4	2
8	5	19	8	2	3	-	5	9	5	3	3
1	3	2		1			1				
	3	2	2						2	-	1
	1	2	2	1							
									1		
12	12	18	18	25	27	20	28	28	20	20	25
		1	2			1			1		1
1	1	1	1			1		1	1	1	
8	12	8	6	8	6	15	3	6	5	2	8
2	23	-	14	6	6	7	3	1	24	13	2
	2	-									2
6	2	-					1	2	1		
5	12	10	8	14	7	11	10	4	5	8	7
1		2	1		1				1		1
4	5	8	7	5	8	8	7	8	10	8	11
	6	2	3	2			-		2	1	1
						1	-	1			1
15	4	5	1	3	6	2	-	-	5	3	5
4	1		6	3	3	5	3	2	3	4	4

?	15.9	13.1	11.3	13.9	10.5
L36-689	H20-694.3	H20-685	H20-679.7	J-22 682.5	J-22 671-6
105	124	107	118	125	146
2	2	-	1	3	2
2	1	1	3	1	1
4	2	4	4	6	5
5	3	7	4	6	2
		1			
1					
30	23	36	39	29	17
		1			
11	3	5		5	
7	20	6	1	5	
	4	4	3	2	2
			3		4
12	5	5	6	5	5
2		1	1		
10	4	4	5	4	9
3		3	4	2	1
			1	2	2
4	6	9	6	2	
2	3	6	4	3	4

APPENDIX C

WELL LOG LOCATIONS USED IN STUDY

	WELL	LOCATION	
1	M. Parks No. 4	1540 WL 660 NL SW¼ Sec. 27	20-21
2	Craig No. 2	1100 NL 220 WL SE¼ Sec. 27	20-21
3	EM Byerley B99	Sec. 30	20-22
4	HB Cox Fe	350 EWL 1200 SNL NW¼ Sec.20	20-22
5	Fuerborn No. 1	Sec. 16	20-22
6	Kretchmar 35	1600 NL 110 WL NW ¼ Sec. 33	20-21
7	North Unit 26	SW NW NE Sec. 4	21-21
8	Schermerhorn S-8	1700 FWL 1350 FSL Sec. 4	21-21
9	Bailey-Lohrengel 9	NE SW NE Sec. 22	21-21
10	Bailey-Bailey No. 2	Sec. 27	21-21
11	C. Hastert No. 11	SW NW SW Sec. 13	20-20
12	C. Hastert No. 10	NW SW SE Sec. 13	20-20
13	C. Hastert No. 20	SW SE SE Sec. 13	20-20
14	C. Hastert No. 24	SE SE SE Sec. 13	20-20
15	North Unit 33	NW N½ of NE¼ Sec. 4	21-21
16	North Unit 21	SW NE¼ NE¼ Sec. 4	21-21
17	North Unit 19	SE SE NE Sec. 4	21-21
18	North Unit 18	NE NE SE Sec. 4	21-21
19	North Unit 16	SW NE SE Sec. 4	21-21
20	Melcher No. 2	Sec. 6	21-20
21	Melcher L10R	1375NSL 330 WEL SE¼ Sec. 7	21-20
22	Wilson F4R	SW SE SW Sec. 8	21-20
23	Kirk 16	SE NE NE Sec. 17	21-20
24	Kirk W13	SE SE Sec. 16	21-20
25	Hunley H32	NW SW NW Sec. 16	21-20
26	Hunley H30	NE SE NW Sec. 16	21-20
27	Kirk 14	NW SW NE Sec. 16	21-20
28	West Hunley No. 17	NE NE NW Sec. 16	21-20
29	East Hunley No. 3	SW NW NE Sec. 16	21-20
30	12 E	430 NSL 330 EWL NW¼ Sec. 15	21-20
31	Weiss No. 7	NE SW NW Sec. 15	21-20
32	West Ware No. 6	NW SE NW Sec. 15	21-20
33	Ware No. K13	C N½ Sec. 15	21-20

	WELL	LOCATION	
34	Andregg No. 1	SE SE SE Sec. 10	21-20
35	Weiss L-19	SE NW NW Sec. 15	21-20
36	Ware No. F14-R	SE SE NW Sec. 15	21-20
37	East Herman No. 4	NE NW SE Sec. 15	21-20
38	C. Parks No. 3	1100 S 660 W SW¼ Sec. 27	20-21
39	M. Parks No. 2	660 WL 1100 NL SW¼ Sec. 27	20-21
40	M. Parks No. 3	1100 WL 660 NL SW¼ Sec. 27	20-21
41	M. Parks No. 4	1540 WL 660 NL SW¼ Sec. 27	20-21
42	Katzer No. 7	SW NE¼ Sec. 27	20-21
43	Katzer No. 4	600 NL 1440 WL NE¼ Sec. 27	20-21
44	Katzer No. 5	440 NL 1880 WL NE¼ Sec. 27	20-21
45	Katzer No. 6	220 EL 220 NL NE¼ Sec. 27	20-21
46	C. Park No. 3	NE SW¼ Sec. 27	20-21
47	Craig No. 2	1100 NL 220 WL SE¼ Sec. 27	20-21
48	Gregg No. 6	Sec. 22	21-19
49	Kellstadt 32 P	W½ NE NE Sec. 34	21-19
50	Babcock No. 2	NW SE SE Sec. 8	22-19
51	Gregg No. 1	SW NW Sec. 22	22-19